

HEAT TRANSFER IN HIGH LAMINAR, TRANSITION AND LOWER  
TURBULENT FLOW REGIMES FOR SQUARE-EDGED  
CONTRACTION ENTRANCE IN A CIRCULAR TUBE

By

JENG-HO CHEN

Bachelor of Science  
National Tsing-Hua University  
Hsin-Chu, Taiwan, R. O. C.  
1978

Master of Science  
National Tsing-Hua University  
Hsin-Chu, Taiwan, R. O. C.  
1980


Submitted to the Faculty of the  
Graduate College of the  
Oklahoma State University  
in partial fulfillment of  
the requirements for  
the degree of  
DOCTOR OF PHILOSOPHY  
May, 1989

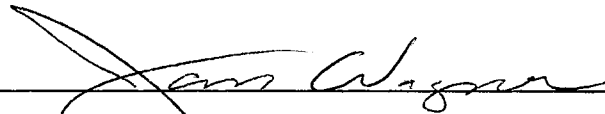
Thesis  
1989 D  
C518h  
cop. 2

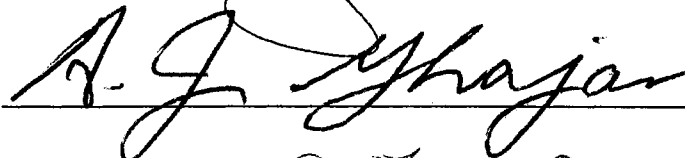
HEAT TRANSFER IN HIGH LAMINAR, TRANSITION AND LOWER  
TURBULENT FLOW REGIMES FOR SQUARE-EDGED  
CONTRACTION ENTRANCE IN A CIRCULAR TUBE

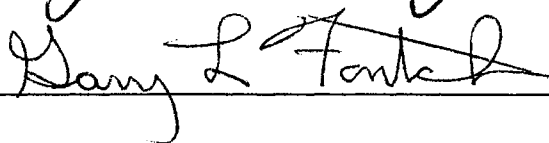
Thesis Approved:


  
Thesis Advisor









  
Dean of Graduate College

C O P Y R I G H T

by

Jeng-Ho CHEN

May 1989

## PREFACE

A tube rolled into a tubesheet in a shell and tube heat exchanger has, to a first approximation, a square-edged entrance. Simultaneous hydrodynamically and thermally developing flow in the tubes is the practical situation in most heat exchangers. The present understanding of combined free and forced convection heat transfer in a circular tube in developing laminar, transition, and turbulent flow regimes is quite limited. Consequently, the combined natural and forced convection heat transfer in high laminar through lower turbulent flow regimes for a tube with a square-edged entrance was investigated.

Distilled water and 28.3 percent, 48.5 percent, 65.0 percent, 92.5 percent, and nearly 100 percent diethylene glycol (DEG) mass fraction DEG-water solutions were used as test fluids in an electrically-heated stainless steel tube. D. C. current passed through the wall of the tube, and heat was generated by the electrical resistance of the wall. Local peripheral wall temperatures were measured at twelve axial locations and the local heat transfer coefficients were calculated. The experiments covered the local bulk Reynolds number range from 121 to 12,400, the local bulk Prandtl number range from 3.5 to 285.0, and the Grashof number range from 930 to 1,040,000.

This study permitted a better understanding of the combined forced and natural convection problem, where both the velocity and the temperature profiles are developing simultaneously. The following correlations were developed to predict the heat transfer coefficient in a straight horizontal circular tube with a square-edged contraction entrance:

#### Laminar

$$Nu = \{4.364 + 0.00106Re^{0.81}Pr^{0.45} (1+14e^{-0.063x/d_i}) + 0.268(GrPr)^{1/4} (1-e^{-0.042x/d_i})\} (\mu_b/\mu_w)^{0.14}$$

where  $121 < Re < 2,100$

$3.5 < Pr < 282.4$

$930 < Gr < 67,300$

#### Upper Transition

$$Nu = 0.00392RePr^{1/3} (1+1.19e^{-0.308x/d_i}) (\mu_b/\mu_w)^{0.14}$$

where  $4,600 < Re < 7,000$

$3.5 < Pr < 7.4$

$45,570 < Gr < 1,040,000$

#### Lower Turbulent

$$Nu = 0.01426Re^{0.86}Pr^{1/3} [1+1.15e^{-x/(3d_i)}] (\mu_b/\mu_w)^{0.14}$$

where  $7,000 < Re < 12,400$

$$3.5 < Pr < 7.4$$

$$45,570 < Gr < 1,040,000$$

### Lower Transition

For Reynolds numbers between 2,100 and 4,600, no satisfactory correlation was derived. Linear interpolation is recommended:

$$y = (Re - 2100) / (4600 - 2100)$$

$$Nu = [ (1-y) \cdot Nu_{Laminar} + y \cdot Nu_{Upper Transition} ]$$

## ACKNOWLEDGMENT

I am deeply indebted to my advisor Professor Kenneth J. Bell for his valuable guidance, precious time and tremendous patience.

I am grateful to my committee members: Drs. G. L. Foutch, C. Gentry, A. Ghajar, and J. Wagner for their concern and help.

I am thankful to: Dr. J. Chandler of the Department of Computer Science and Information, Drs. H. O. Spivey and J. Merz of the Biochemistry Department, Dr. E. J. Eisenbraun of the Chemistry Department, Mr. C. Baker, Mr. E. Elizondo, and Mr. M. Abu-Arabi for their valuable help in many ways.

Special thanks are due to the Pybus', Emmett, Florence, Nani, Sean, and Brooks, for their hospitality and friendship.

My wife Peggy deserves my deepest appreciation for her love, charming, understanding and fulfilling my life. Also, I am very grateful to my parents and parents-in-law. Special appreciations are to my little ones, Patrick and Tiffany.



## TABLE OF CONTENTS

Chapter		Page
	NOMENCLATURE . . . . .	xv
I.	INTRODUCTION . . . . .	1
II.	LITERATURE SURVEY . . . . .	8
III.	EXPERIMENTAL APPARATUS . . . . .	19
	Description of the Equipment . . . . .	19
	Test Section . . . . .	19
	Entrance Chamber . . . . .	22
	Thermocouples . . . . .	23
	Digital Thermocouple Indicator . . . . .	25
	DC Power Source . . . . .	26
	Voltmeter . . . . .	26
	DC Ammeter . . . . .	26
	Heat Exchanger . . . . .	27
	Fluid Bath . . . . .	27
	Pumps . . . . .	27
	Rotameters . . . . .	27
	Test Fluids . . . . .	28
	Calibration Equipment . . . . .	28
IV.	EXPERIMENTAL PROCEDURES . . . . .	29
	Calibration Procedures . . . . .	29
	Start-up and Operating Procedures . . . . .	29
	Some of the Problems Encountered . . . . .	31
V.	DATA REDUCTION . . . . .	33
	Calculation of Overall Heat Balance . . . . .	34
	Calculation of the Local Inside Wall Temperature and Local Inside Wall Heat Flux . . . . .	35
	Calculation of the Local Heat Transfer Coefficient . . . . .	35
VI.	RESULTS AND DISCUSSIONS . . . . .	37
	Effect of Various Parameters on the Average Local Heat Transfer Coefficient . . . . .	38

Chapter	Page
Entrance Effect . . . . .	38
Lower Turbulent Flow . . . . .	40
Transition Flow Regime . . . . .	45
High Laminar Flow Regime . . . . .	51
Comparison with Literature . . . . .	54
Colburn Correlation . . . . .	54
Sieder and Tate Correlation . . . . .	54
Hausen Correlation . . . . .	57
Eubank and Proctor Correlation . . . . .	60
Siegwarth Correlation . . . . .	60
Hong, Morcos and Bergles Correlation . . . . .	67
Morcos and Bergles Correlation . . . . .	67
Sieder and Tate Correlation . . . . .	72
Morcos and Bergles Correlation . . . . .	72
VII. DERIVATION OF THE CORRELATION EQUATION . . . . .	78
Laminar Flow . . . . .	79
Lower Turbulent Flow . . . . .	81
Upper Transition Flow . . . . .	84
Lower Transition Flow . . . . .	87
VIII. CONCLUSIONS AND RECOMMENDATIONS . . . . .	92
Conclusions . . . . .	92
Recommendations . . . . .	93
BIBLIOGRAPHY . . . . .	95
APPENDIX A: CALIBRATION OF THE STREAM THERMOCOUPLES . . . . .	100
Calibration Equipment . . . . .	100
Calibration Procedures . . . . .	100
APPENDIX B: CALIBRATION OF THE SURFACE THERMOCOUPLES . . . . .	102
Calibration Procedures . . . . .	102
APPENDIX C: FLOW RATE CALIBRATION . . . . .	103
Calibration Equipment . . . . .	103
Calibration Procedures . . . . .	103
APPENDIX D: EVALUATION OF THE COMPOSITION OF DIETHYLENE GLYCOL . . . . .	105
Apparatus . . . . .	105
Procedures . . . . .	105
Kinematic Viscosity Method . . . . .	105
Density Method . . . . .	106

Chapter	Page
APPENDIX E: PHYSICAL PROPERTIES . . . . .	108
Water . . . . .	108
Density . . . . .	108
Viscosity . . . . .	109
Specific Heat . . . . .	109
Thermal Conductivity . . . . .	109
Coefficient of Thermal Expansion . . . . .	110
Diethylene Glycol . . . . .	111
Density . . . . .	111
Viscosity . . . . .	111
Thermal Conductivity . . . . .	112
Specific Heat . . . . .	113
Coefficient of Thermal Expansion . . . . .	113
Stainless Steel . . . . .	114
Thermal Conductivity . . . . .	114
Electrical Resistivity . . . . .	114
APPENDIX F: NUMERICAL SOLUTION OF THE WALL TEMPERATURE GRADIENT . . . . .	115
APPENDIX G: ERROR ANALYSIS . . . . .	119
Error Analysis . . . . .	119
Correction of Outside Wall Temperature . . . . .	122
APPENDIX H: EXPERIMENTAL DATA AND CALCULATED RESULTS . . . . .	128
APPENDIX I: COMPUTER LISTING OF THE MAIN PROGRAM . . . . .	141
APPENDIX J: SAMPLE CALCULATION . . . . .	155
Calculation of the Heat Balance . . . . .	156
Rate of Heat Input . . . . .	156
Rate of Heat Output . . . . .	158
Heat Balance . . . . .	159
Calculation of the Local Inside Wall Temperature and the Local Inside Wall Heat Flux . . . . .	159
Calculation of the Local Heat Transfer Coefficient . . . . .	159
APPENDIX K: EXAMPLE PROBLEM . . . . .	161
Laminar Flow . . . . .	161
$X/d_i = 300$ . . . . .	162
$X/d_i = 20$ . . . . .	164
Lower Turbulent Flow . . . . .	165
Transition Flow . . . . .	167

Chapter	Page
APPENDIX L: BEHAVIOR OF THE DEVELOPED CORRELATION . . .	168

## LIST OF TABLES

Table	Page
I. Constants for Equation (II.1) . . . . .	9
II. Range of Properties Measured and Their Accuracy . . . . .	120
III. Percentage Standard Deviations . . . . .	123
IV. Summary of Experimental Data and Calculated Results . . . . .	130

## LIST OF FIGURES

Figure	Page
1. Secondary Flow Pattern . . . . .	3
2. Secondary Flow: Streamlines ,Isothermals and Directions . . . . .	3
3. Regimes for Free, Forced and Mixed Convection for Horizontal Tubes . . . . .	5
4. Local Average Heat Transfer Data of Petukhov and Polyakov . . . . .	11
5. Correlation of Combined Convection of Shannon and Depew . . . . .	15
6. Prediction Plot for Laminar Flow of Water of Bergles and Simonds . . . . .	18
7. Experimental Apparatus . . . . .	20
8. Entrance Configuration of the Test Section . . . . .	21
9. Thermocouple Layout . . . . .	24
10. Local Average Heat Transfer Coefficient $h$ vs $X/d_i$ . . . . .	39
11. $N$ vs $Re$ for All Data Points . . . . .	41
12. $N$ vs $Re$ for Stations 4 to 12 for All Data Points .	42
13. $N$ vs $Re$ for $Re > 7000$ for Stations 4 to 12 . . . . .	44
14. $N$ vs $Re$ for $4600 < Re < 7000$ for Stations 4 to 12	46
15. Temperature Readings for Run 1101 at Station 6 with Local Reynolds Number of 4070 . . . . .	47
16. Temperature Fluctuations for Thermocouple 4-4 Run 1109 with Local Bulk $Re = 7000$ . . . . .	49

Figure	Page
17. Local Surface Temperature for Run 2137 with Local Bulk Reynolds Number from 1796 to 2284 .	53
18. Comparison between the Experimental Heat Transfer Coefficients and the Heat Transfer Coefficients Predicted by Colburn as a Function of Reynolds Number for $121 < Re < 2300$ . . . . .	55
19. Comparison between the Experimental Nusselt Number and the Nusselt Number Predicted by Colburn . .	56
20. Comparison between the Experimental Nusselt Number and the Nusselt Number Predicted by Sieder and Tate as a Function of Reynolds Number for $121 < Re < 2300$ . . . . .	58
21. Comparison between the Experimental Nusselt Number and the Nusselt Number Predicted by Sieder and Tate . . . . .	59
22. Comparison between the Experimental Heat Transfer Coefficients and the Heat Transfer Coefficients Predicted by Hausen as a Function of Reynolds Number for $121 < Re < 2300$ . . . . .	61
23. Comparison between the Experimental Nusselt Number and the Nusselt Number Predicted by Hausen . .	62
24. Comparison between the Experimental Nusselt Number and the Nusselt Number Predicted by Eubank and Proctor as a Function of Reynolds Number for $121 < Re < 2300$ . . . . .	63
25. Comparison between the Experimental Nusselt Number and the Nusselt Number Predicted by Eubank and Proctor . . . . .	64
26. Comparison between the Experimental Heat Transfer Coefficients and the Heat Transfer Coefficients Predicted by Siegwarth as a Function of Reynolds Number for $121 < Re < 2300$ . . . . .	65
27. Comparison between the Experimental Nusselt Number and the Nusselt Number Predicted by Siegwarth .	66
28. Comparison between the Experimental Nusselt Number and the Nusselt Number Predicted by Hong, Morcos and Bergles as a Function of Reynolds Number for $121 < Re < 2300$ . . . . .	68

Figure	Page
29. Comparison between the Experimental Nusselt Number and the Nusselt Number Predicted by Hong, Morcos and Bergles . . . . .	69
30. Comparison between the Experimental Nusselt Number and the Nusselt Number Predicted by Morcos and Bergles as a Function of Reynolds Number for $121 < Re < 2300$ . . . . .	70
31. Comparison between the Experimental Nusselt Number and the Nusselt Number Predicted by Morcos and Bergles . . . . .	71
32. Comparison between the Experimental Nusselt Number and the Nusselt Number Predicted by Sieder and Tate as a Function of Reynolds Number for $4,600 < Re < 12,400$ . . . . .	73
33. Comparison between the Experimental Nusselt Number and the Nusselt Number Predicted by Sieder and Tate . . . . .	74
34. Comparison between the Experimental Nusselt Number and the Nusselt Number Predicted by Petukhov and Popov as a Function of Reynolds Number for $4,600 < Re < 12,400$ . . . . .	75
35. Comparison between the Experimental Nusselt Number and the Nusselt Number Predicted by Petukhov and Popov . . . . .	76
36. Comparison between the Experimental Nusselt Number and the Nusselt Number Predicted by Equation (VII.1) as a Function of Reynolds Number for $270 < Re < 2800$ . . . . .	82
37. Comparison between the Experimental Nusselt Number and the Nusselt Number Predicted by Equation (VII.1) . . . . .	83
38. Comparison between the Experimental Nusselt Number and the Nusselt Number Predicted by Equation (VII.2) as a Function of Reynolds Number for $7000 < Re < 12400$ . . . . .	85
39. Comparison between the Experimental Nusselt Number and the Nusselt Number Predicted by Equation (VII.2) . . . . .	86



Figure	Page
40. Comparison between the Experimental Nusselt Number and the Nusselt Number Predicted by Equation (VII.3) as a Function of Reynolds Number for $4000 < Re < 7000$ . . . . .	88
41. Comparison between the Experimental Nusselt Number and the Nusselt Number Predicted by Equation (VII.3) . . . . .	89
42. Comparison between the Experimental Nusselt Number and the Nusselt Number Predicted by Equations (VII.4) and (VII.5) as a Function of Reynolds Number for $1900 < Re < 5500$ . . . . .	90
43. Comparison between the Experimental Nusselt Number and the Nusselt Number Predicted by Equations (VII.4) and (VII.5) . . . . .	91
44. Interior Nodes . . . . .	116
45. Correction of Outside Wall Temperature . . . . .	124
46. $Nu$ and $\underline{Nu}$ vs $X/d_i$ and $L/d_i$ at $Re = 2,000$ . . . . .	170
47. $Nu$ and $\underline{Nu}$ vs $X/d_i$ and $L/d_i$ at $Re = 1,000$ . . . . .	171
48. $Nu$ and $\underline{Nu}$ vs $X/d_i$ and $L/d_i$ at $Re = 500$ . . . . .	172
49. $Nu$ and $\underline{Nu}$ vs $X/d_i$ and $L/d_i$ at $Re = 10,000$ . . . . .	173
50. $Nu$ and $\underline{Nu}$ vs $X/d_i$ and $L/d_i$ at $Re = 5,500$ . . . . .	174

## NOMENCLATURE

A	= area, $\text{ft}^2$ or $\text{m}^2$
$C_p$	= specific heat of the liquid at the bulk temperature, $\text{Btu}/(\text{lb}_m \cdot ^\circ\text{F})$ or $\text{J}/(\text{kg} \cdot \text{K})$
$d_i$	= inside tube diameter, ft or m
F	= unit conversion factor, $3.412 \text{ Btu}/(\text{hr} \cdot \text{W})$
g	= gravitational acceleration, $\text{ft}/\text{hr}^2$ or $\text{m}/\text{hr}^2$
h	= heat transfer coefficient, $\text{Btu}/(\text{hr} \cdot \text{ft}^2 \cdot ^\circ\text{F})$ or $\text{W}/(\text{m}^2 \cdot \text{K})$
I	= current in the test section, amperes
$I_p$	= number of thermocouples at a station
k	= thermal conductivity, $\text{Btu}/(\text{hr} \cdot \text{ft} \cdot ^\circ\text{F})$ or $\text{W}/(\text{m} \cdot \text{K})$
K	= capillary constant for viscometer
L	= length of the test section, ft or m
$\dot{m}$	= mass flow rate of the liquid flowing through the test section, $\text{lb}_m/\text{hr}$ or $\text{kg}/\text{s}$
N	= $\text{Nu}/[\text{Pr}^{1/3}(\mu_b/\mu_w)^{0.14}]$
P	= pressure, $\text{lb}_f/\text{in}^2$ , or $\text{N}/\text{m}^2$
$Q_{\text{input}}$	= rate of heat input to the test section, $\text{Btu}/\text{hr}$ or W
$Q_{\text{loss}}$	= rate of heat loss from the test section, $\text{Btu}/\text{hr}$ or W
$Q_{\text{output}}$	= heat gained by the test fluid, $\text{Btu}/\text{hr}$ or W
q	= heat flux, $\text{Btu}/(\text{hr} \cdot \text{ft}^2)$ or $\text{W}/\text{m}^2$

$r$	= distance from the centerline to the position, ft or m
$r_i$	= tube inside radius, ft or m
$S$	= standard deviation
$T$	= temperature, °F or °C
$T_i$	= bulk liquid temperature at the inlet of the test section, °F or °C
$T_o$	= bulk liquid temperature at the exit of the test section, °F or °C
$t$	= tube wall thickness, ft or m
$u$	= flow velocity in the test section, ft/hr or m/s
$V$	= voltage drop across the test section, volts
$X$	= distance along the test section from the the beginning of heating, ft or m
$x$	= diethylene glycol(DEG) mass fraction in DEG-water solution
$y$	= independent variable in error analysis
$z$	= distance from the entrance of the test section to the desired position, ft or m

### Dimensionless Parameters

$Gr$	= Grashof number, $g\beta\rho^2d_i^3(T_{wi}-T_b)/\mu^2$
$Gz$	= Graetz number, $PrRe(d_i/X)$
$Nu$	= local average peripheral Nusselt number, $hd_i/k$
$Nu_{Gz}$	= theoretical Nusselt number for constant properties with parabolic velocity profile from equation (II.1)
$Pr$	= local bulk Prandtl number, $C_p\mu/k$
$Pw$	= tube wall parameter, $(hd_i/k)/(d_i/t)$

Ra = Rayleigh number,  $PrGr$   
 Re = local bulk Reynolds number,  $\rho u d_i / \mu$

### Greek Letters

$\beta$  = coefficient of volume expansion,  $1/F$  or  $1/C$   
 $\theta$  = correction time for viscometer, sec,  
 or dimensionless temperature difference,  
 $4(T-T_w)\nu\mu/[r_i Pr(\partial P/\partial X)(\partial T/\partial X)]$  used in  
 Figure 2  
 $\mu$  = fluid viscosity,  $lb_m/(hr \cdot ft)$  or  $Ns/m^2$   
 $\rho$  = fluid density,  $lb_m/ft^3$  or  $kg/m^3$   
 $\nu$  = kinematic viscosity,  $m^2/sec.$   
 $\phi$  = polar angle  
 $\psi$  = dimensionless stream function  
 $\delta$  = electrical resistivity, ohm-in. or ohm-m

### Subscripts

b = for the bulk of the fluid  
 f = at the average fluid film temperature where  
 $T = (T_{wi} + T_b)/2$   
 i = peripheral position (either 1 to 4 or 1 to 8)  
 j = station number (1 to 12)  
 j, i = local peripheral position  
 w = property of tube wall  
 $w_i$  = property at the inside tube surface  
 $w_o$  = property at the outside surface of the tube

## CHAPTER I

### INTRODUCTION

Shell and tube heat exchangers are the most extensively used heat transfer equipment in the petrochemical and chemical process industries. On the tube side of the shell and tube exchanger, the fluid flows through a nozzle into the entrance fluid chamber and usually must turn toward the tube sheet. The fluid must accelerate when it flows into the tubes. Ideally, the entrance shape of the tubes is square-edged, but actual entrances may be reentrant (when the tubes are roller-expanded into the tube sheet) or rounded (typical of welded tubes).

Inside the circular tube, the fluid is subjected to an abrupt contraction at the entrance which may cause turbulence in the fluid. There are developing velocity and temperature profiles at the entrance of the test section, which are further altered by the contraction. Ideally, both profiles are flat at the entrance. Both velocity and temperature profiles start to develop along the tube simultaneously toward the fully-developed profiles. Usually, the velocity profile develops faster than the temperature profile for liquids ( $Pr > 1$ ). Roy (40)

considered three types of development of the profiles: simultaneous development of the velocity and temperature profiles, fully developed velocity and developing temperature profiles, and both profiles fully developed.

Due to the complexity of the entrance flow and the interactions between momentum and energy transfer, these considerations, i.e., entrance effects on heat transfer, are usually ignored in heat transfer calculations and only fully developed momentum and energy transfer are considered. However, the factors that are ignored may influence considerably the performance of heat exchangers, especially those having relatively short tubes.

Once heating starts in the tube, the flow may change from the laminar flow regime to transition flow regime along the tube due to the change in physical properties caused by the change of temperature. The flow in the direction of the tube axis is referred to as primary.

Application of heat to the tube wall produces a temperature difference in the fluid. The fluid near the tube wall has a higher temperature and lower density than the fluid close to the centerline of the tube. For the cooling case, the fluid near the tube wall has a lower temperature and higher density than the fluid close to the centerline of the tube. This temperature difference may produce a secondary flow due to natural convection as shown in Figure 1. In Figure 1, the secondary flow forms a pair of vortices which are symmetrical in the vertical plane.



Figure 1: Secondary Flow Pattern,(25) a)  $ReRa = 20,000$   
b)  $ReRa = 90,000$  and c)  $ReRa = 160,000$

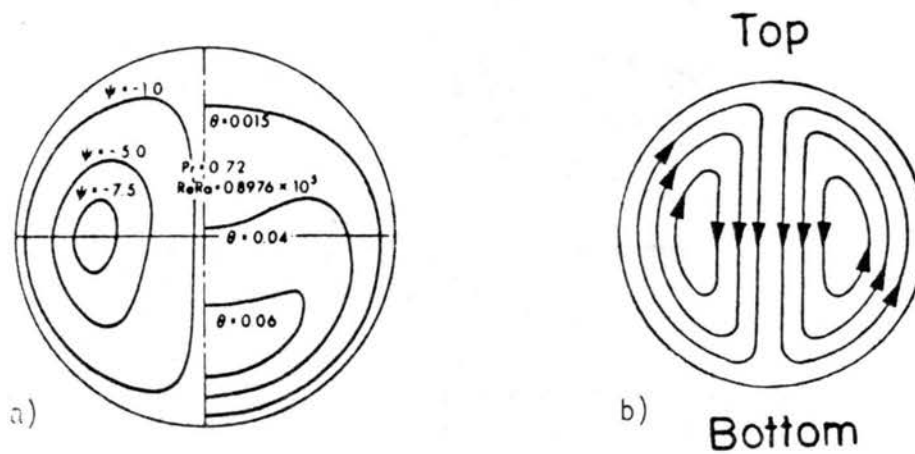


Figure 2: Secondary Flow a) Streamlines and Isotherms(15)  
b) Directions(1)  $\Psi$  is the Dimensionless Stream Function.  $\theta$  is Dimensionless Temperature.

The fluid near the tube wall rises toward the top of the tube along the tube wall, and then flows vertically from the top of the tube toward the bottom of the tube. Therefore, viewed in the direction of the fluid flow, the secondary flow on the right side of the tube is counterclockwise while that on the left hand side is clockwise. This secondary flow affects the flow pattern as well as the temperature profile. Figure 2 gives the streamlines and isotherms, showing the effect of the secondary flow.

The boundary between natural, mixed and forced convection can be determined from the local heat transfer data. The ratio of the heat transfer coefficient at the top of the tube ( $h_{top}$ ) to the heat transfer coefficient at the bottom of the tube ( $h_{bottom}$ ) should be close to 1.0 for forced convection and is much less than 1.0 for a case in which natural convection dominates. Forced convection heat transfer is primarily dependent on the Reynolds number and the Prandtl number. Natural convection primarily depends upon the Grashof number (which accounts for the variation in density of the test liquid) and the Prandtl number. Figure 3 shows the regimes for free, mixed, and forced convection for a horizontal tube (22).

In this thesis, the entrance effects and the development of natural and forced convection flow patterns and heat transfer rates were investigated in the high laminar, transition and early turbulent flow regimes for a



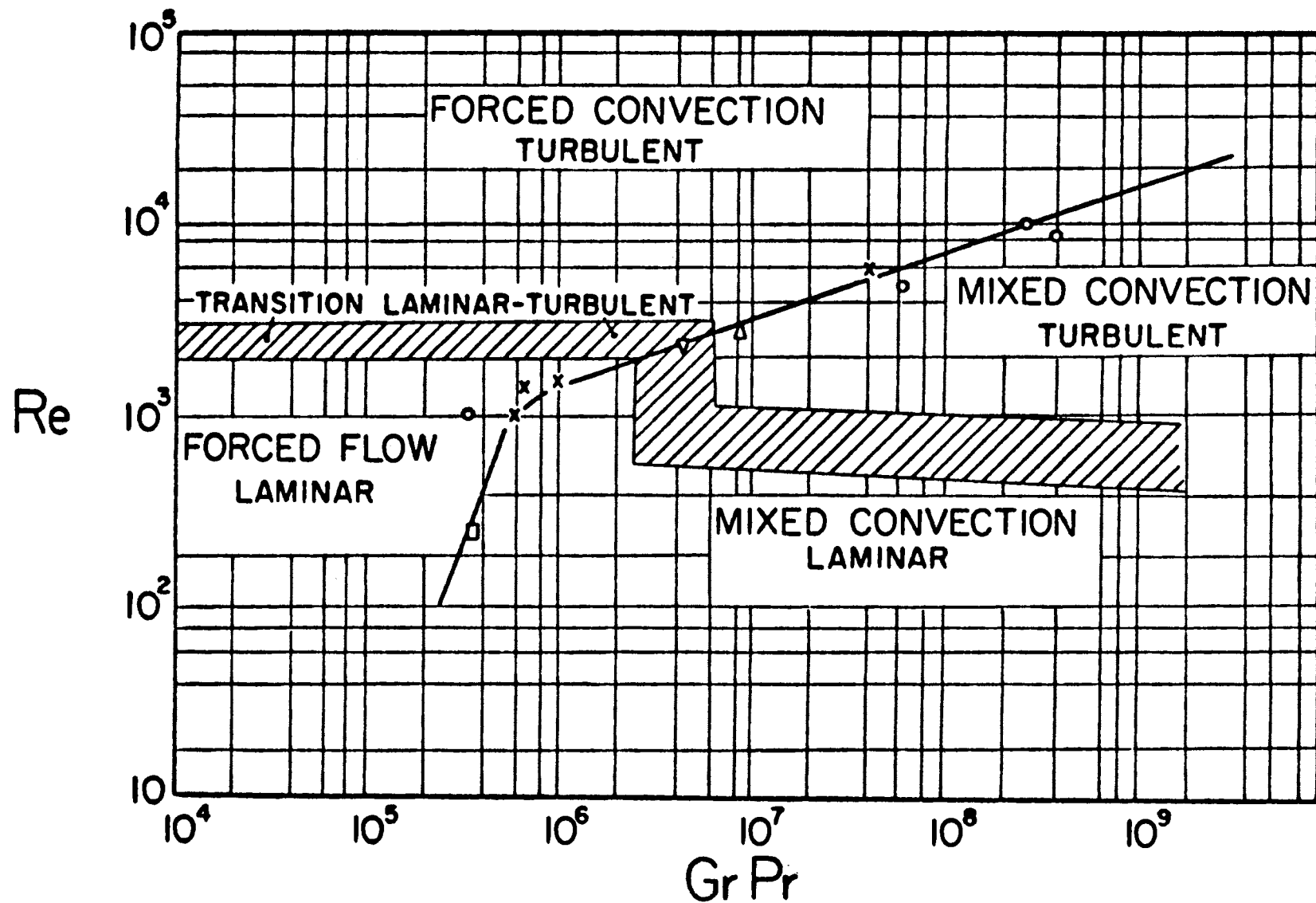


Figure 3: Regimes for Free, Forced and Mixed Convection for horizontal Tubes(22).  $10^{-2} < Pr_i/L < 1$

circular horizontal electrically-heated straight tube with a square-edged entrance. Peripheral conduction of heat in the tube wall was included in the calculations. The test fluids were distilled water and diethylene glycol (DEG)-distilled water solutions.

Local outside wall temperatures were measured and the local peripheral heat transfer coefficients were calculated at twelve stations along the axis of the tube. The experiments included 48 runs. Distilled water was used as the test fluid in 10 runs, over a local bulk Reynolds number range of 2,470 to 12,400, a local bulk Prandtl number range of 3.5 to 7.9 and a Grashof number range of 45,570 to 1,040,000. DEG-distilled water solutions were used as test fluid for 38 runs, over a DEG concentration range of 28.3 to 99.9 mass percent, a local bulk Reynolds number range of 121 to 4,372, and a local bulk Prandtl number range of 16.4 to 282.4; the local Grashof number varied from 930 to 67,300.

These experiments permit a better understanding of the effect of an abrupt contraction at the entrance and the development of natural and forced convection profiles in the tube. Some runs also showed flow regime transitions (e.g. from laminar to transition, or transition to turbulent) along the tube during the heating process. Correlations which predict the local peripheral average heat transfer coefficient in a circular tube downstream from a square-edged entrance are introduced for the various

flow regimes.

## CHAPTER II

### LITERATURE SURVEY

Numerous analytical and numerical solutions have been proposed for combined forced and free convection in horizontal tubes. The usual boundary conditions are: uniform and specified wall heat flux with fully developed flow, constant surface temperature with fully-developed flow, and uniform heat flux with simultaneously developing temperature and velocity profiles. These solutions have been thoroughly reviewed by Shah and London (42) and Kakac, Shah and Bergles (16).

Analytical solutions for the heat transfer in laminar flow without free convection (i.e., with constant physical properties) have been studied by many researchers. The solution proposed by Siegel, Sparrow and Hallman (46) has been widely accepted and has been used as a standard solution without free convection in many articles (3, 13, 14, 32, 43, 44). They derived the following equation analytically for the local average Nusselt number with a fully developed laminar velocity profile for constant heat flux:

$$Nu = \frac{2}{\frac{11}{48} + \sum_{n=1}^{\infty} C_n R_n e^{-\left(\frac{\beta_n}{Re Pr} \frac{x}{T_o}\right)}} \quad (II.1)$$

where  $\beta_n$ ,  $R_n$ , and  $C_n$  are given in the Table I. But as we can see in Figure 4 (constant property analysis with parabolic velocity profile), the pure forced convection prediction gives lower values of heat transfer coefficients than experimental values (with varying physical properties) by Petukhov and Polyakov (32). The higher the heat flux, the higher the deviation from the pure forced convection prediction. And the higher the heat flux, the higher the density variation and the Rayleigh number will be.

Experimental data are abundant for various fluids on combined forced and free convection in the laminar flow regime (1, 3, 7, 13, 14, 21, 22, 24-28, 32-34, 38, 43-45, 47). These results are generally inconsistent with one another. And there is a scarcity of literature on the transition and early turbulent flow regimes.

Ede (7, 8) applied uniform heat flux to study the effects of free convection on fluid flow. The test fluids were water and air at Reynolds numbers from 300 to 100,000. Electrically-heated aluminum-brass pipes, with inside diameters ranging from 0.5 to 2 in. (12.7 to 50.8 mm) and wall thicknesses up to 0.279 in. (7.1 mm), were used. The inlet geometries included an abrupt convergence and an abrupt divergence with diameter ratios 2/1 and 1/2 respectively. At each station (at a given axial distance

Table I  
CONSTANTS FOR EQUATION (II.1)

n	$\beta_n$	$R_n$	$C_n$
1	25.6796	-0.492517	0.403483
2	83.8618	0.395508	-0.175111
3	174.1670	-0.345872	0.105594
4	296.5360	0.314047	-0.073280
5	450.9470	-0.291252	0.055036
6	637.3870	0.259852	-0.043483
7	855.8500	-0.259852	0.035597

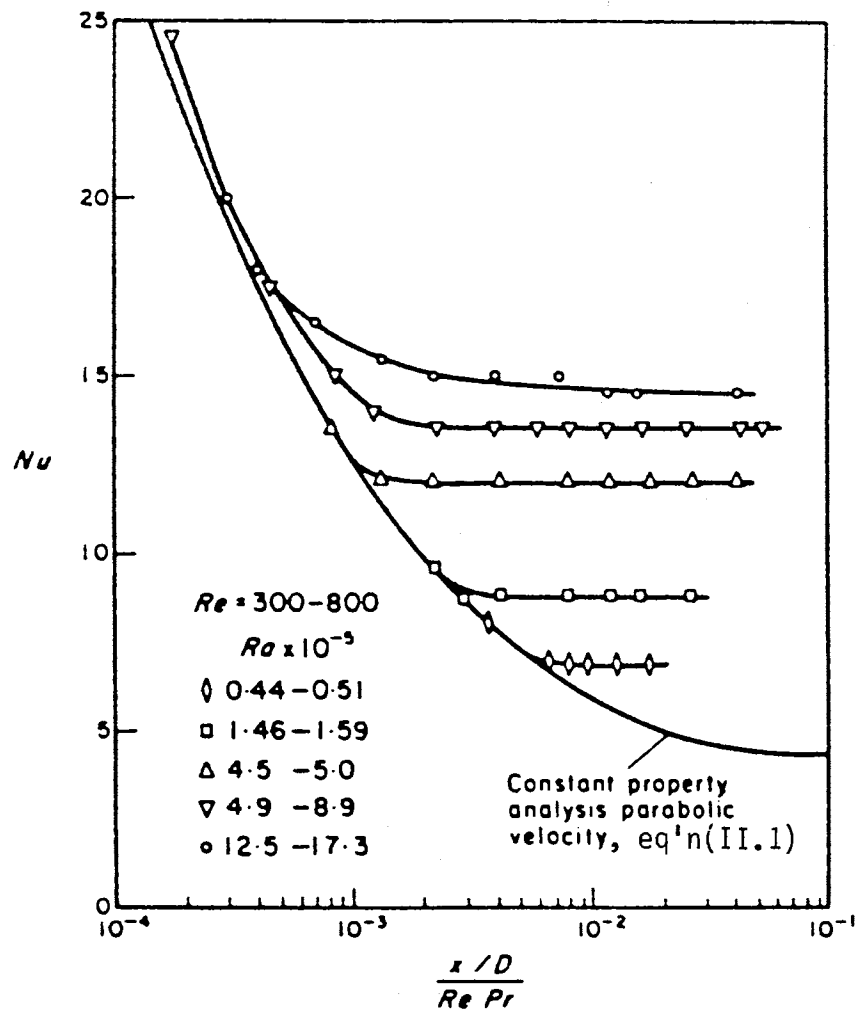


Figure 4: Local Average Heat Transfer Data of Petukhov and Polyakov(32)

from the inlet), five thermocouples were uniformly spaced around the periphery. Ede found that there was no consistent variation in Nusselt number with Grashof number less than 100,000 in the laminar flow regime ( $Re < 2,300$ ). He presented the following correlation (without a Reynolds number in it) for local average Nusselt number for laminar flow for  $Re < 2,300$ :

$$Nu = 4.36(1+0.06Gr^3) \quad (II.2)$$

No transition or turbulent flow correlations were presented.

McComas and Eckert (21) investigated experimentally the effect of free convection on laminar flow heat transfer in a uniformly heated horizontal tube. Air was used as the test fluid. The Reynolds numbers varied from 100 to 900 and the Grashof number ranged from 0.33 to 1,000. They compared high Grashof number runs to runs at the same Reynolds number but with negligible free convection (very low Grashof number) and found that buoyancy created a secondary flow, which increased as the ratio of Grashof number to Reynolds number increased.

Mori et al. (26) experimentally studied the effect of buoyancy on forced convection heat transfer in uniformly heated (constant heat flux) horizontal tubes. The Reynolds number ranged from 100 to 13,000. They passed air through a brass tube with 1.4-in. (35.6 mm) inside diameter. The tube



was heated by means of 0.02-in. (0.5 mm) nichrome wires wound around the tube at constant pitch to give approximately a constant heat flux. A single wall temperature point was measured at each station. A correlation equation was obtained for laminar flow:

$$Nu = 0.6 (Re Ra)^{1/5} \left\{ 1 + \frac{1.8}{(Re Ra)^{1/5}} \right\} \quad (II.3)$$

Petukhov et al. (32-35) performed an investigation of local heat transfer with distilled water flowing in a tube heated by an alternating current directly through the wall. The stainless steel tube had an inside diameter of 0.743-in. (18.84 mm) and 0.014-in. (0.366 mm) wall thickness. The length of the heated section was 99 inside diameters while the length of upstream calming section was 96 inside diameters. Temperatures at various axial and peripheral locations were measured. A plot of average local Nusselt numbers versus  $(X/d_i)/(RePr)$  showed the combined free and forced convection effect on heat transfer as shown in Figure 4. Their correlation for the asymptotic Nusselt number in fully developed free convection for Reynolds number from 300 to 800 and Rayleigh number from 44,000 to 1,730,000 is:

$$Nu = 4.36 \left\{ 1 + \left( \frac{GrPr}{1.8 \times 10^4} \right)^{0.045} \right\} \quad (II.4)$$

Shannon and Depew (43, 44) studied free convection

effects in an electrically-heated (DC, wall resistance) stainless steel tube with 0.305-in. (7.75 mm) i.d., 0.035-in. (0.89 mm) wall, 20-ft. (6.1 m) heated length, and 40-in. (1.02 m) long calming section. Average peripheral temperatures at 10 stations along the tube wall were measured (one thermocouple at each station) by thermocouples soldered to a copper strap around the tube periphery which was insulated from the tube wall by a thin layer of tape. For water (Prandtl number around 10, at a temperature close to 0 °C), the Reynolds numbers ranged from 120 to 2,300 (43), Grashof numbers ranged up to 250,000 and Graetz numbers varied from 1.5 to 1,000. For ethylene glycol with inlet temperature at 32°F, the Reynolds numbers varied from 6 to 300, Grashof numbers went up to 2,800 and Prandtl numbers varied from 26 to 500, while the Graetz numbers ranged from 3 to 4,800 (44). Shannon and Depew's results showed the presence of natural convection. Their data were correlated by the parameter  $(GrPr)^{1/4}/Nu_{Gz}$  as shown in Figure 5.  $Nu_{Gz}$  is the theoretical local Nusselt number for constant properties and constant heat flux from Siegel, Sparrow and Hallman (46), which is Equation (II.1).

Hussain and McComas (14) studied the effect of free convection for Reynolds numbers between 670 and 3,800 and Grashof numbers between 10,000 and 1,000,000 for air flowing in a 1-in. (25.4 mm) i.d., 118-in. (3 m) long uniformly heated horizontal circular tube. They found that, at Reynolds numbers below 1,200 and far from the entrance,

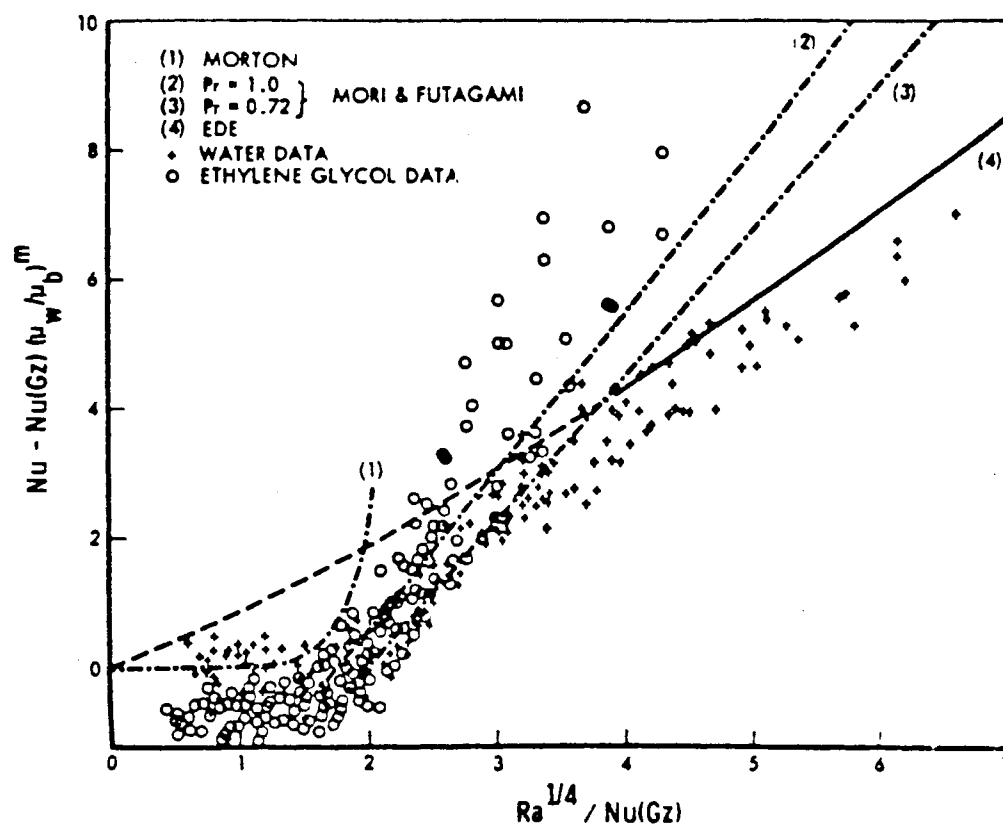


Figure 5: Data for Combined Convection of Shannon and Depew(43)

the heat transfer was below the pure forced flow prediction with constant physical properties, Equation (II.1). For large Reynolds numbers, the results were higher than the pure forced flow predictions. They also observed significant peripheral wall temperature variations, as much as 13°F (7°C) for a wall to bulk temperature difference of 50.4°F (28°C) for the upper range of Grashof numbers investigated.

Siegwarth et al. (47) analyzed the effect of the secondary flow on the temperature field and the primary flow at the outlet of a long, electrically-heated tube. Constant heat flux was assumed. They developed a model for the flow field by dimensional reasoning and found that the secondary flow controls the rate of heat transfer. Their model showed good agreement with the data measured by Readal (38). For constant viscosity and very large Prandtl number, the equation is:

$$Nu = 0.471(GrPr)^{1/4} \quad (II.5)$$

Bergles and Simonds (3) studied visually and experimentally the effects of free convection on laminar flow of water in horizontal circular tubes with constant heat flux. The tubes were Pyrex E-C Coated Tube with length of 30-in. (0.76 m) and i.d. of 0.433-in. (11 mm). Four thermocouples were placed circumferentially 90° apart at the same axial position. Heat was generated in the tube

coating to provide constant heat flux and nearly zero heat conduction around the tube circumference. Bergles and Simonds developed a correlation plot similar to Petukhov's, shown as Figure 6.

Morcos and Bergles (24) considered the effects of fluid property variations on laminar flow heat transfer for fully-developed velocity profile in electrically-heated horizontal tubes (glass and stainless steel tubes). They obtained the following correlation equation:

$$Nu_f = \left\{ (4.36)^2 + \left[ 0.055 \left( \frac{Gr_f Pr_f^{1.35}}{Pw^{0.25}} \right)^{0.4} \right]^2 \right\}^{1/2} \quad (II.6)$$

where  $Pw = (hd_i/k_w)(d_i/t)$  and  $h$  = local circumferential average heat transfer coefficient. The ranges of parameters tested were

$$4 \leq Pr \leq 175$$

$$30,000 \leq Ra \leq 1,000,000$$

$$2 \leq Pw \leq 66$$

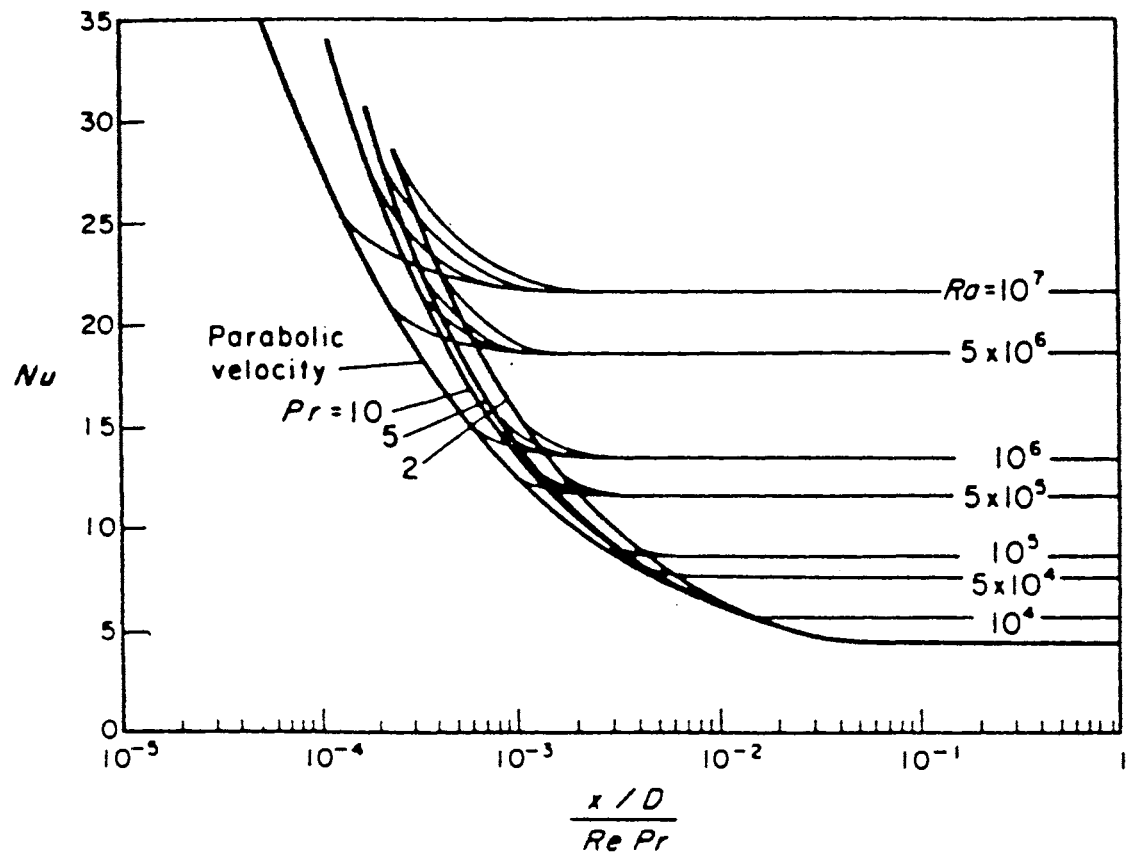


Figure 6: Prediction Plot for Laminar Flow of Water of Bergles and Simonds(3)

## CHAPTER III

### EXPERIMENTAL APPARATUS

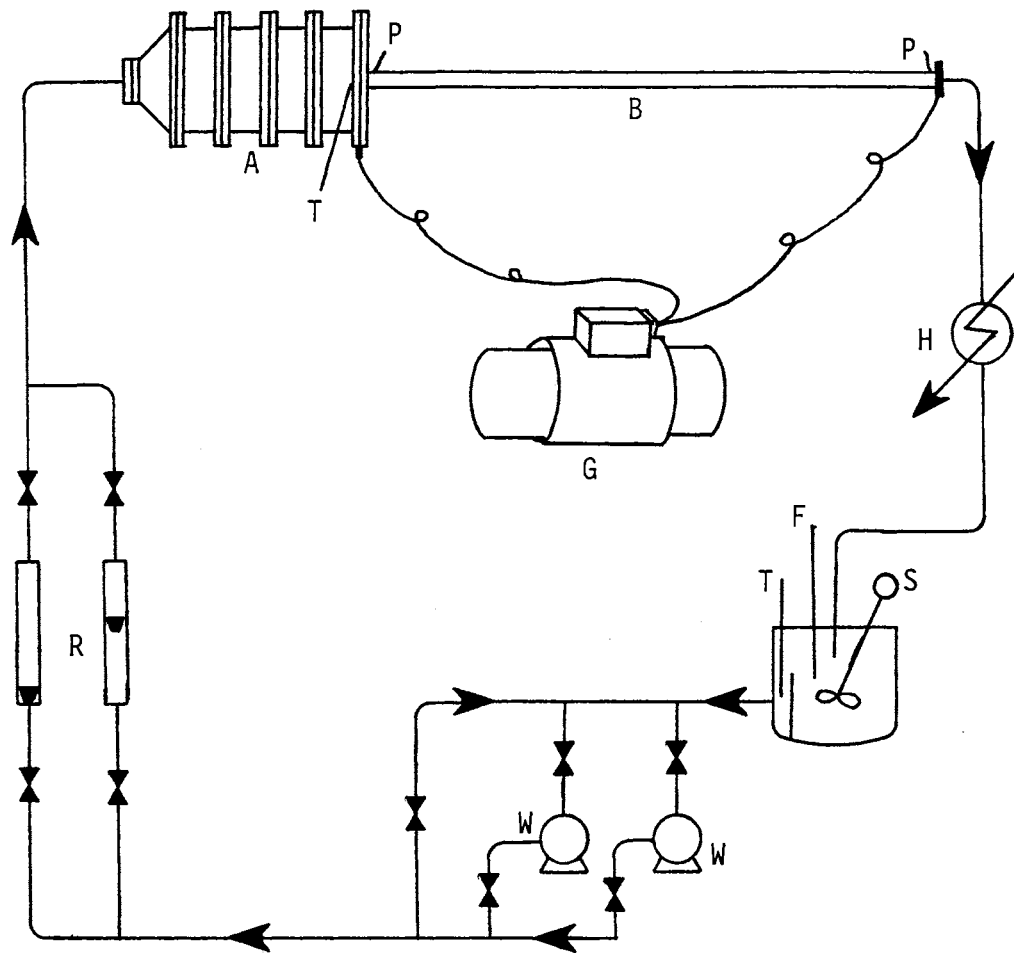
Heat transfer in high laminar, transition and early turbulent flow regimes was studied in a horizontal circular tube with a square-edged entrance. The experimental setup is shown in Figure 7. The entrance configuration of the test section is shown in Figure 8. Distilled water, almost pure diethylene glycol (DEG) and various DEG concentrations in DEG-distilled water solutions were used as test fluids. The experimental set-up and equipment are basically similar to those used by Moshfeghian (28) and Abdelmessih (1).

#### Description of the Equipment

##### Test Section

The test section was a seamless 316 stainless steel circular tube with an average inside diameter  $0.6327 \pm 0.0006$  inch ( $16.070 \pm 0.015$  mm) and outside diameter  $0.7520 \pm 0.0005$  inch ( $19.100 \pm 0.013$  mm). The tube was purchased from Precision Fitting and Tubing Company. The total length of the test section was 155.5 inches (3.95 m).

The test section was wrapped by woven fiberglass tape, followed by bonded fiberglass tape and pipe insulation, and



A: Entrance Chamber

B: Test Section

F: Heating Coil

G: Generator

H: Heat Exchanger

P: Pressure Gauge

R: Rotameter

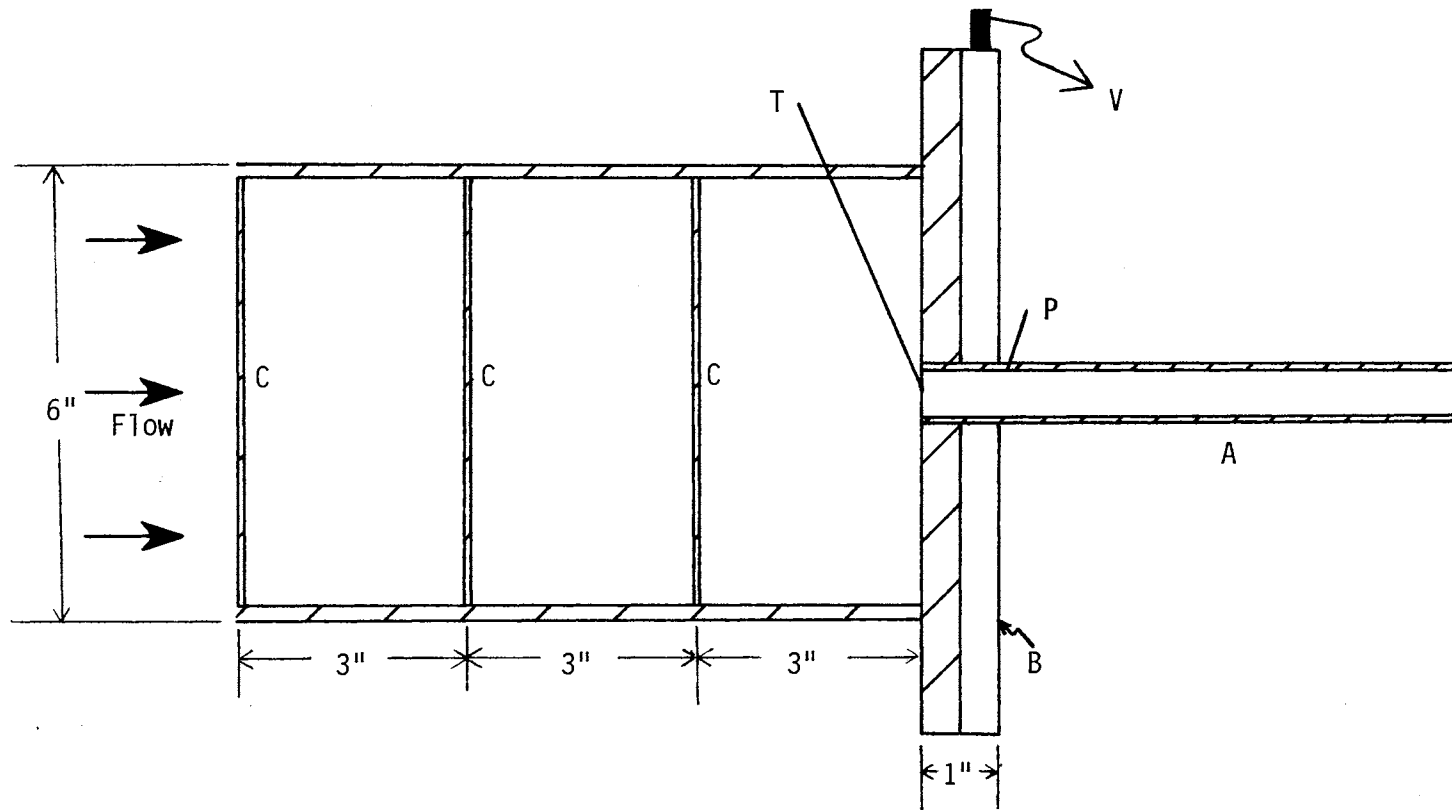
S: Stirrer

T: Thermocouple

W: Pump

Figure 7: Experimental Apparatus





- |                  |                                       |
|------------------|---------------------------------------|
| A: Test Section  | P: Pressure Tap                       |
| B: Copper Flange | T: Thermocouple                       |
| C: Screen        | V: Copper Bar, Connected to Generator |

Figure 8: Entrance Configuration of the Test Section

secured with insulating tape. The total thickness of these materials was approximately one inch.

Two pressure taps (2-inch long with 1/16-in. (1.59 mm) o.d.) were silver-soldered to each end of the test section and were connected to a mercury manometer. A 1/4-inch-thick, one-inch-wide, and four-inch-long copper bar was silver-soldered to the exit end of the test section. The entrance end of the test section was silver-soldered to a copper flange, 1/2-in. (12.7 mm) thick by 6-in. (152.4 mm) diameter.

#### Entrance Chamber

The entrance chamber was used to produce a uniform velocity distribution in the test fluid before entering the test section and was constructed from acrylic plastic. The combination of the entrance chamber and the test section produced a square-edged entrance configuration for the test section. Figure 8 shows the dimensions of the entrance chamber.

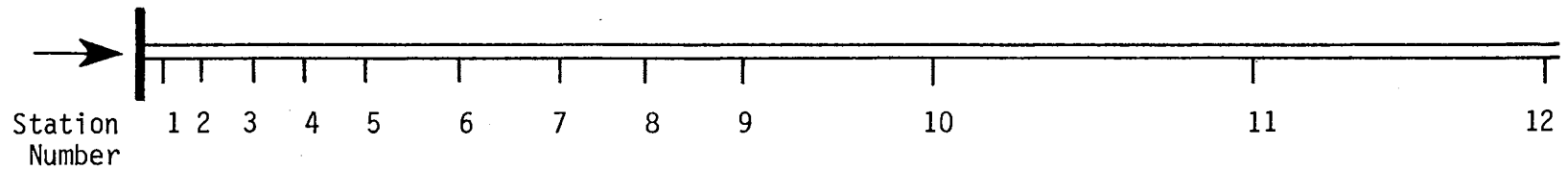
The entrance chamber consisted of a 6-inch diameter acrylic plastic cylinder with three perforated plates perpendicular to the cylinder center axis. Each stainless steel perforated plate had uniformly distributed 3/16-in. (4.76 mm) diameter holes with equilateral triangle pitch. Also there were uniformly distributed 1/16-in. (1.6 mm) diameter holes between the larger holes. These perforated plates were used to generate a uniform velocity profile.

The entrance chamber was constructed by the Physics Department Shop.

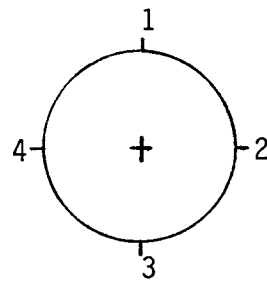
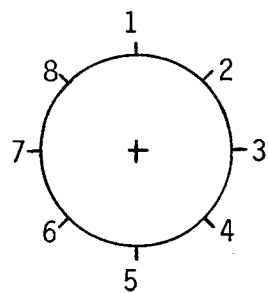
### Thermocouples

Figure 9 shows the positions of the 12 thermocouple stations. Stations 2, 3, 5 and 7 have eight thermocouples which were placed 45 degrees apart around the tube periphery. Stations 1, 4, 6, 8, 9, 10, 11 and 12 have four thermocouples each; the thermocouples were placed 90 degrees apart around the periphery. Copper-constantan thermocouple wire, Omega TT-T-36, with teflon wrapped insulation was used. All thermocouple beads were fabricated with a thermocouple welder in the laboratory.

Each thermocouple carried two numbers. The first number specified the station number from 1 to 12 starting from the tube entrance. The second number, from either 1 to 8 (for eight thermocouple stations) or 1 to 4 (for four thermocouple stations), indicated the location of the thermocouple around the periphery of the tube. The thermocouples at each station were always numbered so that 1 was on the top of the tube. For a four-thermocouple station, 3 was on the bottom of the tube, 2 was 90° clockwise looking from the tail of the fluid flow, and 4 was at 270° clockwise from the top. For an eight-thermocouple station, 5 was on the bottom of the tube, 2, 3 and 4 were on the right half of the station looking from



Station Number	1	2	3	4	5	6	7	8	9	10	11	12
$X/d_i$	2.4	7.1	13.4	26.0	38.6	51.2	63.8	76.5	101.7	126.9	177.3	244.3
Number of Thermocouples	4	8	8	4	8	4	8	4	4	4	4	4



+: Tail of Fluid Flow

Figure 9: Thermocouple Layout

the tail of the fluid flow, 45° apart, and 6, 7 and 8 were on the left half of the station, 45° apart.

Thermocouple beads were fixed on the outside of the test section by Omegabond 101. Omegabond 101 is an epoxy adhesive having a high thermal conductivity (0.6 Btu/(hr·ft·F)) and very high electrical resistivity ( $10^{13}$  ohm-m). A very thin layer (approximately 0.2 mm) of the adhesive was placed at the intended point of thermocouple attachment and allowed to set. This prevented the thermocouple beads from being in direct electrical contact with the tube. Thermocouple beads were held with tape and clamps at the intended point of thermocouple attachment. Another thin layer of adhesive was put on the thermocouple beads to fix them on the desired position.

The thermocouple lead wires were connected to a rotary switch board at the instrument panel. The thermocouple lead wires were held along the tube for about 10 mm. The rotary switch board was connected to a Doric thermocouple digital indicator.

#### Digital Thermocouple Indicator

A T-type model DS 350-T3 Doric thermocouple digital indicator was used to display temperature in degrees Fahrenheit with a claimed accuracy of  $\pm 0.3$  °F (0.17 °C) (6). Instrument repeatability is stated to be 0.1 °F (0.056 °C).

### DC Power Source

A Lincolnweld SA-750 electric welder generated constant voltage DC current, which passed through the test section between the copper bar and copper flange, thus generating heat internally in the wall due to the electric resistance of the wall. The DC power generator has a maximum output power of 30 KW. The duty cycle rating of the SA-750 is 750 amperes at 40 volts, continuous duty (19).

### Voltmeter

A Numatron, a digital readout voltmeter produced by Leeds and Northrup Company, was used to measure the voltage drop through the test section. It was calibrated by the manager of the Electronics Laboratory in the School of Electrical and Computer Engineering at Oklahoma State University. The readout is accurate within  $\pm 0.05$  volt.

### DC Ammeter

The current passing through the wall of the stainless steel test section was measured with a Weston 931 ammeter. It has a range of 0 to 750 amperes DC. It was placed in parallel with a 50-millivolt shunt. It was calibrated by the manager of the Electronics Laboratory in the School of Electrical and Computer Engineering at Oklahoma State University. The readout is accurate within one percent of its full scale, i.e.,  $\pm 7.5$  amperes.

### Heat Exchanger

A 4.3-ft<sup>2</sup> (0.40-m<sup>2</sup>), 1-4 shell and tube heat exchanger manufactured by American Standard Company was used to cool the fluid from the test section. The cooling fluid was utility water.

### Fluid Bath

A 15 gallon plastic tank with a mixer was used as test fluid bath. It was made by U. S. Plastic Corp.

### Pumps

A sliding vane pump was used to pump the fluid through the experimental loop. It was manufactured by Eastern Industries, Inc. (Model VW-5-A). It has a maximum capacity of 1.2 gpm of water.

Another sliding vane pump manufactured by Floctec Inc. was used for higher flow rates. It has a maximum capacity of 10 gpm of water.

### Rotameters

Two Fischer and Porter rotameters, FP-3/4-G10 and FP-1-35-G11, were used for fluid flow measurements. They have 1.96 and 11 gpm capacities of water respectively. The details of the rotameter calibration are listed in Appendix C.

### Test Fluids

Distilled water, and 28.3 percent, 48.5 percent, 66 percent, 92.5 percent, and nearly 100 percent (by mass fraction) DEG-water solutions were used as test fluids. Technical grade DEG (99.9 % as tested by the author) was purchased from Sargent-Welch Scientific Company.

### Calibration Equipment

Auxiliary equipment was used for the calibration of the measuring instruments. The temperature and flow calibration equipment and procedures are included in Appendices A and C, respectively. The apparatus for the determination of the viscosity is described in Appendix D.



## CHAPTER IV

### EXPERIMENTAL PROCEDURES

#### Calibration Procedures

The thermocouples that measured the inlet bulk, exit bulk, bath and room temperatures, together with the thermocouple switch board and the thermocouple indicator were calibrated against a platinum thermometer. The calibration procedure and data for these thermocouples are given in Appendix A. Calibration data of the thermocouples that measured the outside wall temperatures of the test section are included in Appendix B. Appendix C has the flow rate calibration procedure. The procedure for calculating the composition of DEG-distilled water solution is given in Appendix D.

#### Start-Up and Operating Procedure

The fluid flow loop was tested by running water at maximum flow rate. All leaks were eliminated before putting on insulation.

The following procedures were followed for each run:

1. The valves were checked and adjusted to the desired position.
2. The cooling water was turned on to the heat

exchanger.

3. The pump was started and the fluid flow rate was adjusted to the desired value by means of the flow control valve.
4. The Numatron voltmeter was turned on.
5. The DC generator was started with the polarity switch in the neutral position and allowed to run for at least 30 minutes to warm up.
6. After the test fluid had circulated at constant temperature for one hour, the room, bath, inlet bulk and exit bulk temperatures were recorded.
7. The DC current through the test section was started by switching the polarity to positive. The DC current was adjusted to the desired value by varying the output control knob of the generator.
8. If, after at least 90 minutes of steady state operation, the inlet bulk, exit bulk, and station 12 temperature were observed to be stable, the following data were taken:
  - a. the inlet and exit bulk fluid temperatures
  - b. fluid flow rate (rotameter reading)
  - c. the room temperature and bath temperature
  - d. the DC current flowing through the wall of the test section
  - e. the voltage drop across the section
  - f. the output readings of the 64 thermocouples

attached to the outside wall surface of the section

- g. the pressure drop across the test section.
- 9. The data collected in step 8 were gathered again after twenty minutes. Four to six sets of data were collected for each run depending upon the flow regime.
- 10. The DC generator was shut off.
- 11. After the Numatron reached 0, it was shut off.
- 12. The cooling water was shut off.
- 13. To calculate the heat loss at the exit of the test section, the bath temperature was set to slightly above the exit bulk fluid temperature. The inlet bulk, exit bulk and bath temperatures were recorded after running the test fluid at the set temperature for one hour.
- 14. The pump, mixer and thermocouple indicator were shut off.

#### Some of the Problems Encountered

The thermocouple readings from the Omega 350 thermocouple indicator shifted while the experiment was proceeding. This was due to an increase in the room temperature. The Omega 350 thermocouple indicator was replaced by the Doric 350-T3 and the problem disappeared. Also, the air circulation in the room was improved and the room temperature was kept below 80 °F.

In the early experiments, the temperature profile at the first thermocouple station was not symmetric. This was eliminated by increasing of the entrance tube length into the plastic chamber and rearrangement of the pipe loop.

## CHAPTER V

### DATA REDUCTION

The computer program used by Abdelmessih(1) was modified to reduce the experimental data using the IBM 3081. The listing of the modified computer program is presented in Appendix H. The outside wall temperatures were measured along the test section at 12 stations. The average bulk fluid temperature was assumed to vary linearly with axial distance along the test section. The average bulk fluid temperature was used to calculate the local values of the dimensionless groups.

The physical properties of the test fluids and tube wall were evaluated as functions of temperature and compositions as given in Appendix E. Those correlations were incorporated into the computer program for reducing the data.

The following procedures were used to reduce the data:

1. Calculation of the overall heat balance.
2. Calculation of the local inside wall temperatures and the local inside wall radial heat fluxes.
3. Calculation of the local heat transfer coefficients.

Details of the procedures follow and a sample calculation is presented in Appendix J.

### Calculation of the Overall Heat Balance

The overall heat balance for each run is calculated as follows:

1. The rate of heat input to the fluid is calculated from the power input to the test section and the heat loss from the test section. The heat loss from the test section is the arithmetic mean between:

- a. the heat loss when the test fluid is run at constant temperature equal to the inlet bulk temperature, and
- b. the heat loss when the test fluid is circulated at a constant temperature equal to the exit bulk temperature.

$$Q_{\text{input}} = F \cdot I \cdot V - Q_{\text{loss}} \quad (\text{V.1})$$

2. The heat absorbed by the fluid is calculated from the mass flow rate, inlet and outlet temperatures, and the specific heat calculated at the average bulk temperature:

$$Q_{\text{output}} = \dot{m} \cdot C_p \cdot (T_o - T_i) \quad (\text{V.2})$$

3. The error in the heat balance is calculated as follows:

$$\% \text{ error} = 100\% \cdot \frac{Q_{\text{input}} - Q_{\text{output}}}{Q_{\text{input}}} \quad (\text{V.3})$$

### Calculation of the Local Inside Wall Temperature and the Local Inside Wall Heat Flux

The computer program in Appendix H corrects the measured outside wall temperature according to the calibration in Appendix B. Then the inside wall temperature and the inside heat flux corresponding to each thermocouple location are computed using a two-dimensional relaxation calculation. In the numerical solution, it is assumed that peripheral and radial wall conduction are significant, while axial conduction is negligible. Also, the solution accounts for the heat losses to the surroundings and the variation of the physical properties of the tube wall with temperature. The derivation of the numerical solution is given in Appendix F.

### Calculation of the Local Heat Transfer Coefficient

From the local inside wall temperature, the local inside wall heat flux, local bulk fluid temperature, the local heat transfer coefficient can be calculated as follows:

$$h_{ji} = q_{ji} / (T_{wji} - T_{bj}) \quad (\text{V.4})$$

The subscript 'j' denotes the station number and 'i'

denotes the peripheral position.

The average peripheral heat transfer coefficient at a thermocouple station is calculated by two different methods

$$h = \frac{1}{I_p} \cdot \sum_{i=1}^{I_p} \left\{ \frac{(Q/A)_i}{(T_{wi} - T_b)} \right\} \quad (V.5)$$

$$h = \left\{ \sum_{i=1}^{I_p} \left( \frac{q_i}{I_p} \right) \right\} / \left\{ \left[ \sum_{i=1}^{I_p} \left( \frac{T_{wi}}{I_p} \right) \right] - T_b \right\} \quad (V.6)$$

where  $I_p$  is the number of thermocouples at station  $j$ .

The average peripheral heat transfer coefficients obtained from Equations (V.5) and (V.6) were then used to determine the average peripheral Nusselt numbers for each thermocouple station. The Nusselt number based on (V.6) is used in the rest of the thesis, unless otherwise indicated. The physical properties of the test fluid used in determining the dimensionless groups were evaluated at the bulk temperature at each station.



## CHAPTER VI

### RESULTS AND DISCUSSION

Experimental data were gathered for local bulk Reynolds numbers ranging from 121 to 12,400, local bulk Prandtl numbers from 3.5 to 282.4, and local bulk Grashof numbers from 930 to 1,040,000. The test fluids were distilled water and distilled water-DEG solutions (with DEG mass fraction ranging from 28.3 % to 99.9 %). The experiments were performed with nominally constant wall heat flux with the average heat flux ranging from 1,620 to 11,800 Btu/(hr·ft<sup>2</sup>) (or 5.1 to 37.2 kW/m<sup>2</sup>). Only two sets out of 48 sets of data have heat balance errors beyond the range from -1.5% to +6.4%. The average absolute heat balance error is 2.31%. The local bulk fluid velocity ranges from 0.31 ft/sec (0.094 m/sec) to 5.21 ft/sec (1.59 m/sec).

Appendix H shows a typical set of data and calculated results which include uncorrected outside surface temperatures, corrected outside surface temperatures, Reynolds number at the inside wall, inside surface temperatures, local bulk fluid temperatures, inside surface heat fluxes, peripheral heat transfer coefficients, local average heat transfer coefficients, ratios of the average

heat transfer coefficient to those predicted by literature correlations, and local average values for dimensionless groups.

### Effect of Various Parameters on the Average Bulk Local Heat Transfer Coefficient

Parameters which affect the average bulk local heat transfer coefficients are divided into: entrance effect, lower turbulent flow, high laminar flow, and transition flow.

#### Entrance Effect

The entrance effect is defined as the enhancement of heat transfer by the acceleration and/or turbulence created by the entrance configuration. Figure 10 shows typical profiles of local average heat transfer coefficient for several runs. In Figure 10, the entrance effect is identified as the increase in local heat transfer coefficient for low  $X/d_i$ . The entrance effect seemed to be damped out after 12.5 tube diameters (station 3) for the flow in the low turbulent flow regime ( $Re > 7,000$ ). In the transition flow regime ( $2,100 < Re < 7,000$ ), the entrance effect extends as far as 40 diameters. And the effect seems to exceed over 60 diameters in the high laminar flow regime ( $120 < Re < 2,100$ ).

The magnitude of the entrance effect seems to be

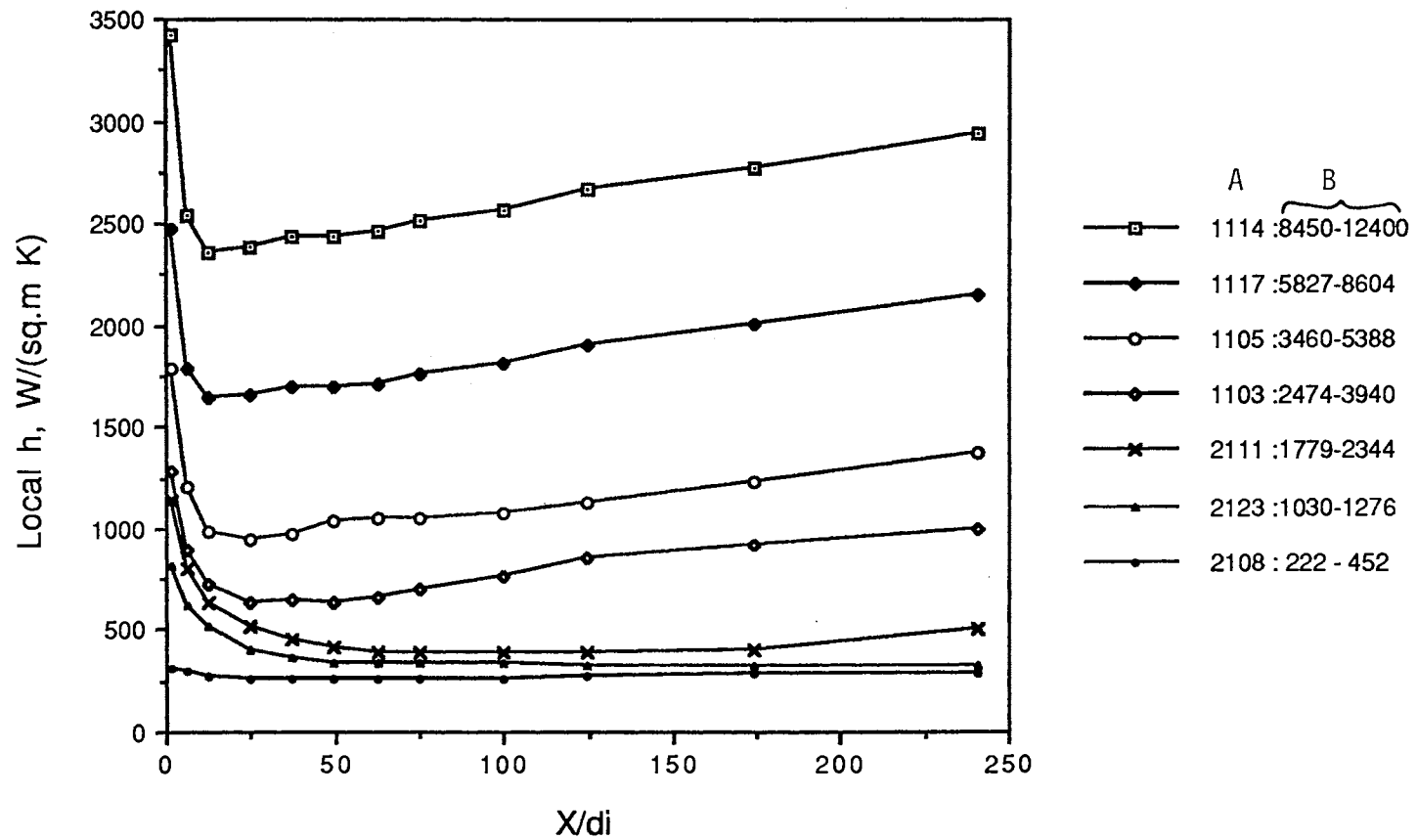


Figure 10: Local Average Heat Transfer Coefficient  $h$  vs  $X/d_i$ .  
 A is Run Number. B is the Local Average Reynolds Number at Station 1 to the Local Average Reynolds Number at Station 12.

inversely related to the Reynolds number. For example, for run 1114 (Re ranges from 8450 at station 1 to 12400 at station 12), the ratio of the heat transfer coefficient at station 1 to station 3 is  $3425/2364 = 1.45$ , while the ratio of the heat transfer coefficient at station 1 to station 4 for run 1103 (Re ranges from 2474 at station 1 to 3940 at station 12) is  $1279/631 = 2.03$ .

### Lower Turbulent Flow

Figure 11 shows  $N$  vs  $Re$  for all data points. The lower turbulent flow regime is defined as flows with bulk Reynolds numbers ranging from 7,000 to 12,500. The Sieder and Tate equation (44):

$$Nu = 0.023Re^{0.8}Pr^{1/3}(\mu_b/\mu_w)^{0.14} \quad (VI.1)$$

holds for fully developed turbulent flow. The group  $N = Nu/[Pr^{1/3}(\mu_b/\mu_w)^{0.14}]$  should be dependent on Reynolds number only. There are not many points above the major data diagonal on the figure beyond station 3. This is due to the fact that entrance effects do not exist or have little influence on the flow after station 3. To eliminate entrance effects, the figure was replotted for stations 4 to 12 as shown in Figure 12. There seems to be a break in slope at  $Re \sim 7,000$ , and the data points begin to spread for  $Re < 4600$ .

The nature of the fluid flow through a square-edged

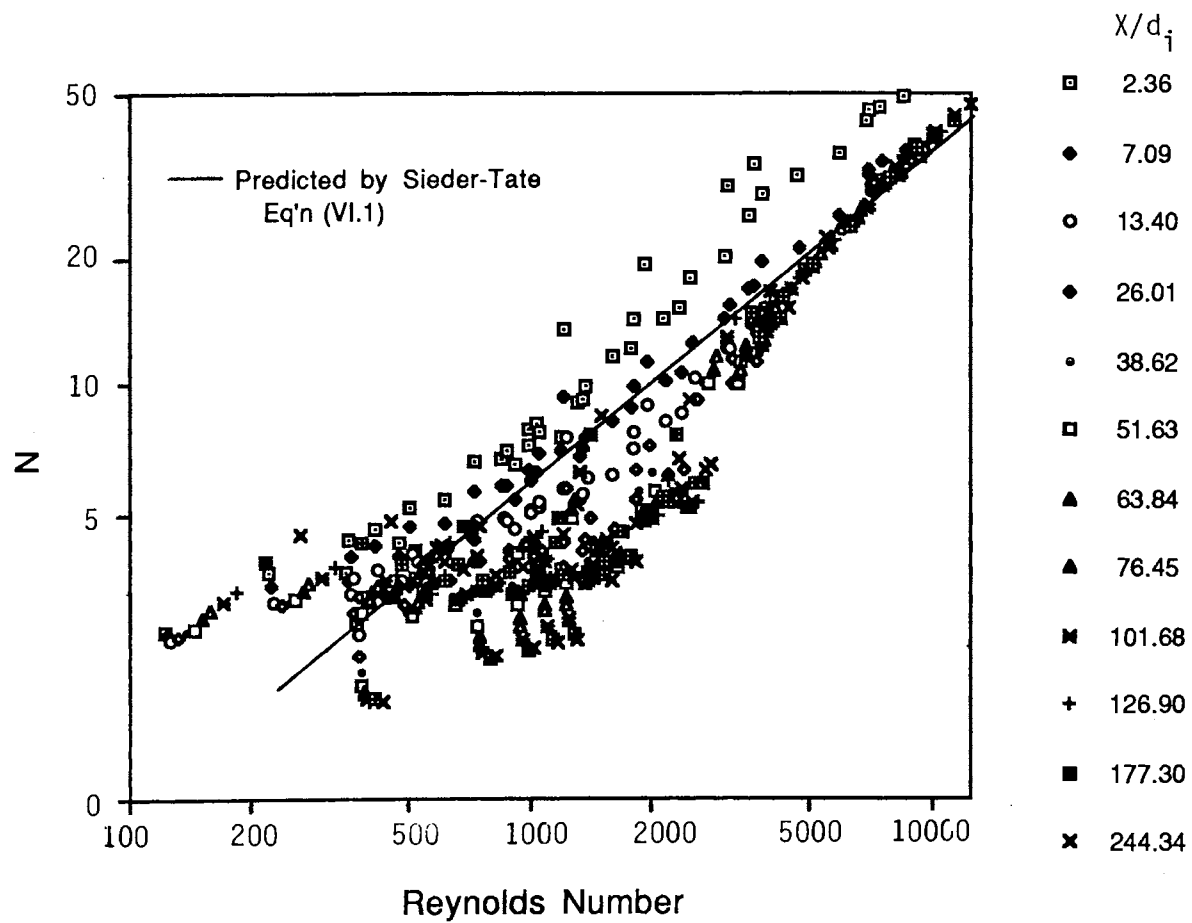


Figure 11: All Data Points for  $N = Nu / (Pr^{1/3} (\mu_b / \mu_w)^{0.14})$  vs Reynolds Number

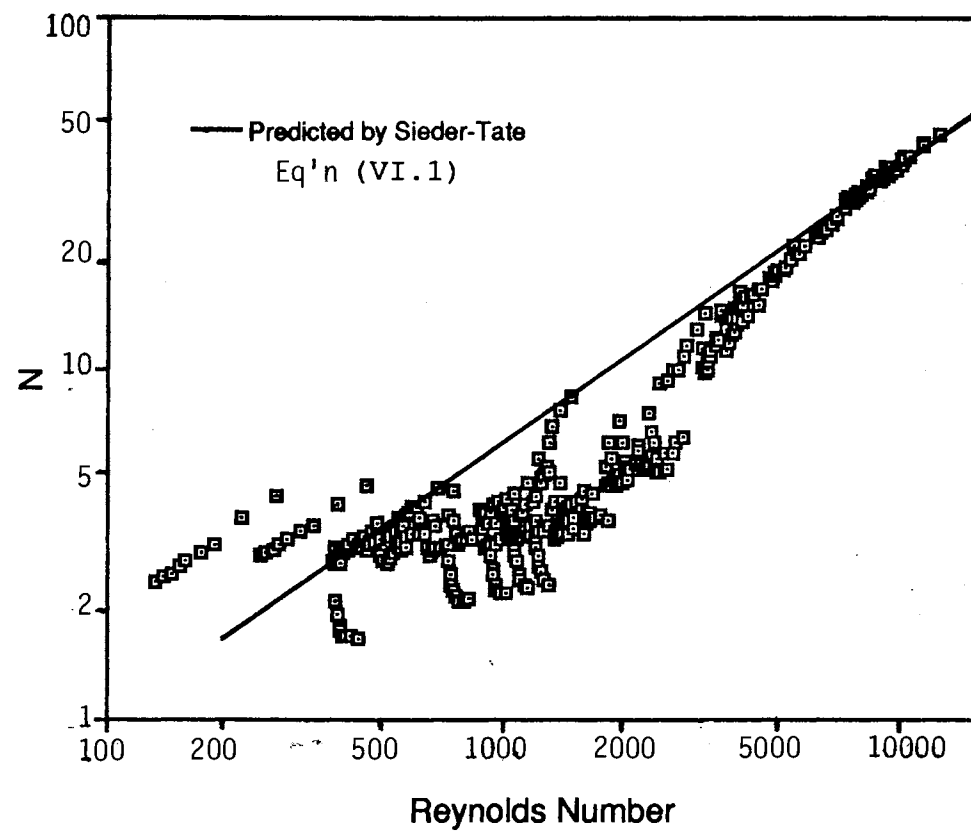


Figure 12: N vs Re for Stations 4 to 12 for all Data Points

entrance is well understood. The stream of fluid entering the tube continues to converge further after entering the tube until it reaches a minimum jet cross-sectional area called the vena contracta. The stream then diverges until it fills the tube (reattachment). At reattachment, the velocity profile is probably very uniform and then both the velocity and temperature profiles begin to be established.

Figure 13 shows  $N$  vs  $Re$  for  $Re > 7000$ . This is considered to be the lower turbulent flow regime. A simple least square curve fitting gives:

$$Nu = 0.01424 Re^{0.86} Pr^{1/3} (\mu_b/\mu_w)^{0.14} \quad (VI.2)$$

In the lower turbulent flow regime, the ratio of the experimental heat transfer coefficient at the top of the tube to the heat transfer coefficient at the bottom of the tube,  $h_{top}/h_{bottom}$ , is generally greater than 0.92 and less than 1.02. A value less than 1.0 implies that there is some natural convection existing in the lower turbulent flow regime. In most cases,  $h_{top}/h_{bottom}$  is greater than 0.95. But there is no apparent relationship between the  $h$  ratios and the other dimensionless groups. This may be due to the effect of  $h_{top}/h_{bottom}$  term being too close to 1.0. Both the flow condition and temperature readings were very stable in all cases in this flow regime.

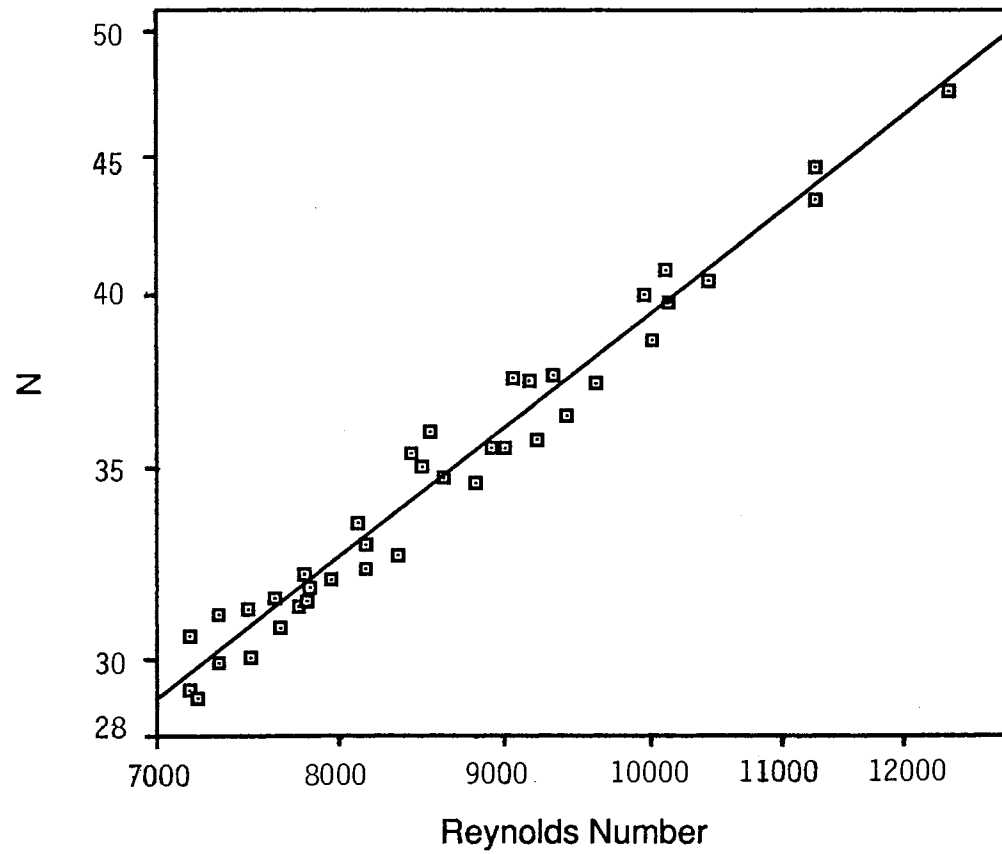


Figure 13: N vs Re for Reynolds Numbers Greater Than 7,000 and for Stations 4 to 12



### Transition Flow

The transition flow regime is defined as flows with bulk Reynolds numbers between 2,100 and 7,000. And the transition flow regime is divided into the upper transition flow, for  $4,600 < Re < 7,000$ , and lower transition flow,  $2,100 < Re < 4,600$ . In the upper transition flow regime, a Sieder-Tate type relationship holds as we can see in Figure 14. However, the curve is somewhat steeper than Figure 13. A simple least square fit gives:

$$Nu = 0.00298 Re^{1.03} Pr^{1/3} (\mu_b/\mu_w)^{0.14} \quad (VI.3)$$

for stations 4 to 12.

Transition flow is the end result of the growth of initially small, probably random disturbances in the flow. Small disturbances due to noises or slight vibrations of solid surfaces are always present in the background of any flow. Under some conditions in the flow, these disturbances are damped out, whereas at other conditions they are amplified. Transition flow is affected by many factors such as tube roughness, inlet geometry, and natural convection in the flow (49). The complexities of these parameters and their interactions discourage many researchers' hope for a definite picture of the nature of the transition flow.

Figure 15 shows the temperature readings for run 1101 at station 6 which had a bulk local Reynolds number of 4,070. Seven readings were taken for each thermocouple

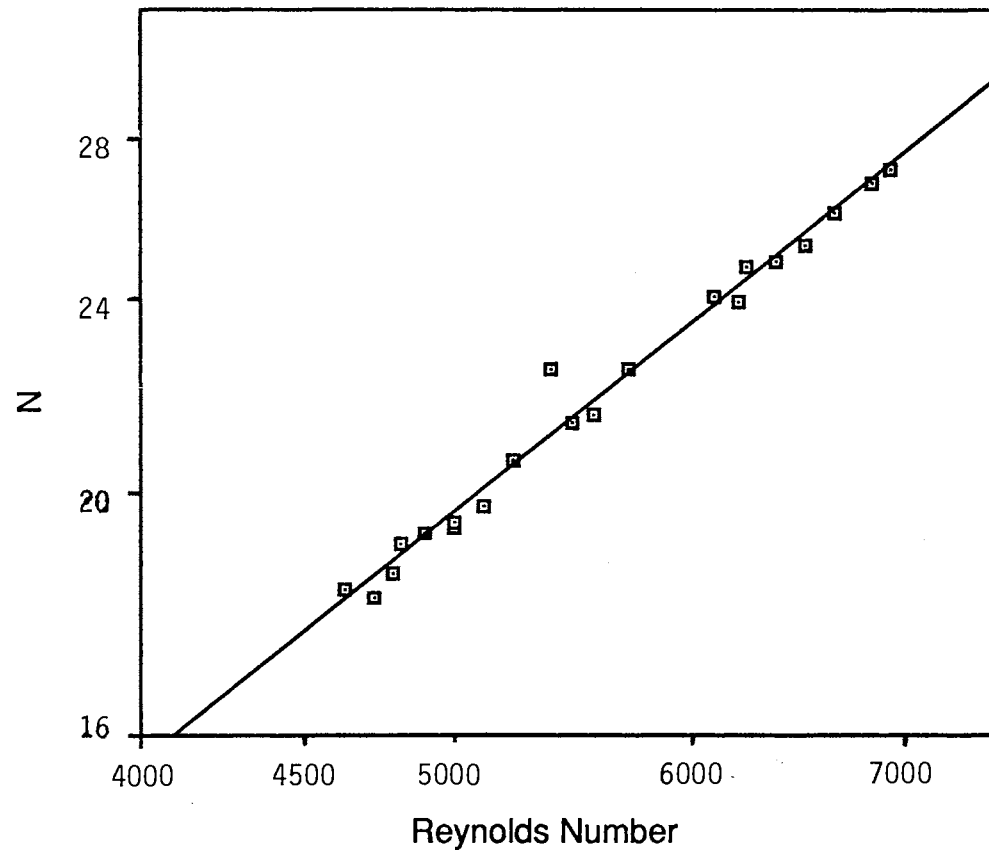


Figure 14: N vs Re for Reynolds Numbers between 4,600 and 7,000 and for Stations 4 to 12

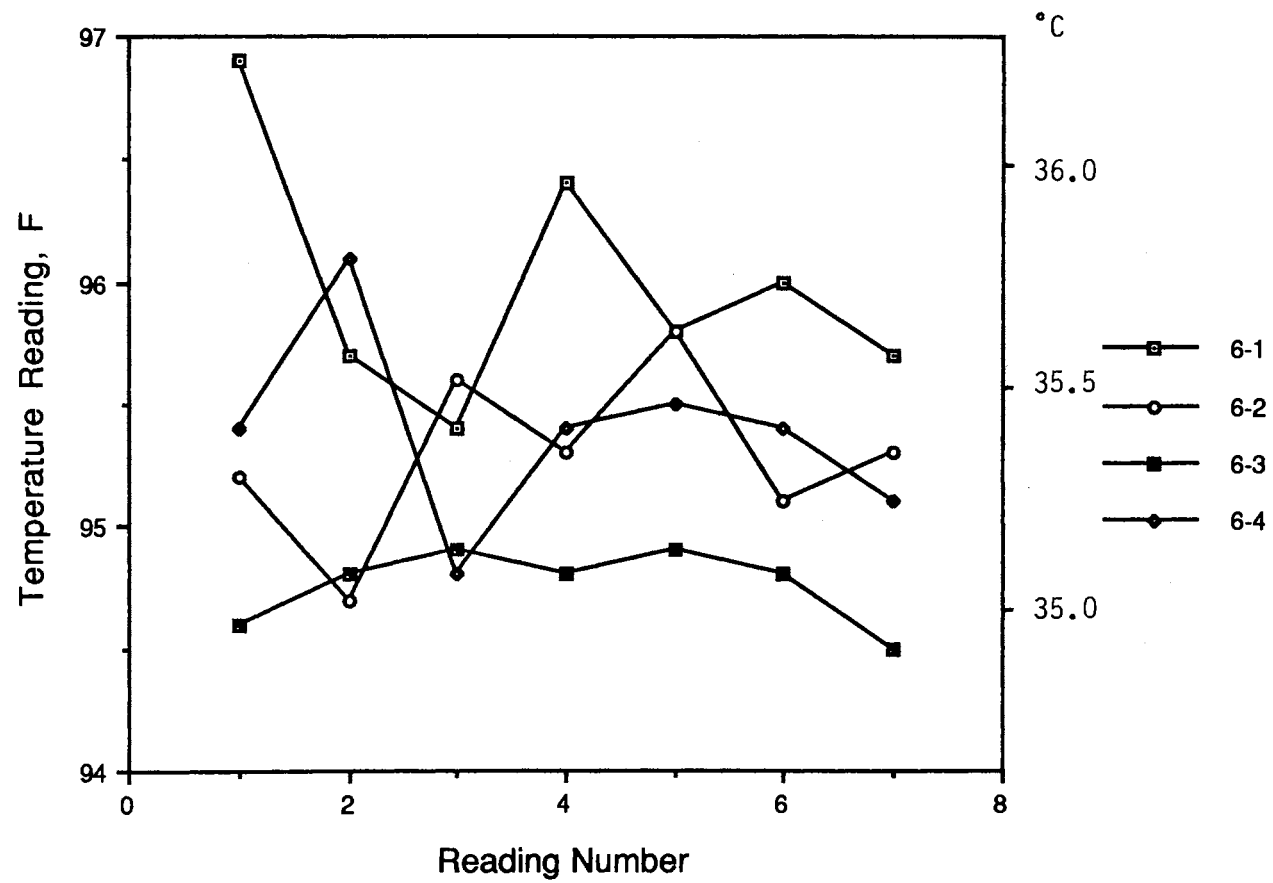


Figure 15: Temperature Readings for Run 1101 at Station 6  
with Local Average Reynolds Number of 4,070

position over the period of forty minutes. The maximum difference among the readings for the same position was up to 1.5 °F. In some other runs, this difference was observed to be as large as 10 °F or higher. Usually, the average of these readings will be very close to the average readings from the corresponding position on the opposite side wall at the same station.

Figure 16 shows the fluctuations of the readings for thermocouple 4-4 for run 1109 with a local average  $Re$  around 7000. No accurate time period was recorded. But the interval between two readings was about 10 seconds. The entire period was about 20 minutes.

In the original experiment conducted by Reynolds (37) in 1883, he found that no turbulence occurs for fully developed flow for  $Re$  less than about 2,000, no matter how rough and noisy the entrance conditions are.

In our experiments for simultaneous developing hydrodynamic and thermal profiles with square-edged entrance, instability, as defined by temperature fluctuations, was found in the runs with local bulk Reynolds number ranging from 886 to 7,750. It seems that the local inside wall Reynolds number is a better criterion for the instability of the temperature readings than the local bulk Reynolds number.

$Re_w$  is defined as the Reynolds number calculated using liquid density and viscosity evaluated at the inside wall temperature. For a position showing instability at a local

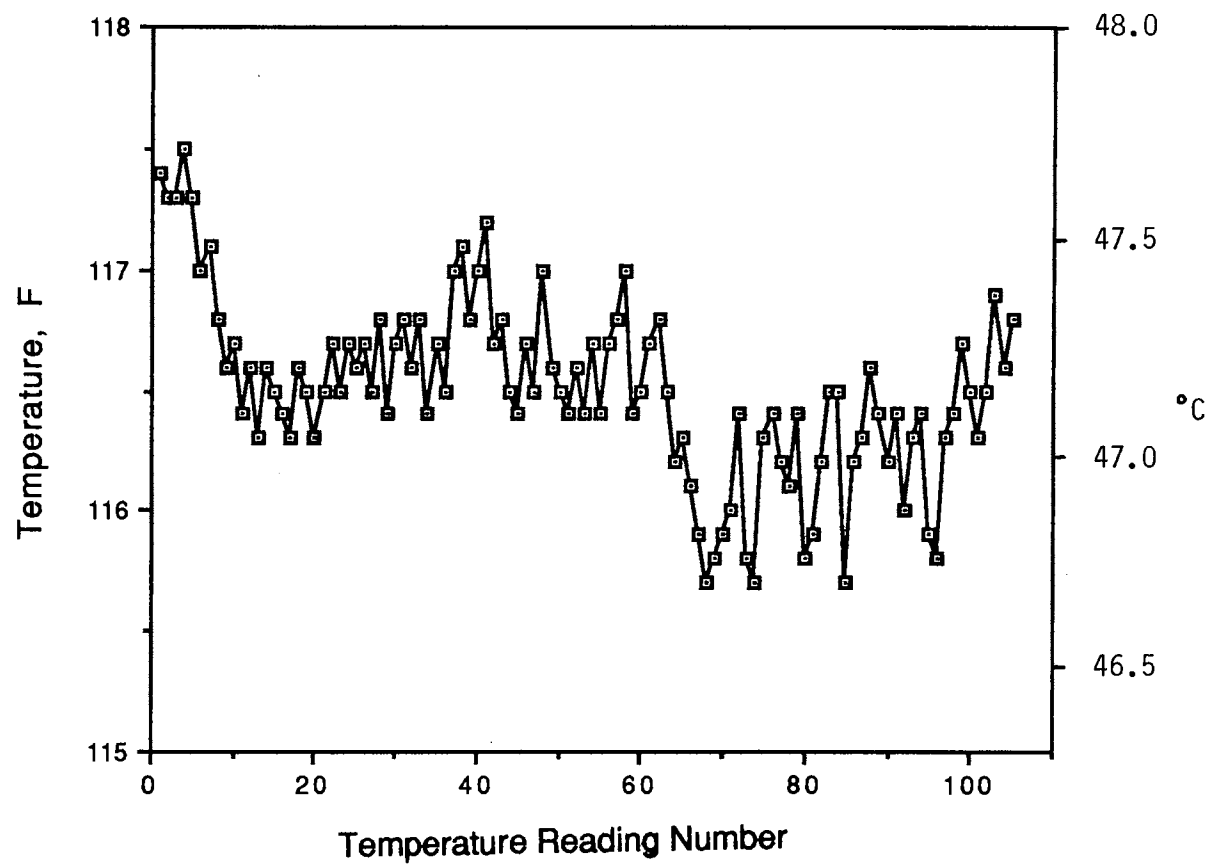


Figure 16: Temperature Fluctuations for Thermocouple 4-4  
Run 1109 with Local Average Reynolds Number  
of 7,000. Approximate Time between Readings  
12 Seconds.

bulk  $Re = 886$ , the average Reynolds number at the inside wall,  $Re_w$ , was 2,390. And the local inside surface temperature was 125.41 °F (51.90 °C) and the bulk temperature was 68.17 °F (20.10°C). This implies that the instability is a local phenomenon and depends upon the local conditions. All instability occurred in the positions with  $Re_w$  from 2,100 to 10,600 except two positions with  $Re_w = 1900$  ( $Re = 1,210$ ) and  $Re_w = 1,920$  ( $Re = 1,035$ ) respectively.

But not all the temperature readings at the positions with  $Re_w$  in the range of 2,100 to 10,600 showed instability. Few points with  $Re_w$  larger than 9,000 (or  $Re > 7,000$ ) showed instability. Only two points showed instability for  $Re_w$  above 10,000. For data with  $Re_w$  in the range of 2,100 and 10,000, only about 33 per cent of the data points showed strong fluctuations in temperature ( $\pm 1.5$  °F about the mean of the total range). About 14 per cent of the points showed minor fluctuations (between 1.5 °F and 0.7 °F), and around 53 per cent of the points showed little fluctuation (less than 0.6 °F).

It is believed that the introduction of disturbance will possibly trigger turbulence. This was shown in the experiments. With similar local bulk Reynolds number, the positions near the entrance of the test section have the tendency to be more unstable in the temperature readings than the positions farther away from the entrance. This was

presumably caused by the disturbance of the flow induced by the square-edged entrance. In some runs, only the early stations (1 to 5) showed instability while stations 6 to 12 showed no fluctuations in the temperature readings, even though the entire run was in the transition flow regime. The disturbance caused by the entrance configuration was damped after a couple of tube diameters.

In some runs, the instability in temperature readings showed on only some of the thermocouples at the same station. The top thermocouple reading in the station may be fluctuating while the other three thermocouple readings are relatively stable. Generally, the top position has a greater tendency to be unstable than the bottom positions.

#### High Laminar Flow

The high laminar flow regime is defined as flows with bulk Reynolds numbers from 120 to 2,100. Practically, the difficulty for interpreting and correlating laminar flow heat transfer is due to the fact that fluids in this flow regime usually have properties, especially viscosity, which are very strongly dependent on temperature. In the case of heating, the fluid near the wall is warmer, and less dense than the bulk fluid in the core. As a consequence, two upward currents flow along the tube side walls and the denser fluid near the center of the tube flows downward. This generates two vortices superimposed on the primary forced convective flow. The above phenomena also exist

in the turbulent flow. However, turbulent flow heat transfer is much higher than for laminar flow. Therefore, the temperature difference and the secondary flow are not so apparent.

Figure 17 shows wall temperature readings for run 2137 (DEG mass fraction 0.283) which has local bulk Reynolds numbers from 1,769 (station 1 with bulk temperature 59.94 °F) to 2,284 (station 12 with bulk temperature 73.24 °F), local bulk Prandtl number from 26.32 to 20.18, local average heat flux 3210 Btu/(hr·ft<sup>2</sup>) (or 10,130 W/m<sup>2</sup>), and  $h_{top}/h_{bottom}$  from 1.00 to 0.252. As fluids flow along the tube, the secondary flow initiates and therefore the temperature difference between the top and the bottom of the tube starts to increase. In run 2137, the temperature difference between the top and the bottom position is -0.06 °F at station 1 and 35.71 °F at station 12. This temperature difference ranges from 0 to 2.8 °F for lower turbulent flow ( $10,000 < Re_{w,avg} < 15,000$ ), from 0.8 to 35.6 °F for transition flow ( $2,100 < Re_{w,avg} < 10,000$ ), and from 19.2 to 46.8 °F for laminar flow ( $100 < Re_{w,avg} < 2,100$ ).

Also, as we can see in Figure 17, from station 5 to 10, the temperature readings at the bottom position did not change very much (from 97.00 to 97.54 °F). This indicates that natural convection took away some of the heat generated at the bottom positions. And the temperature readings at the top positions from stations 5 to station 10



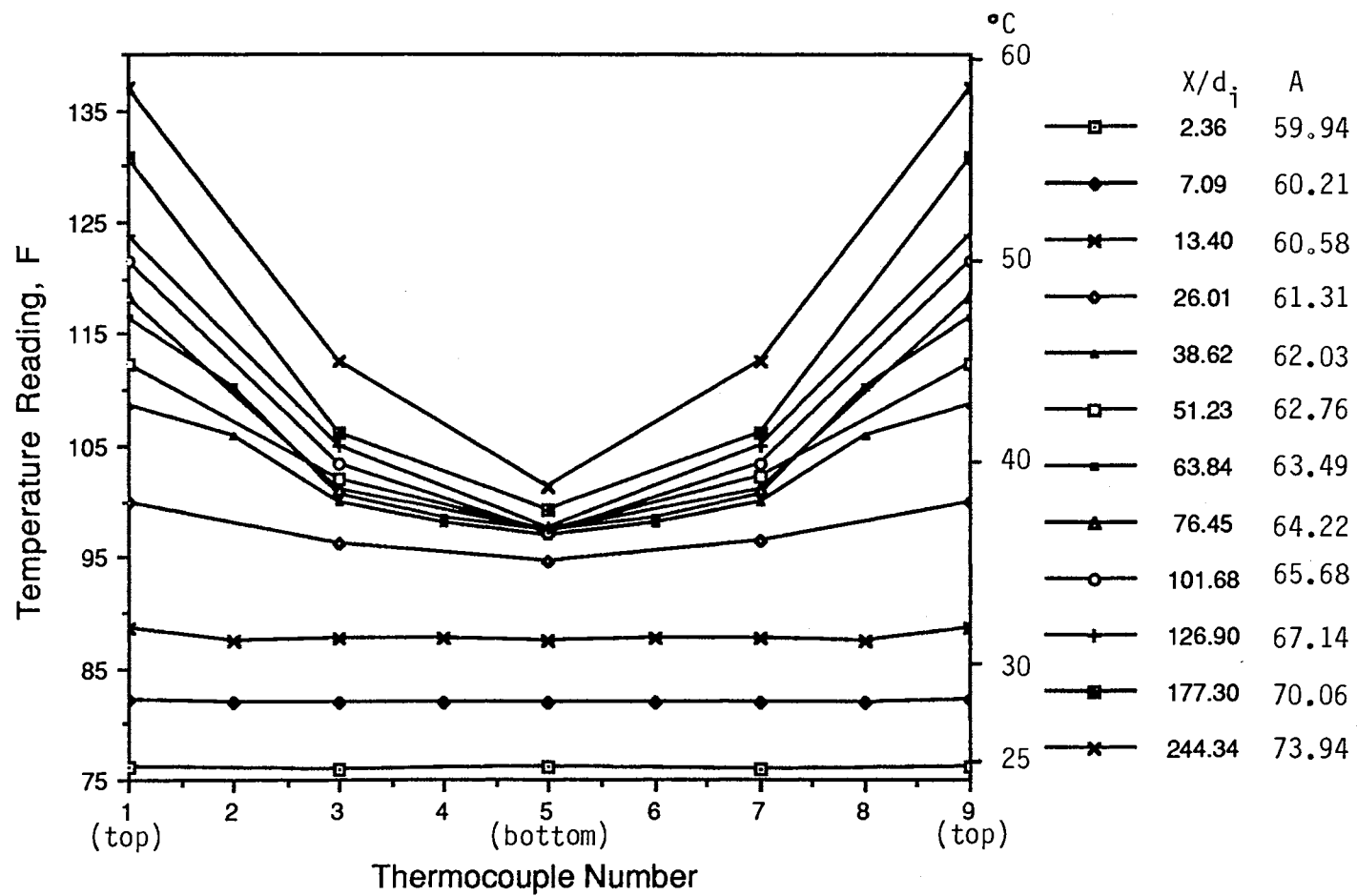


Figure 17: Local Surface Temperatures for Run 2137 with Local Bulk Reynolds Numbers Ranging from 1,769 at Station 1 to 2,284 at Station 12. A is Local Bulk Fluid Temperature F.

increased dramatically from 108.57 to 123.85 °F. This indicates that natural convection brought some hot liquid from the bottom positions to the top positions.

### Comparison with Literature

Most literature correlations are based on the overall average properties including Nusselt number for the entire tube. In order to compare these correlations with our local average Nusselt number obtained from the experiments, these overall average Nusselt numbers, denoted by  $Nu$  in this section, are multiplied by  $X$  and then differentiated with respect to  $X$ . We call these Nusselt numbers the 'local' Nusselt numbers, denoted by  $Nu$ .

### Colburn Correlation

Colburn(5) correlated his experimental data for laminar flow and obtained:

$$\underline{Nu} = 1.5(RePr_d/X)^{1/3} (\mu_b/\mu_w)^{1/3} (1+0.015Gr^{1/3}) \quad (VI.4)$$

The Colburn equation for local Nusselt number is:

$$Nu = (RePr_d/X)^{1/3} (\mu_b/\mu_w)^{1/3} (1+0.015Gr^{1/3}) \quad (VI.5)$$

Colburn recognized the importance of natural convection in laminar flow in a straight horizontal tube. Figures 18 and 19 show that Colburn overpredicted the Nusselt number for most of the runs with  $X/d_i$  less than 50 and underpredicted for  $X/d_i$  greater than 50.

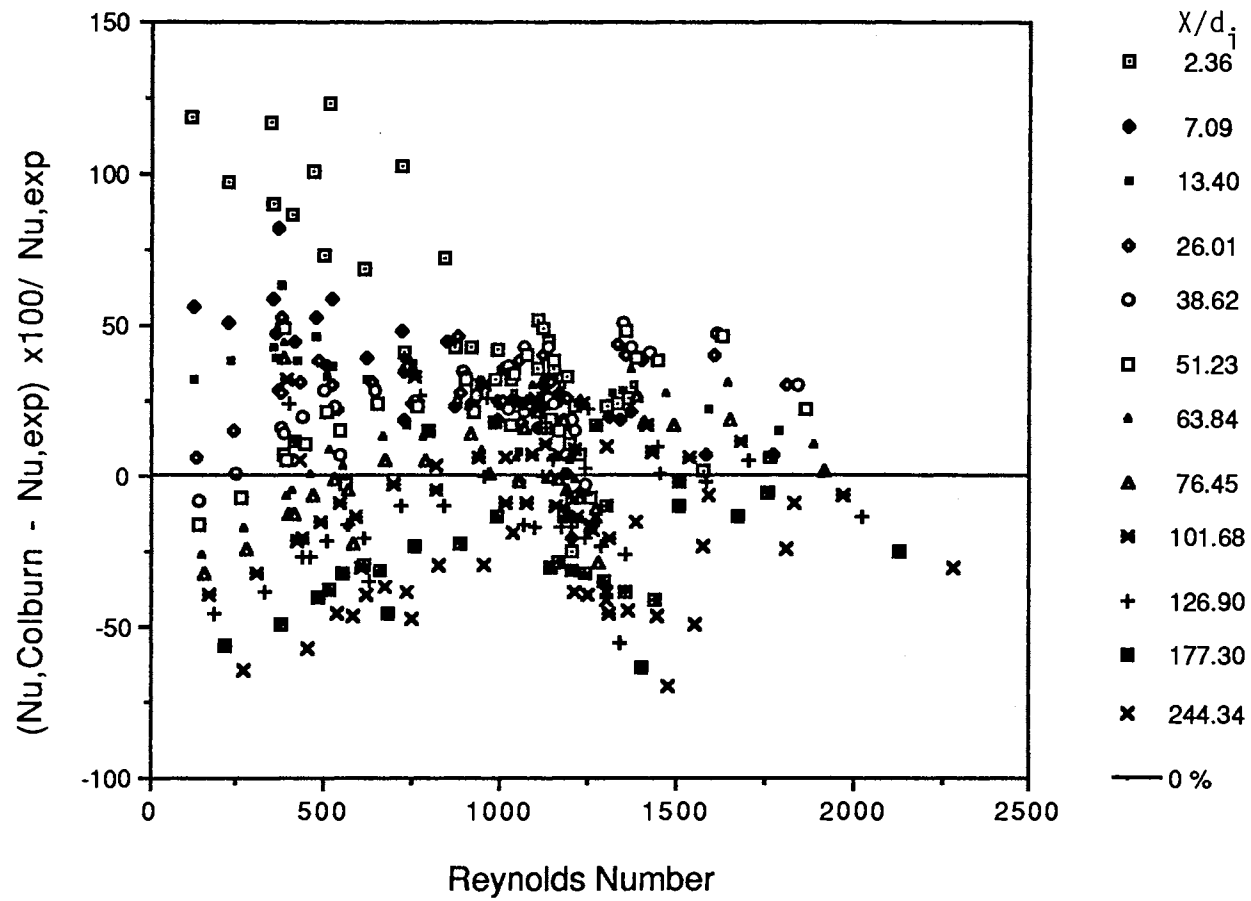


Figure 18: Comparison between the Experimental Heat Transfer Coefficients and the Heat Transfer Coefficients Predicted by Colburn as a Function of Reynolds Number for  $121 < Re < 2,300$ .

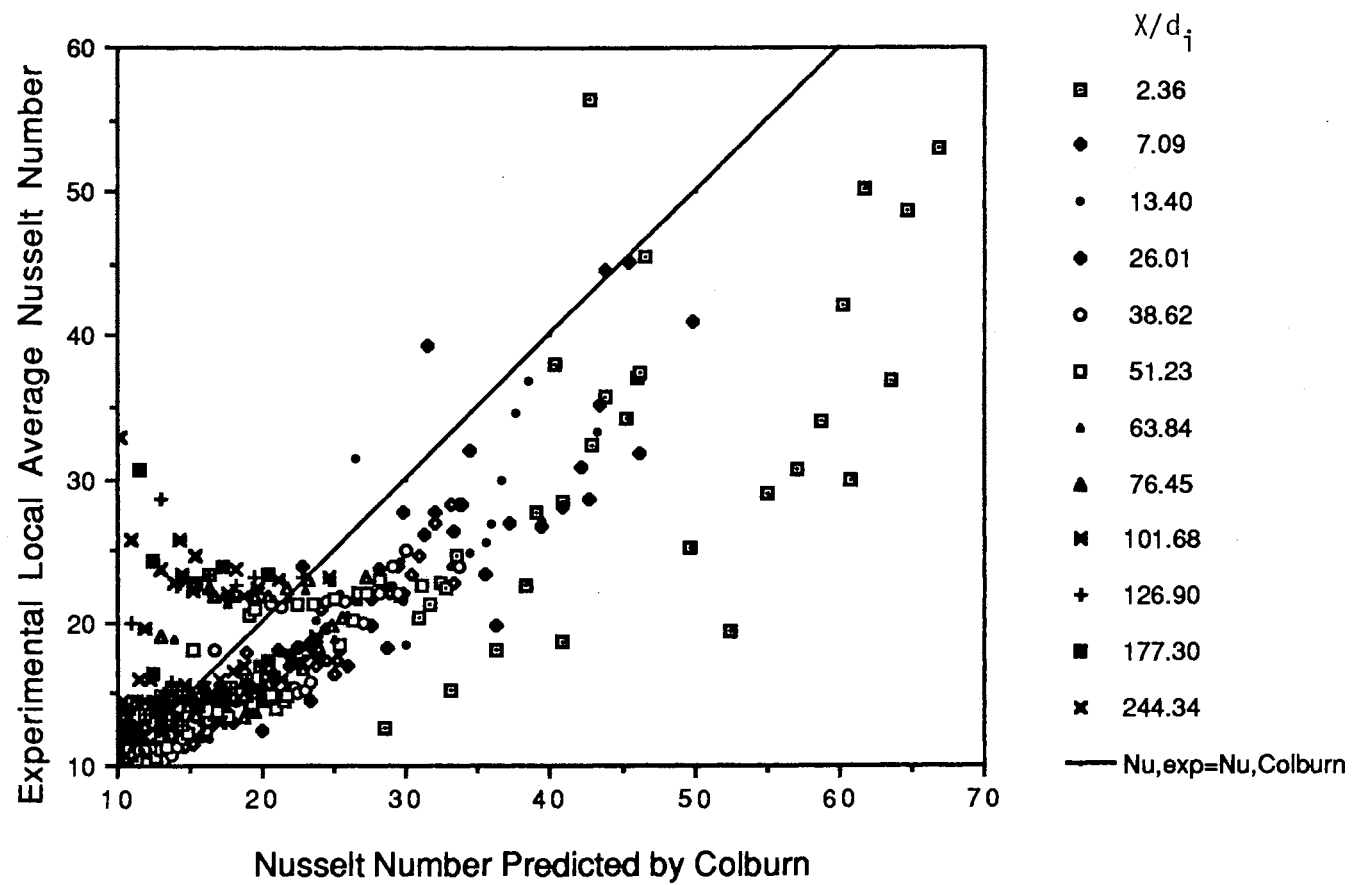


Figure 19: Comparison between the Experimental Nusselt Number and the Nusselt Number Predicted by Colburn

### Sieder and Tate Correlation

Sieder and Tate (45) correlated their data and obtained the following equation for laminar flow inside a straight tube from their experimental data:

$$\underline{Nu} = 1.86(\text{RePr}_i/X)^{1/3} (\mu_b/\mu_w)^{0.14} \quad (\text{VI.6})$$

This equation is converted to:

$$Nu = 1.24(\text{RePr}_i/X)^{1/3} (\mu_b/\mu_w)^{0.14} \quad (\text{VI.7})$$

The Sieder-Tate equation does not take into account the effect of natural convection. Also, for extremely long tubes, the Nusselt number predicted by Sieder and Tate approaches zero which is contradictory to the theoretical fully developed Nusselt number, 4.364, for laminar flow with uniform heat flux. Figures 20 and 21 show that Sieder and Tate overpredicted the Nusselt number for  $X/d_i$  less than 40 and underpredicted the Nusselt number for  $X/d_i$  greater than 40 for most runs.

$(\mu_b/\mu_w)^{0.14}$  is empirical and is called the Sieder-Tate term.

### Hausen Correlation

The Hausen equation (12) predicts the average Nusselt number for constant wall temperature and fully developed velocity profile:

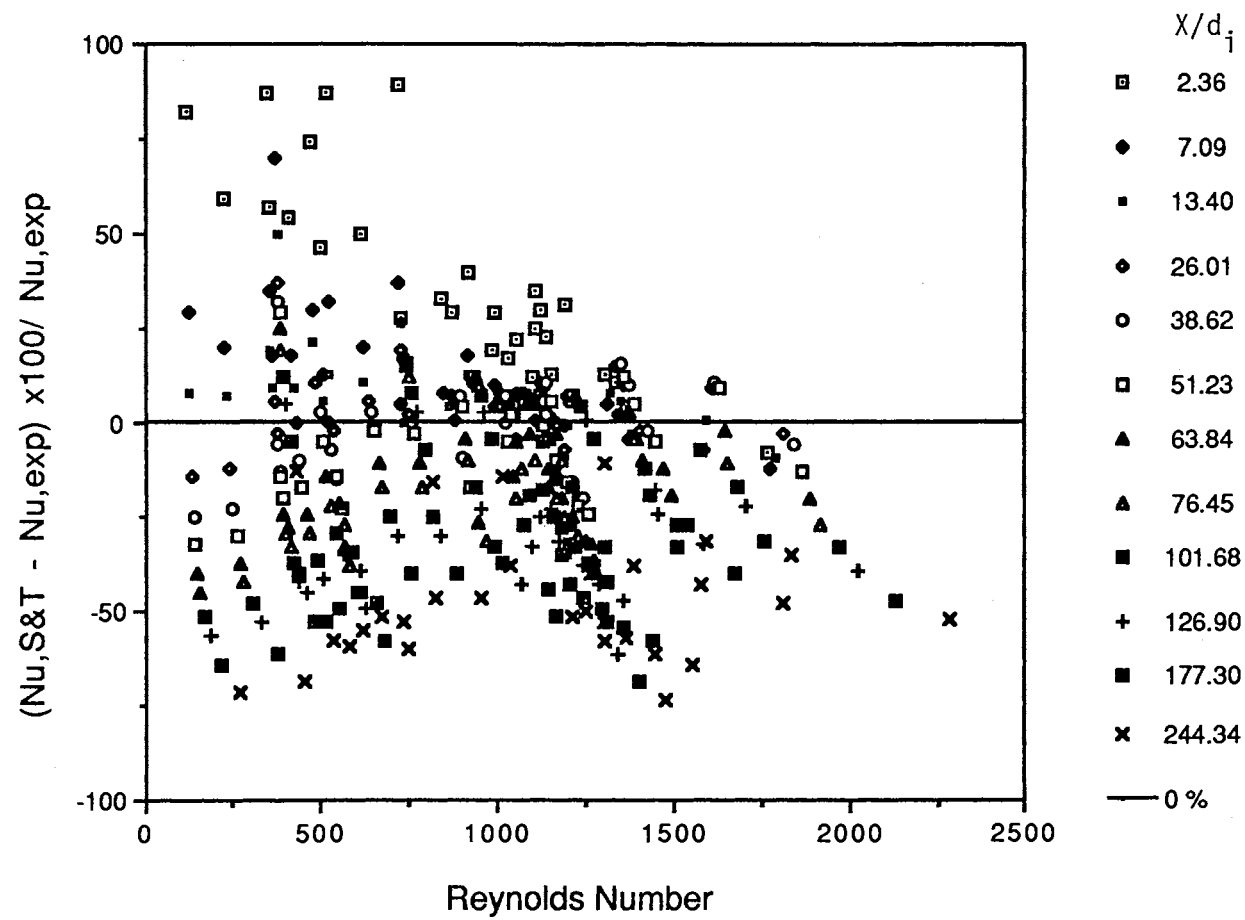


Figure 20: Comparison between the Experimental Nusselt Numbers and the Nusselt Number Predicted by Sieder and Tate as a Function of Reynolds Number for  $121 < Re < 2,300$

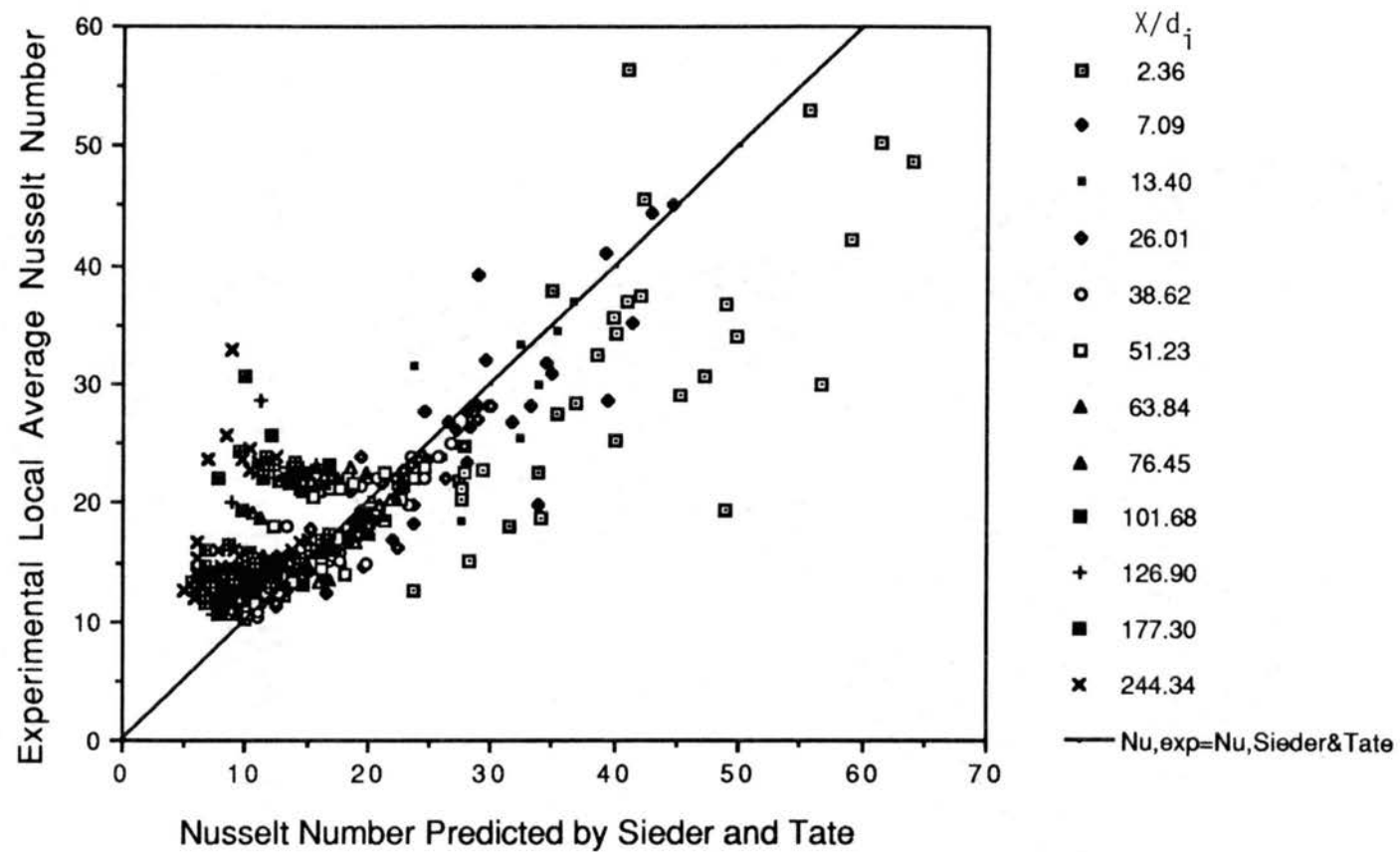


Figure 21: Comparison between the Experimental Nusselt Numbers and the Nusselt Numbers Predicted by Sieder and Tate

$$\underline{Nu} = \{3.66 + 0.0668Gz / (1 + 0.04Gz^{2/3})\} (\mu_b/\mu_w)^{0.14} \quad (VI.8)$$

The converted form is:

$$Nu = \{4.364 + [(0.0445Gz + 0.00356Gz^{5/3}) / (1 + 0.04Gz^{2/3})^2]\} (\mu_b/\mu_w)^{0.14} \quad (VI.9)$$

This equation does not consider the natural convection effects. The 3.66 term in equation (VI.8) was changed to 4.364 for the constant heat flux. Also the Sieder-Tate term for viscosity correction was added to the Hausen equation. Figures 22 and 23 show that Hausen overpredicted the Nusselt number for  $X/d_i$  less than 100 and underpredicted the Nusselt number for  $X/d_i$  greater than 100 for most runs.

#### Eubank and Proctor Correlation

Eubank and Proctor(9) introduced the following equation for laminar flow in horizontal tubes:

$$\underline{Nu} = 1.75\{Gz + 0.04(GrPrd_i/X)^{0.75}\}^{1/3} (\mu_b/\mu_w)^{0.14} \quad (VI.10)$$

$$Nu = 1.75\{Gz + 0.04(GrPrd_i/X)^{0.75}\}^{1/3} (\mu_b/\mu_w)^{0.14} - 0.583[Gz + 0.03(GrPrd_i/X)^{0.75}] / [Gz + 0.04(GrPrd_i/X)^{0.75}]^{2/3} (\mu_b/\mu_w)^{0.14} \quad (VI.11)$$

Figures 24 and 25 show that Eubank and Proctor overpredicted the Nusselt number for  $X/d_i$  less than 30 and underpredicted for  $X/d_i$  greater than 30 for most runs.

#### Siegwarth Correlation

The Siegwarth equation (II.4) is for fully developed



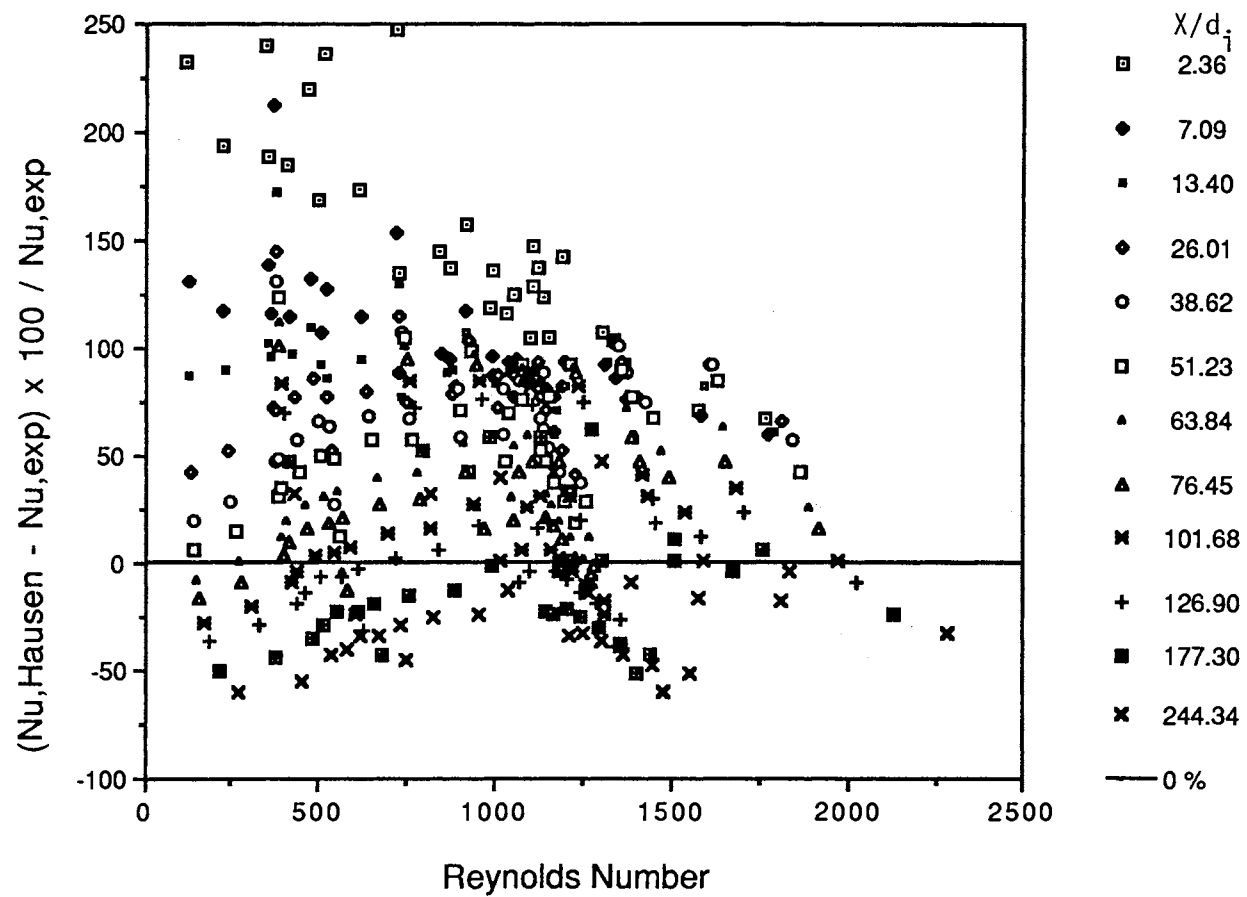


Figure 22: Comparison between the Experimental Nusselt Numbers and the Nusselt Number Predicted by Hausen as a Function of Reynolds Number for  $121 < Re < 2,300$

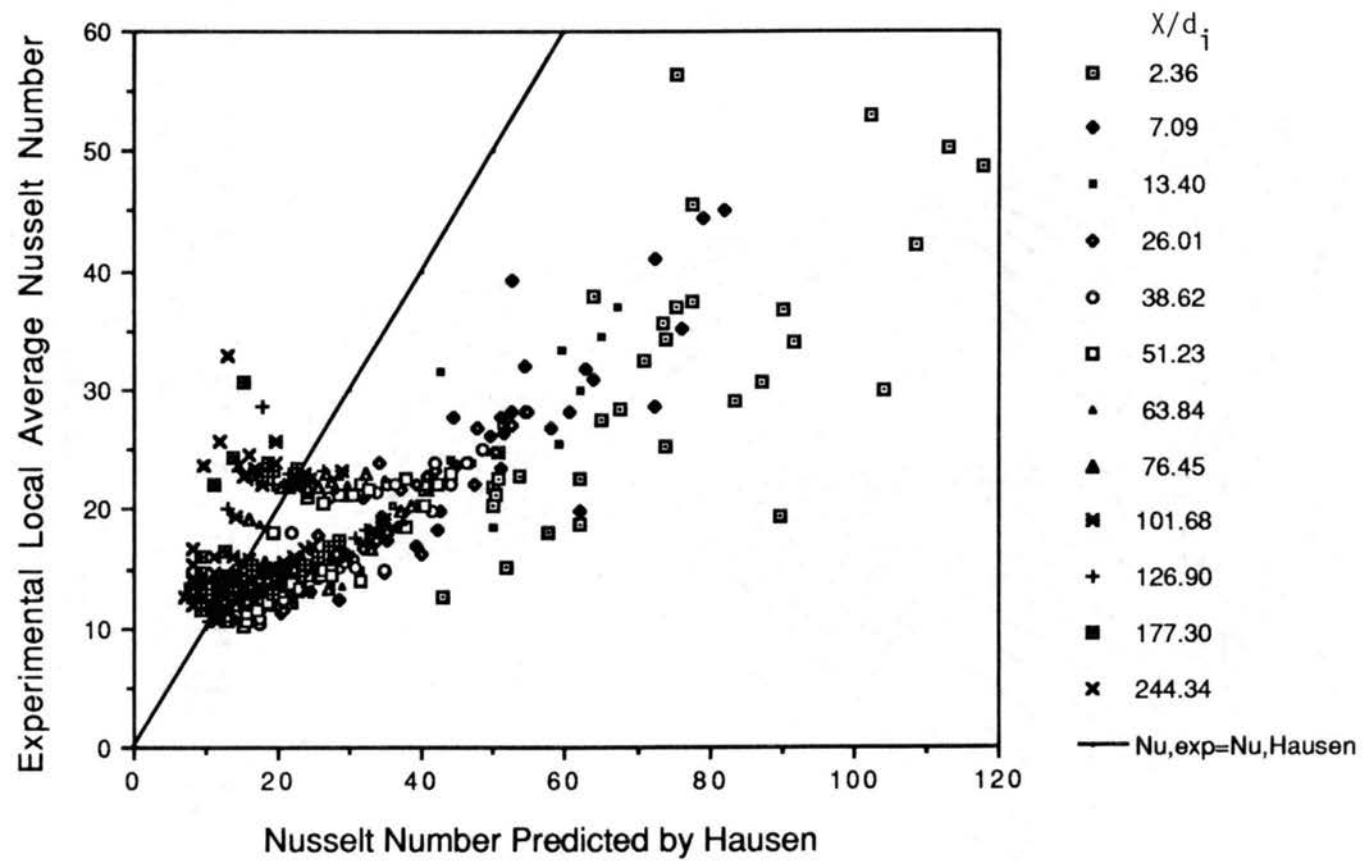


Figure 23: Comparison between the Experimental Nusselt Numbers and the Nusselt Numbers Predicted by Hausen

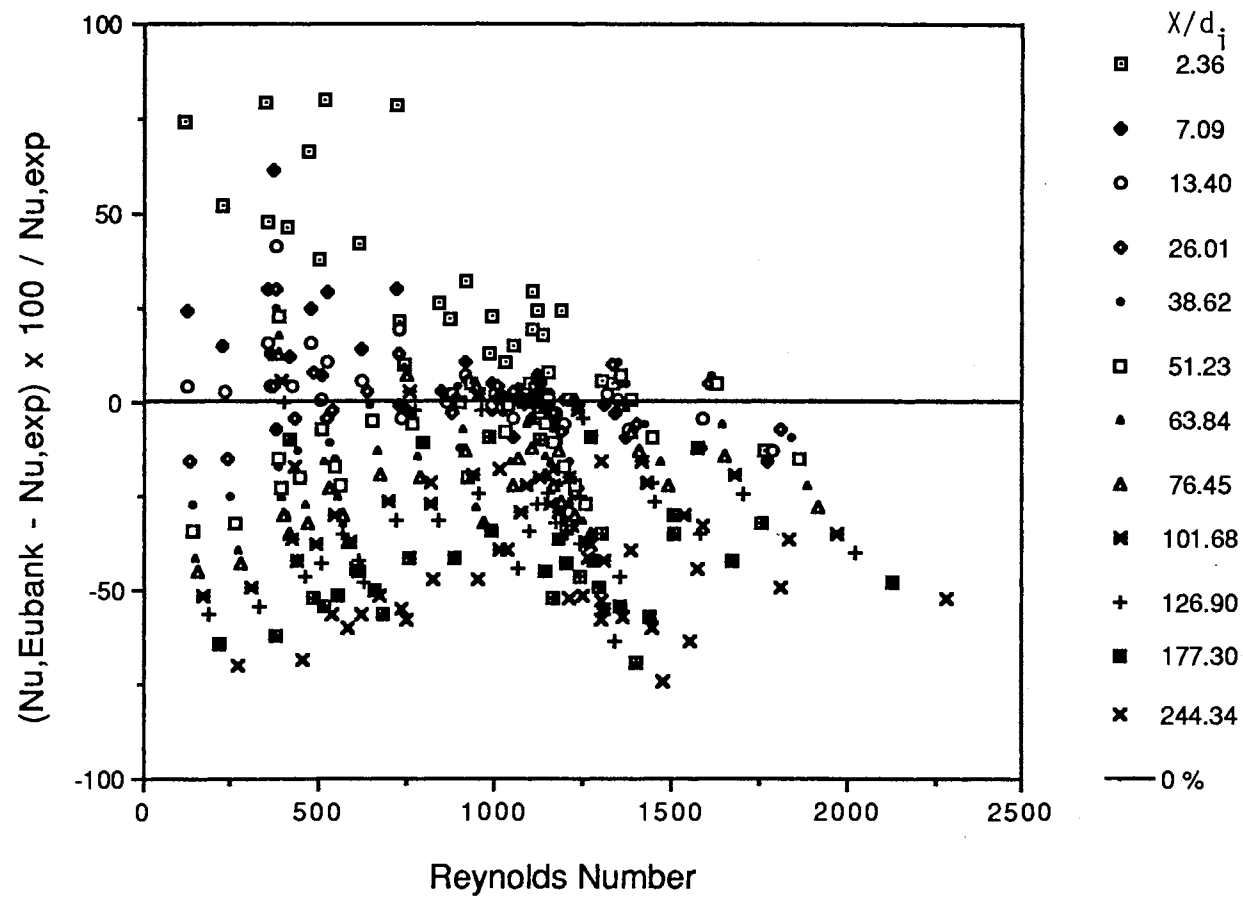


Figure 24: Comparison between the Experimental Nusselt Numbers and the Nusselt Numbers Predicted by Eubank and Proctor as a Function of Reynolds Number for  $121 < Re < 2,300$

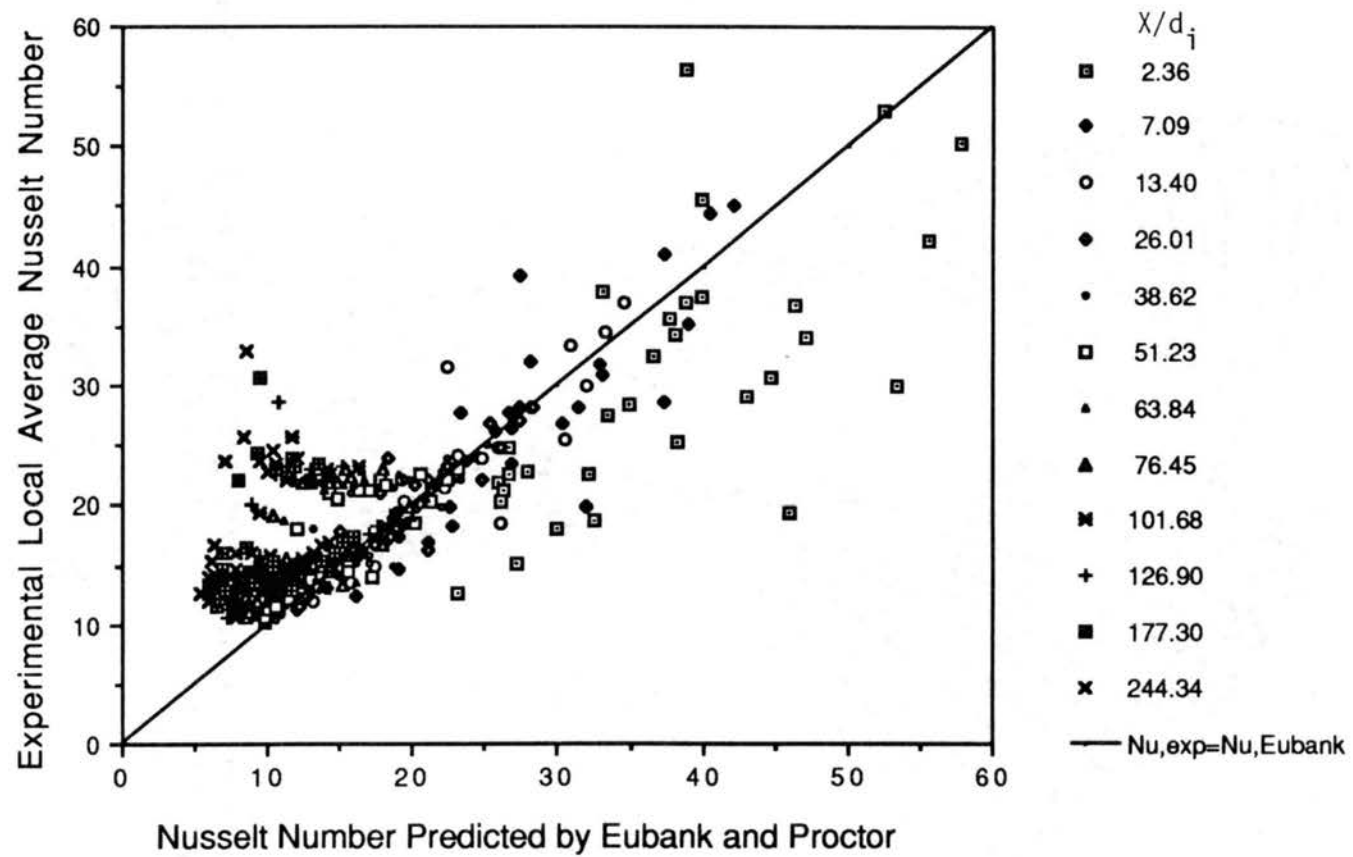


Figure 25: Comparison between the Experimental Nusselt Numbers and the Nusselt Numbers Predicted by Eubank and Proctor

laminar flow in straight tubes. Figures 26 and 27 show that Siegwarth underpredicted the Nusselt number for  $X/d_i$  less than 50. Generally, it predicts within  $\pm 25\%$  for  $X/d_i$  over 50. But the Siegwarth correlation does not take into account the fully developed forced convection component.

#### Hong, Morcos and Bergles Correlation

Hong, Morcos and Bergles (13) presented the following correlation for laminar flow in horizontal circular tubes with constant heat flux:

$$Nu_f = 0.378Gr_f^{0.28}Pr_f^{0.33}/Pw^{0.12} \quad (VI.12)$$

where  $Pw = (hd_i/K_w)(d_i/t)$

All of the dimensionless groups are calculated at the film temperature, which is defined as  $T_f = (T_{wi} + T_b)/2$ .

As shown in Figures 28 and 29, the Hong, Morcos and Bergles correlation underpredicted the Nusselt number for most of the runs with  $X/d_i$  less than 50 and overpredicted the Nusselt number by about 10% for most of the runs with  $X/d_i$  greater than 50. Figures 28 and 29 show the comparisons between the experimental Nusselt numbers and the predicted Nusselt numbers.

#### Morcos and Bergles Correlation

The Morcos and Bergles equation (II.5) for fully developed laminar flow in a straight tube was compared with

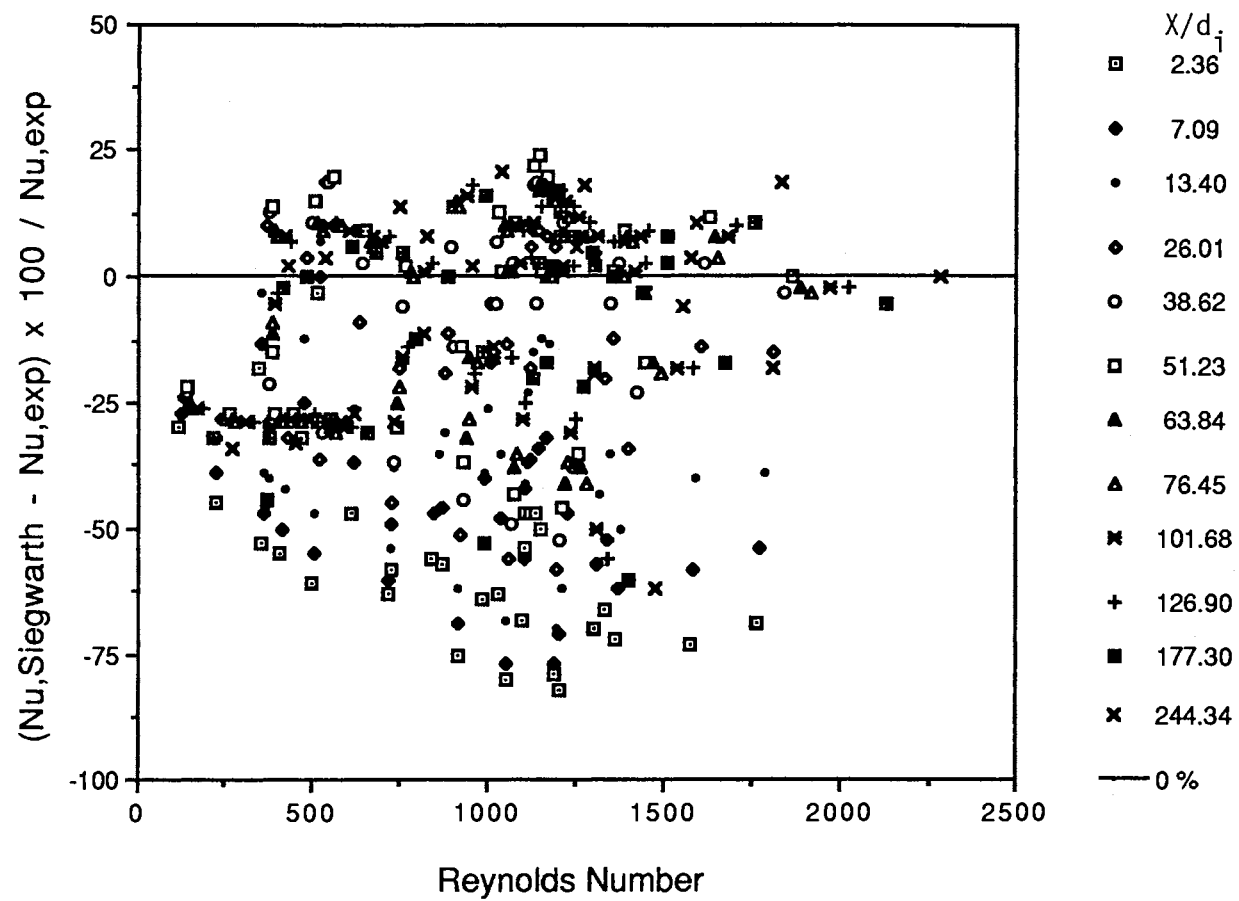


Figure 26: Comparison between the Experimental Nusselt Numbers and the Nusselt Numbers Predicted by Siegwarth as a Function of Reynolds Number for  $121 < Re < 2,300$ .

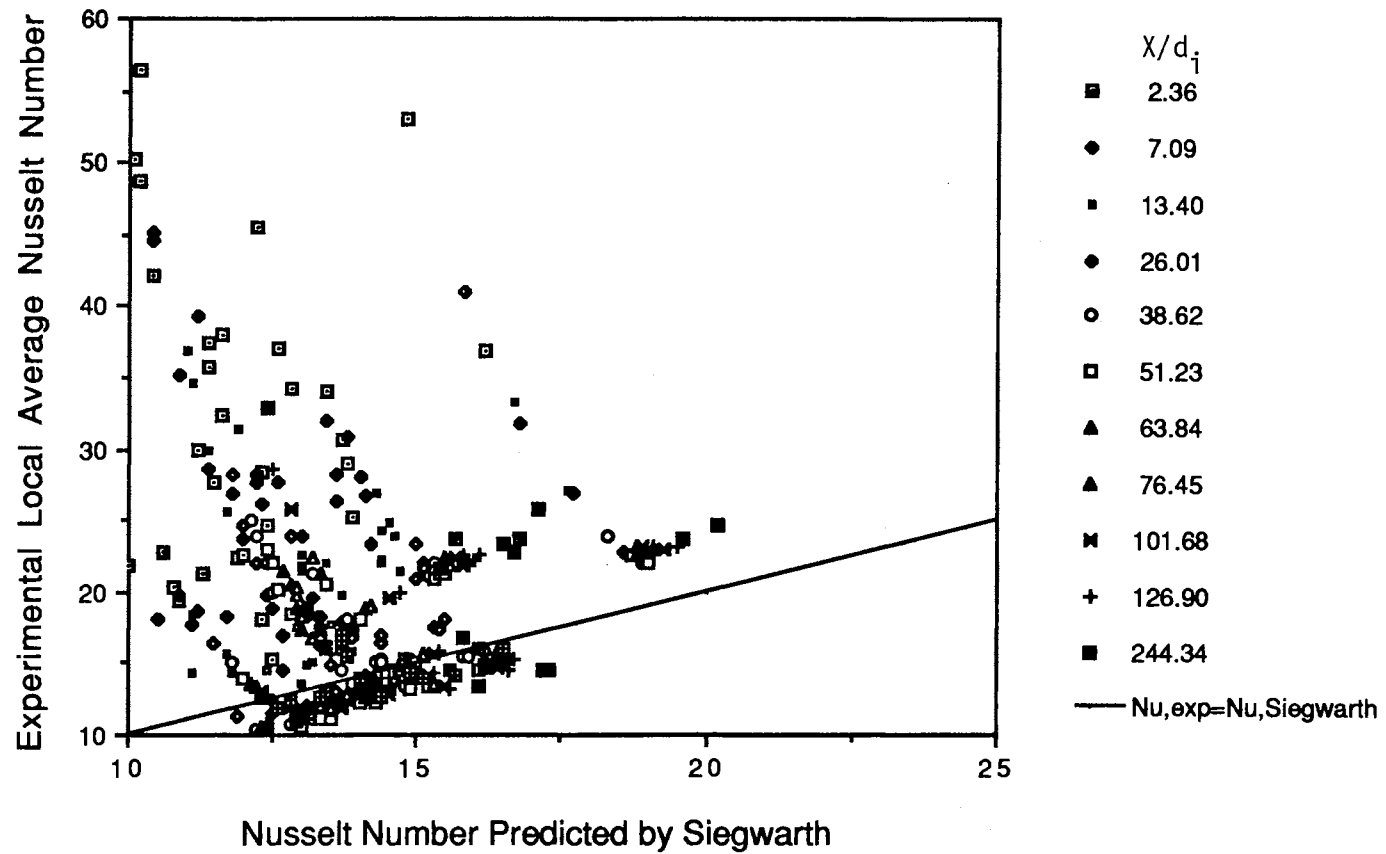


Figure 27: Comparison between the Experimental Nusselt Numbers and the Nusselt Numbers Predicted by Siegwarth

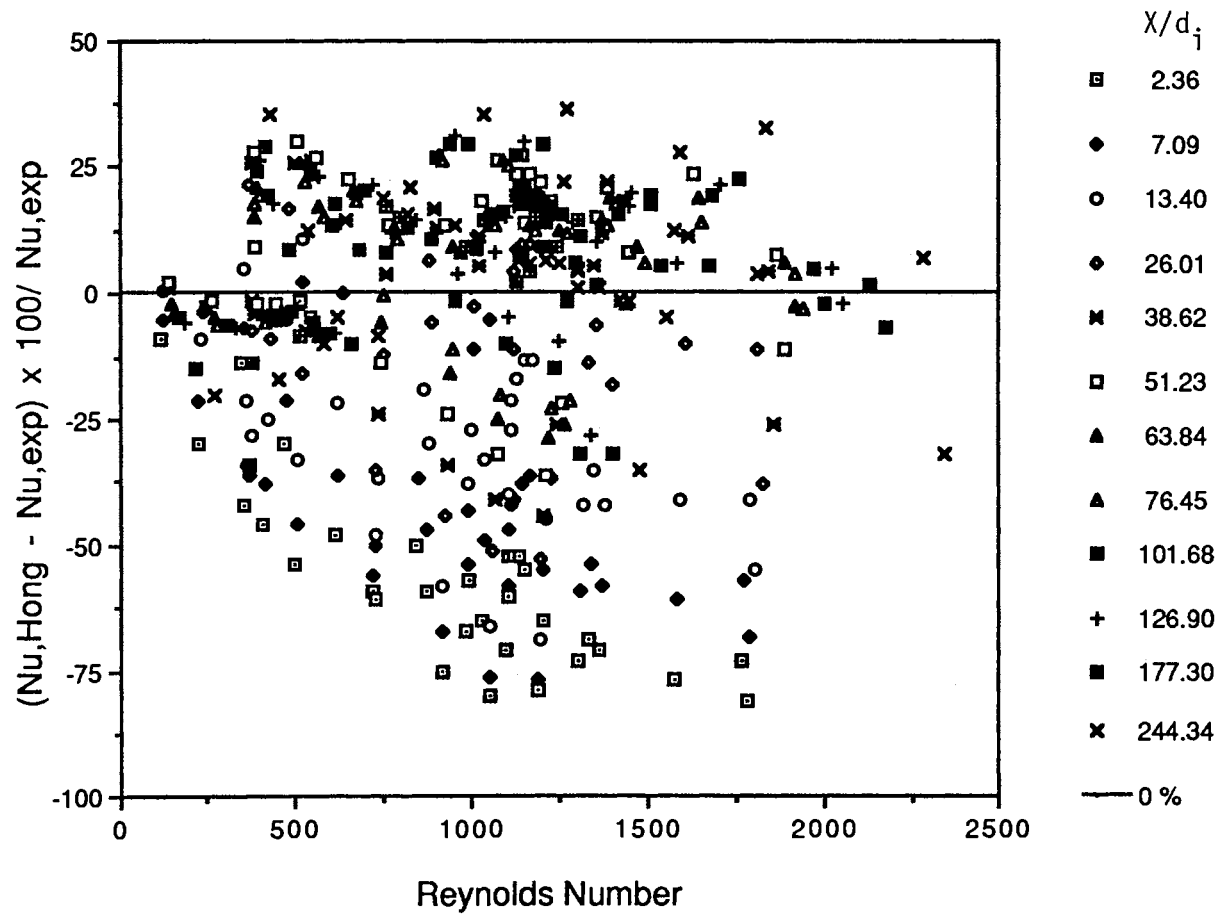
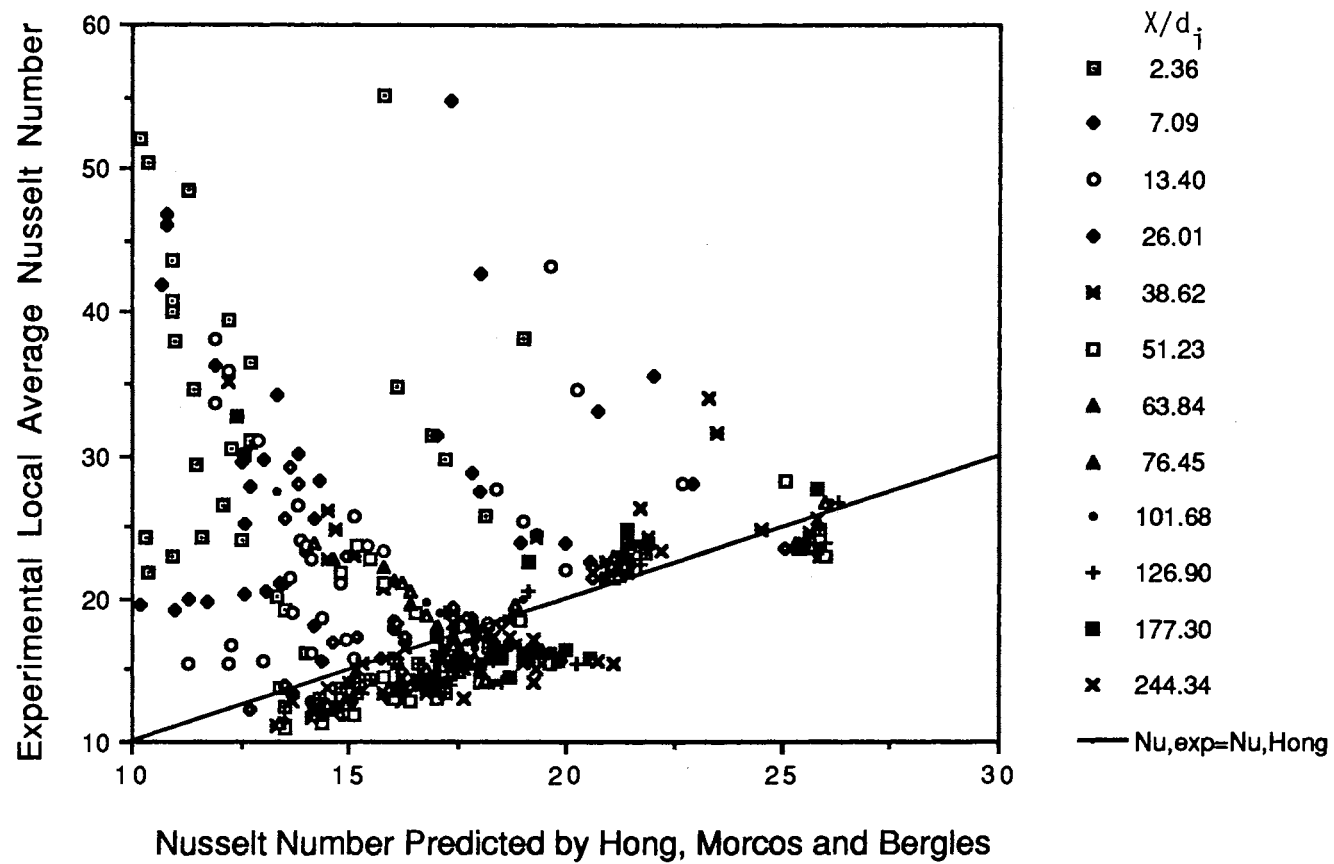


Figure 28: Comparison between the Experimental Nusselt Numbers and the Nusselt Numbers Predicted by Hong, Morcos, and Bergles as a Function of Reynolds Number for  $121 < Re < 2,300$





experimental results at each station. The dimensionless groups in equation (II.5) were calculated at the film temperature.

As shown in Figures 30 and 31, the Morcos and Bergles correlation behaved very similar to the Hong, Morcos and Bergles correlation. The Morcos and Bergles correlation also overpredicted the Nusselt number for stations far away the entrance.

#### Sieder and Tate Correlation

Sieder and Tate (44) presented the following correlation for turbulent flow in horizontal tubes:

$$Nu = 0.023 \cdot Re^{0.8} Pr^{1/3} (\mu_b/\mu_w)^{0.14} \quad (VI.13)$$

As shown in Figures 32 and 33, the Sieder-Tate correlation for turbulent flow underpredicted the Nusselt number for all runs with  $X/d_i < 10$ . For  $X/d_i > 10$ , the Sieder-Tate correlation underpredicted all runs with  $Re$  greater than 7,000 by less than 10 %.

#### Petukhov and Popov Correlation

Petukhov and Popov (35) presented the following correlation for turbulent flow in horizontal tubes:

$$Nu = \frac{\xi Re Pr / 8}{1.07 + 12.7 \sqrt{\xi / 8} (Pr^{2/3} - 1)} \quad (VI.14)$$

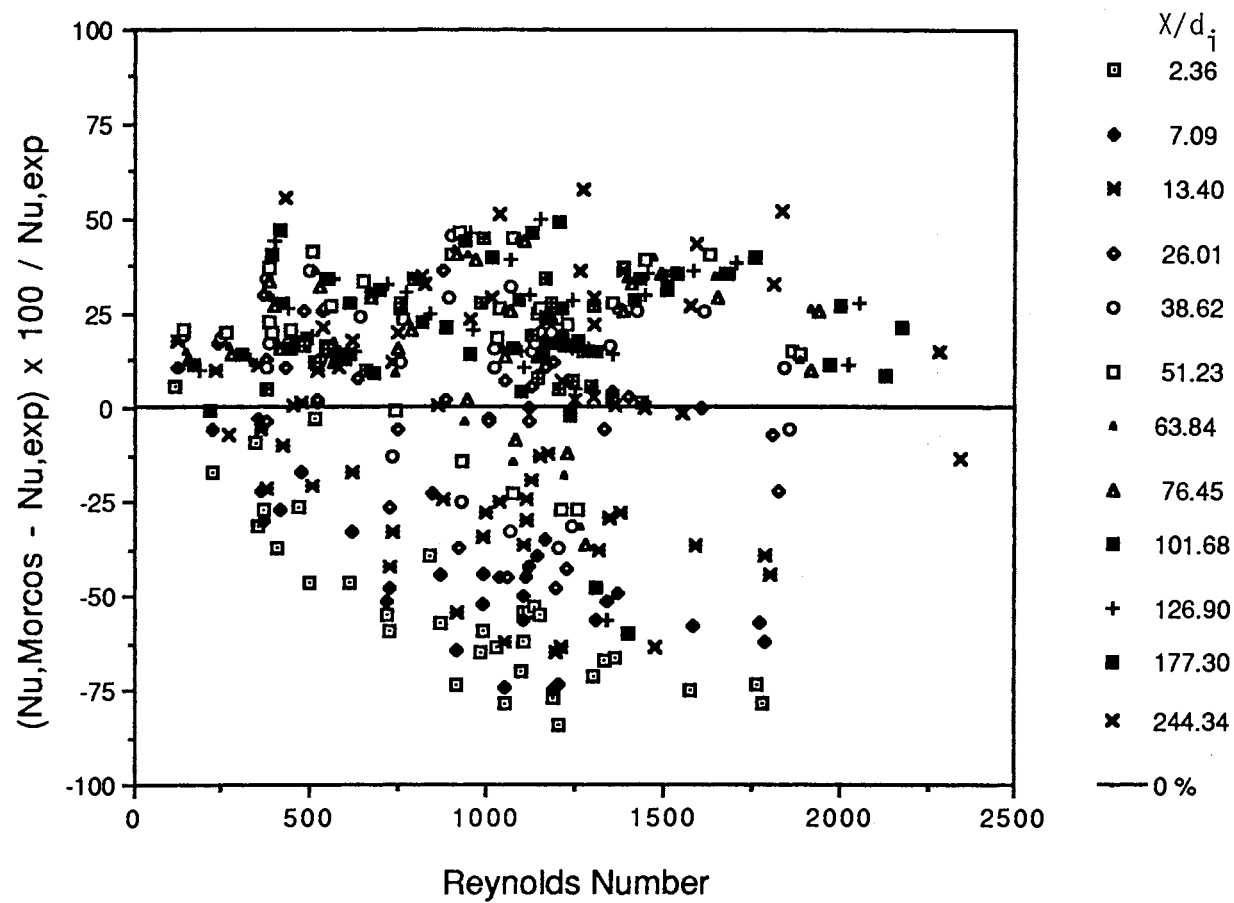


Figure 30: Comparison between the Experimental Nusselt Numbers and the Nusselt Numbers Predicted by Morcos and Bergles as a Function of Reynolds Number for  $121 < Re < 2,300$

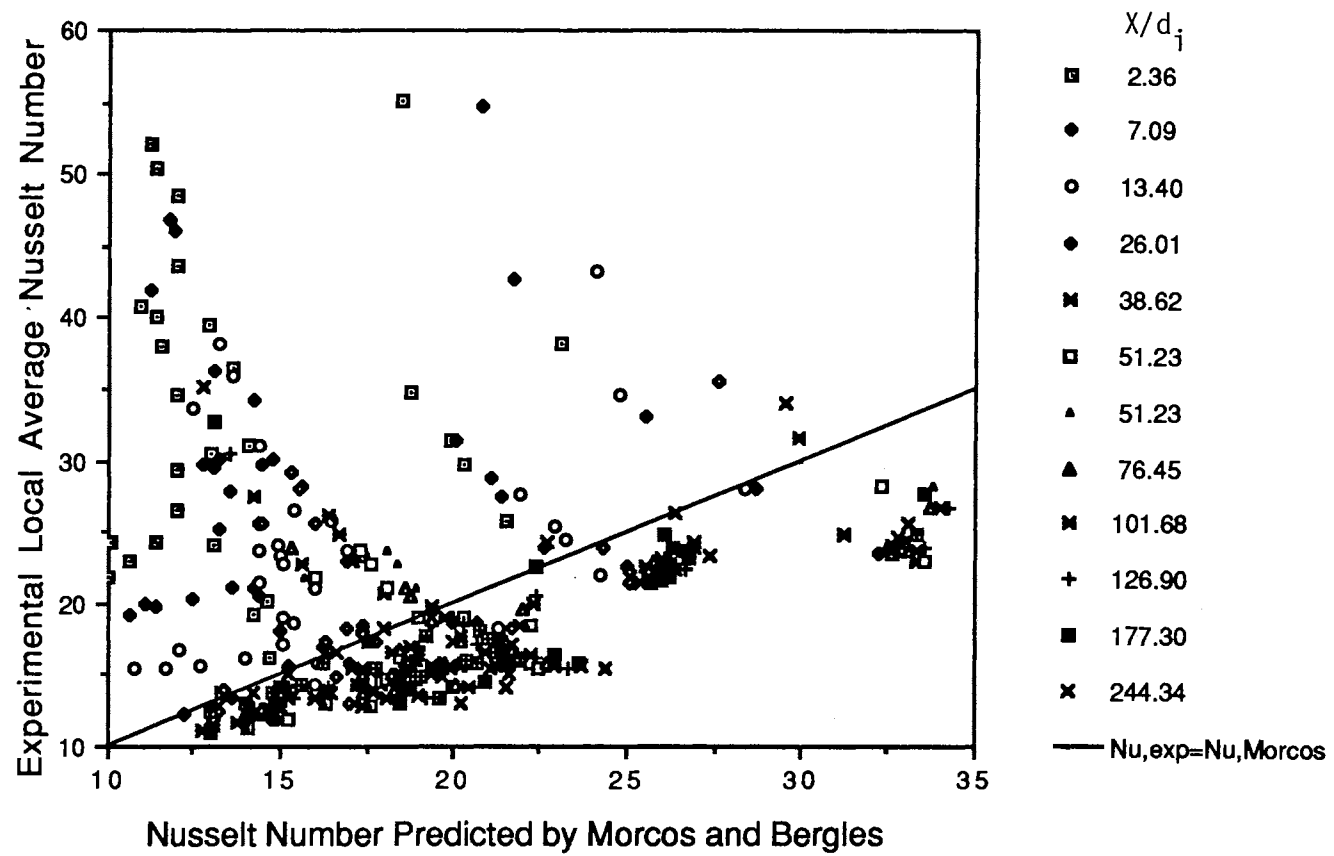


Figure 31: Comparison between the Experimental Nusselt Numbers and the Nusselt Numbers Predicted by Morcos and Bergles

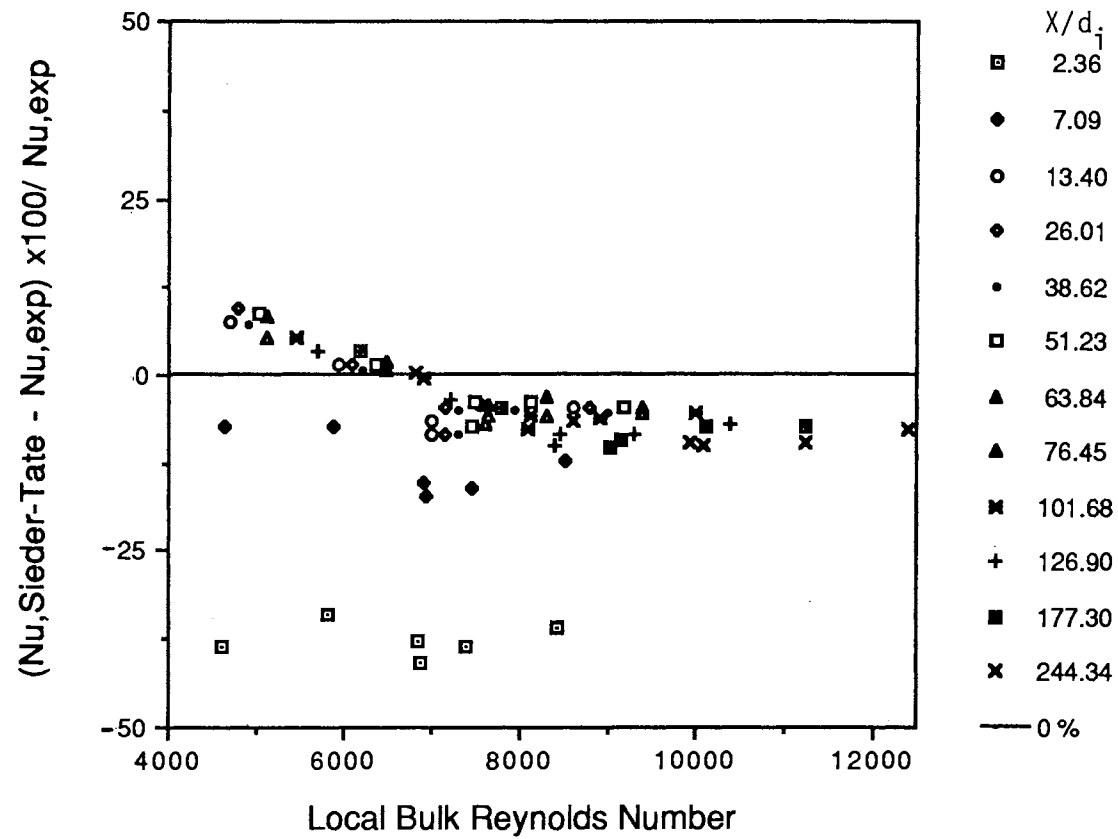


Figure 32: Comparison between the Experimental Nusselt Numbers and the Nusselt Numbers Predicted by Sieder and Tate as a Function of Reynolds Number for  $4,600 < Re < 12,400$

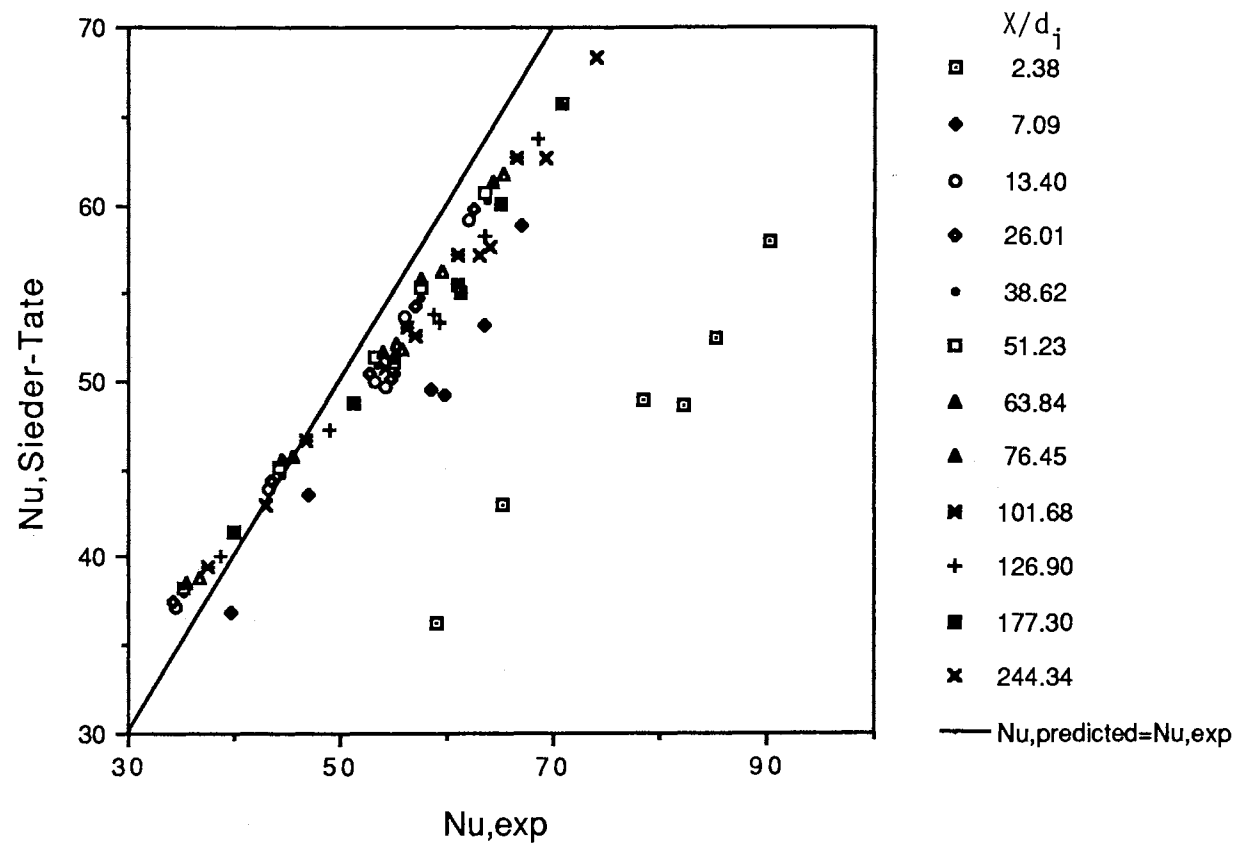


Figure 33: Comparison between the Experimental Nusselt Numbers and the Nusselt Numbers Predicted by Sieder and Tate

where  $\xi = \frac{1}{[1.82 \cdot \log_{10}(\text{Re}) - 1.64]^2}$

As shown in Figures 34 and 35, the Petukhov-Popov correlation for turbulent flow underpredicted the Nusselt number for all runs with  $X/d_i < 5$ . For  $X/d_i > 10$ , the Petukhov-Popov correlation overpredicted all runs. With Re greater than 7,000 The Petukhov-Popov correlation overpredicted by less than 10 %. For  $X/d_i > 200$ , the deviations are less than 5 %. The Petukhov-Popov correlation predicts the Nusselt numbers in the lower turbulent slightly better than the Sieder-Tate correlation, i.e. eq'n (VI.1).

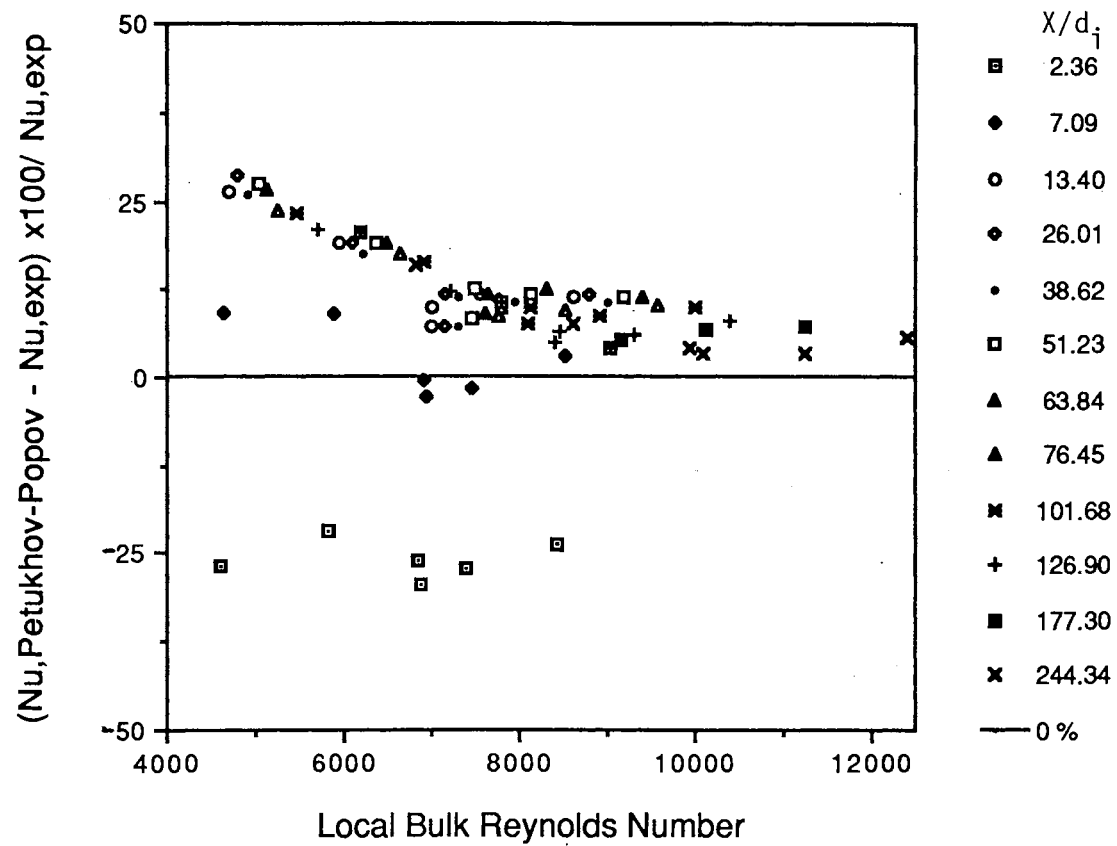


Figure 34: Comparison between the Experimental Nusselt Numbers and the Nusselt Numbers Predicted by Petukhov and Popov as a Function of Reynolds Number for  $4,600 < Re < 12,400$



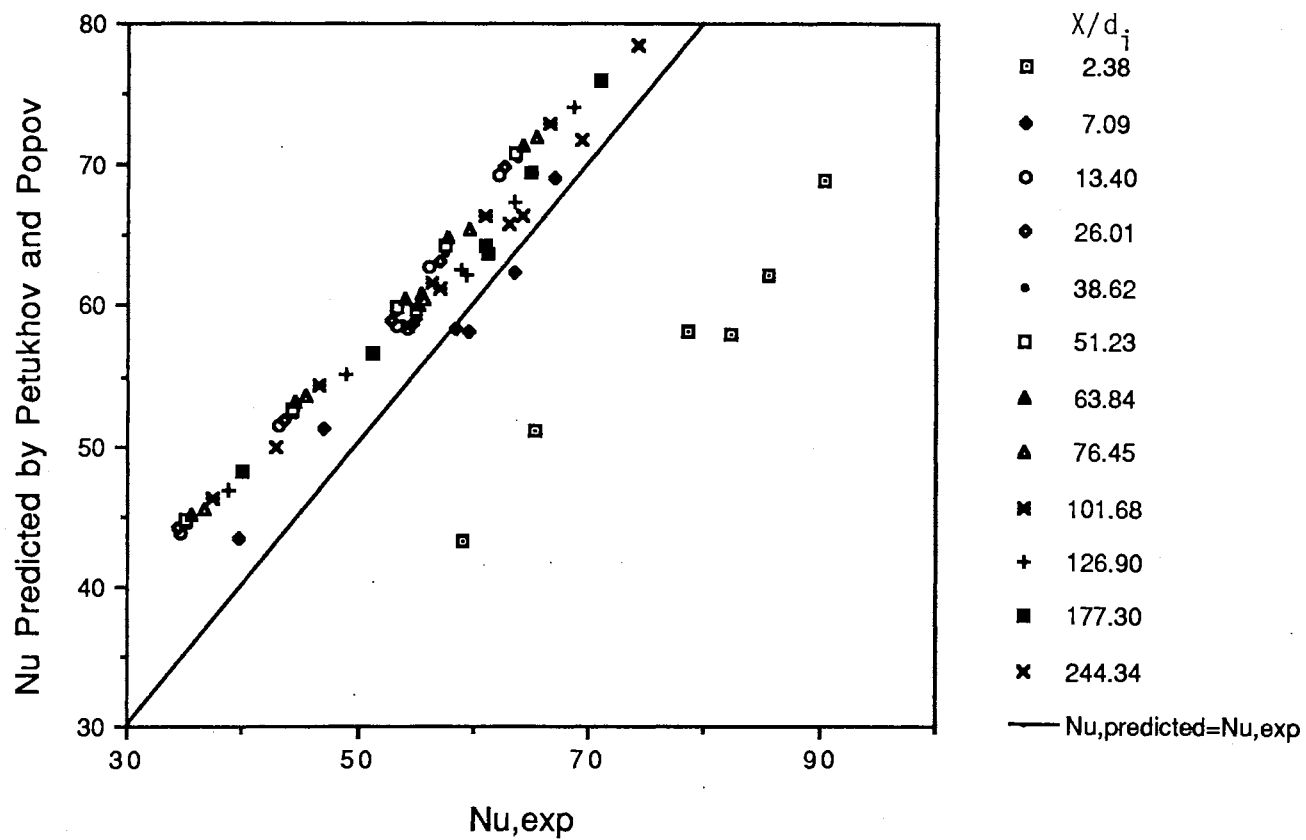


Figure 35: Comparison between the Experimental Nusselt Numbers and the Nusselt Numbers Predicted by Petukhov and Popov

## CHAPTER VII

### DEVELOPMENT OF THE CORRELATIONS

Experimental data were gathered for 48 runs. For each run, data were collected at 12 stations along the length of the tube. Each station has either 4 or 8 peripheral positions. The heat transfer coefficients at each station were averaged by equation (V.6).

Most of the literature correlations were developed for straight circular tubes. The Hausen equation (VI.8) and the Sieder and Tate equation (VI.6) do not explicitly include the effects of natural convection. Although the Hong, Morcos and Bergles equation (VI.12) and the Morcos and Bergles equation (II.5) considered the natural convection, their correlations are in principle only applicable to the fully developed flow in a straight tube. Since none of the literature correlations are directly applicable to the present case (which is typical of the real situation in heat exchangers), it was necessary to develop a correlation that predicts the heat transfer coefficients for simultaneously developing velocity distributions and heat transfer in a straight round tube.

## Laminar Flow

For simultaneously developing velocity profile and heat transfer, three phenomena contribute towards the heat transfer process; these phenomena are the entrance effect, the forced convection(primary) flow, and the natural convection(secondary) flow. For purposes of developing the correlation, we have assumed that the forced convection and natural convection terms are additive. We also assume that there are entrance effects on both forced convection and natural convection. Therefore, we can express the local average heat transfer coefficient equation in the following form:

$$\begin{aligned} \text{Nu} = & (\text{forced convection expression}) \cdot (\text{entrance effect term}) \\ & + (\text{natural convection expression}) \\ & \cdot (\text{entrance effect term}) \end{aligned} \quad (\text{VII.1})$$

The forced convection expression consists of two terms. The first term of the forced convection expression is the value for the developed velocity and temperature profile, calculated by equation (II.1),  $\text{Nu} = 48/11 = 4.364$ . The entrance effect for the forced convection contribution is very large at the entrance region and decreases dramatically after that; this effect is assumed to be a function of the Reynolds and Prandtl numbers. An exponential function  $[1+A \cdot \exp(-B \cdot X/d_1)]$  is introduced to account for the entrance effect on forced convection.

The natural convection expression is expected to be a function of the Grashof number and the Prandtl number, probably a function of their product. Natural convection is negligible at the entrance and increases toward the fully-developed value with distance. An exponential function  $[1 - \exp(-C \cdot X/d_i)]$  is introduced to account for the entrance effect on natural convection.

Experimental data for laminar flow,  $Re < 2,100$ , were correlated for 396 points, where each point represents one of the stations for each run. The resulting correlation for local average Nusselt number is:

$$Nu = \{4.364 + 0.00106Re^{0.81}Pr^{0.45} \cdot [1 + 14.0\exp(-0.063X/d_i)] + 0.268(GrPr)^{1/4} [1 - \exp(-0.042X/d_i)]\} \cdot (\mu_b/\mu_w)^{0.14} \quad (VII.1)$$

Equation (VII.1) is valid for:

$$121 \leq Re \leq 2,100$$

$$3.5 \leq Pr \leq 282.4$$

$$930 \leq Gr \leq 67,300$$

The Sieder and Tate viscosity correction factor,  $(\mu_b/\mu_w)^{0.14}$ , has been included in the correlation. The dimensionless groups are calculated at the local bulk fluid temperature. A computer program originally written by Chandler(4) and modified by the author (with the normalization techniques to increase the accuracy of predicting the exponents) was used to fit the experimental data to equation (VII.1).

Equation (VII.1) was compared with the experimental

data as shown in Figures 36 and 37. Equation (VII.1) has an absolute average deviation of 2.90 and an absolute average per cent deviation of 12.9 %.

Equation (VII.1) has two limiting cases. For the first case, close to the entrance with  $X$  nearly zero, the forced convection is magnified fourteen times by the entrance effect term and the natural convection term is nearly zero. The second case is for large  $X$ , for which the natural convection term reaches 57 % of the predicted contribution from the fully developed natural convection from the Siegwarth equation.

#### Lower Turbulent Flow

For Reynolds numbers greater than 7,000, natural convection does not appear to be a major factor in the heat transfer. Nusselt number is no longer a function of the Grashof and Prandtl numbers' product which accounts for the natural convection contribution. As we can see from Figure 13, the Nusselt number is a function of Reynolds number to the 0.86 power. There is an entrance effect on the forced convection. By using the same fitting program, the following correlation is obtained:

$$Nu = 0.01426Re^{0.86}Pr^{1/3}\{1+1.15\exp[-X/(3.0\cdot d_i)]\}\cdot(\mu_b/\mu_w)^{0.14} \quad (VII.2)$$

Equation (VII.2) is valid for:

$$7,000 \leq Re \leq 12,400$$

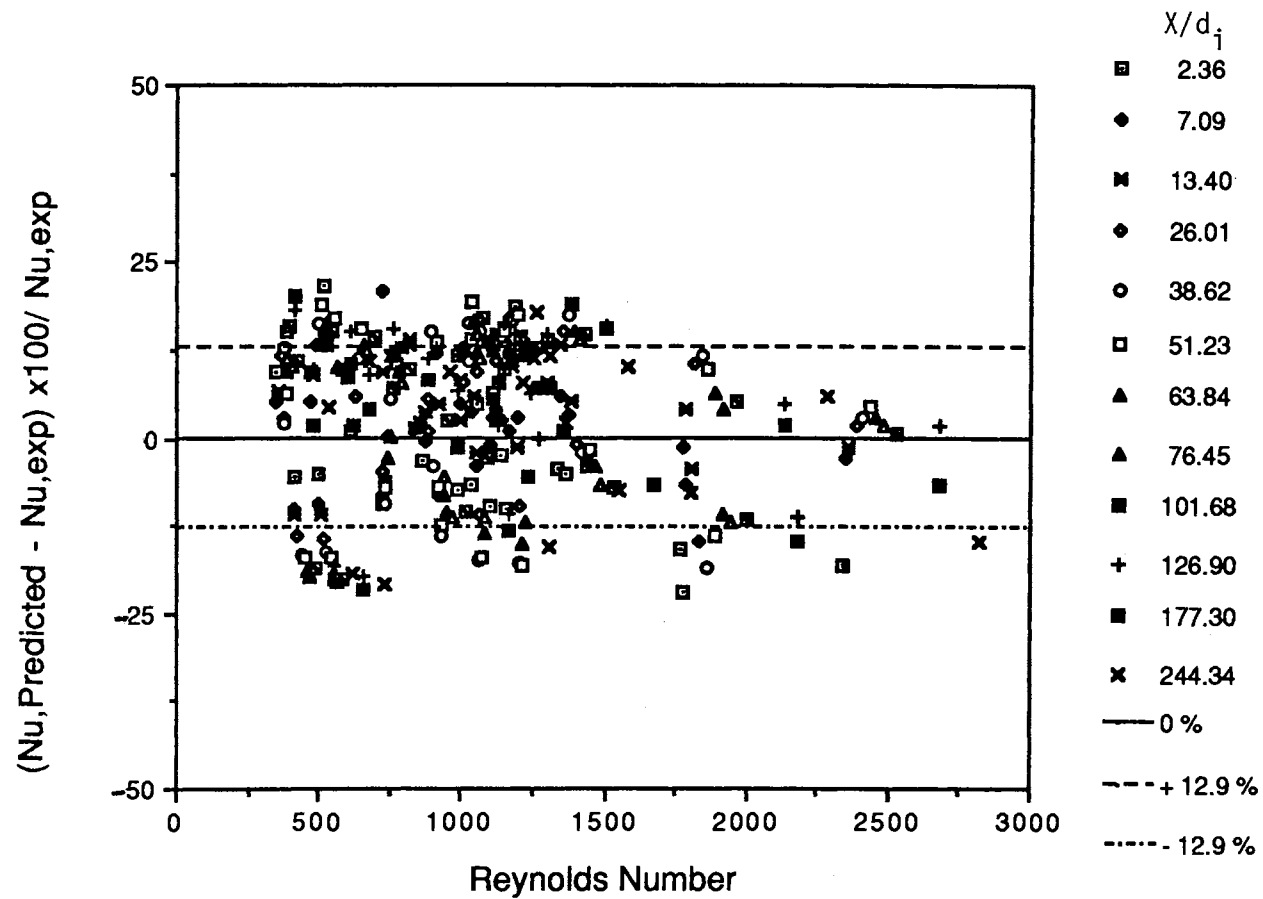


Figure 36: Comparison between the Experimental Nusselt Number and the Nusselt Number Predicted by Equation (VII.1) as a Function of Reynolds Number for  $270 < Re < 2,800$

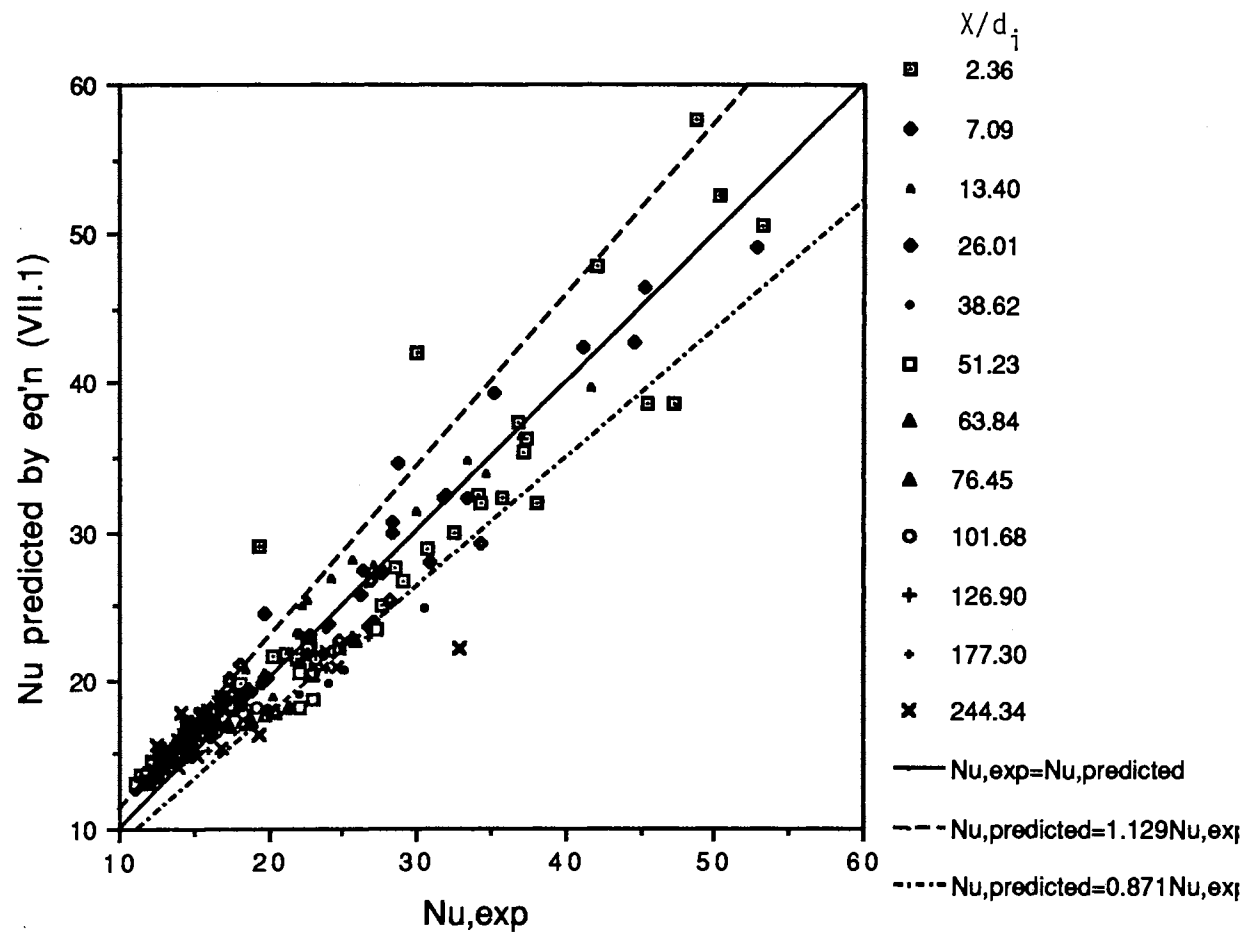


Figure 37: Comparison between the Experimental Nusselt Number and the Nusselt Number Predicted by Equation (VII.1)

$$3.5 \leq Pr \leq 7.4$$

$$45,570 \leq Gr \leq 1,040,000$$

Equation (VII.2) was compared with the experimental data as shown in Figures 38 and 39. Equation (VII.2) has a lower magnitude of entrance effect, 1.15 times the fully-developed value, than equation (VII.1). Also equation (VII.2) shows an entrance effect on the section close to the entrance for  $X/d_i$  less than 14 only.

#### Upper Transition Flow

The flow with Reynolds numbers between 4,600 and 7,000 is defined as upper transition flow. In the upper transition flow, the Nusselt number behaves very similarly to the lower turbulent flow. As we can see in Figure 14, the Nusselt number is a function of Reynolds number to the 1.03 power and the Prandtl number to the  $1/3$  power. Also, natural convection does not appear to be a major factor in heat transfer and the Nusselt number is no longer a function of the product of the Grashof number and Prandtl number as shown in Figure 14. By using the same fitting program, the following correlation is obtained:

$$Nu = 0.00392 Re Pr^{1/3} \{1 + 1.19 \exp(-0.308 X/d_i)\} \cdot (\mu_b/\mu_w)^{0.14} \quad (VII.3)$$

Equation (VII.3) is valid for:

$$4,600 \leq Re \leq 7,000$$

$$3.5 \leq Pr \leq 7.4$$

$$45,570 \leq Gr \leq 1,040,000$$



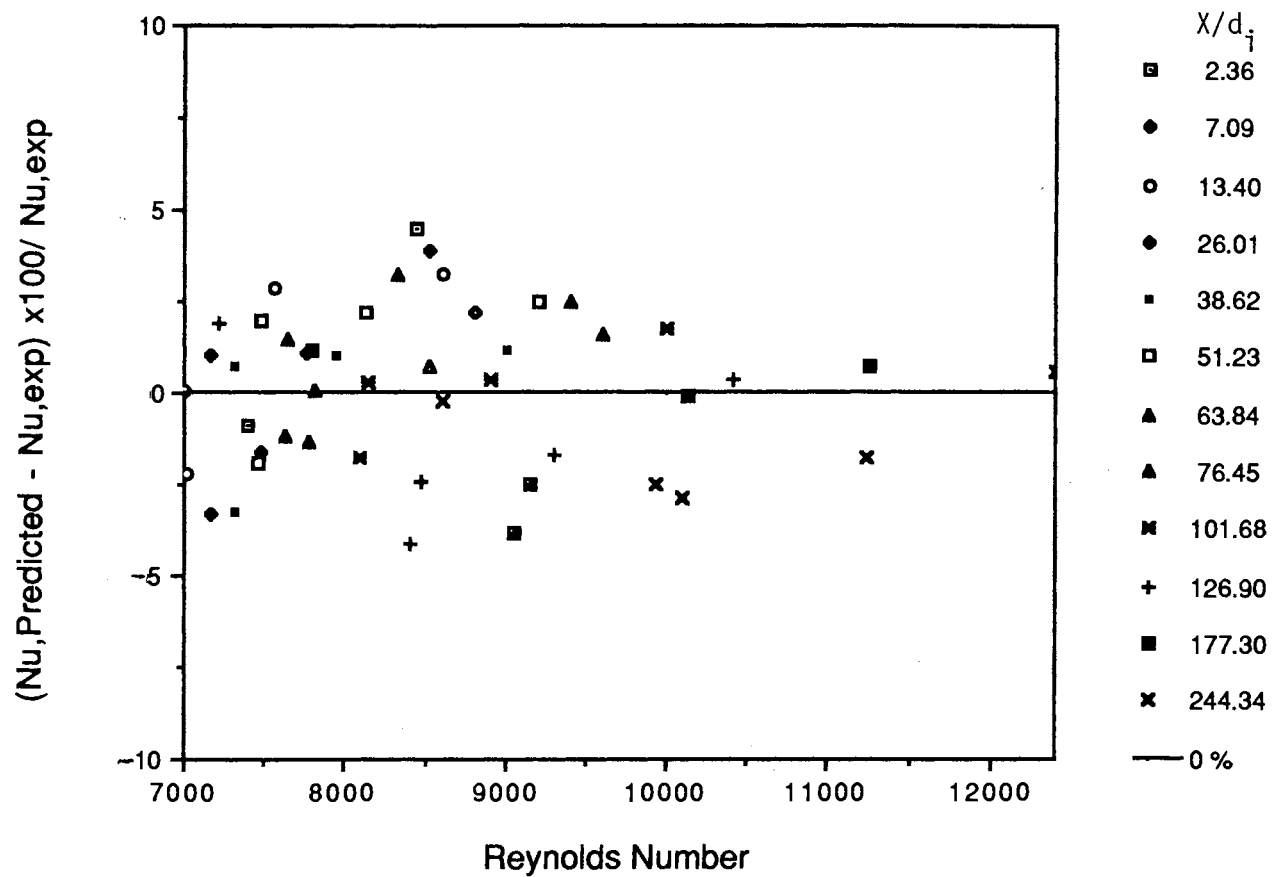


Figure 38: Comparison between the Experimental Nusselt Numbers and the Nusselt Numbers Predicted by Equation (VII.2) as a Function of Reynolds Number for  $7,000 < Re < 12,400$

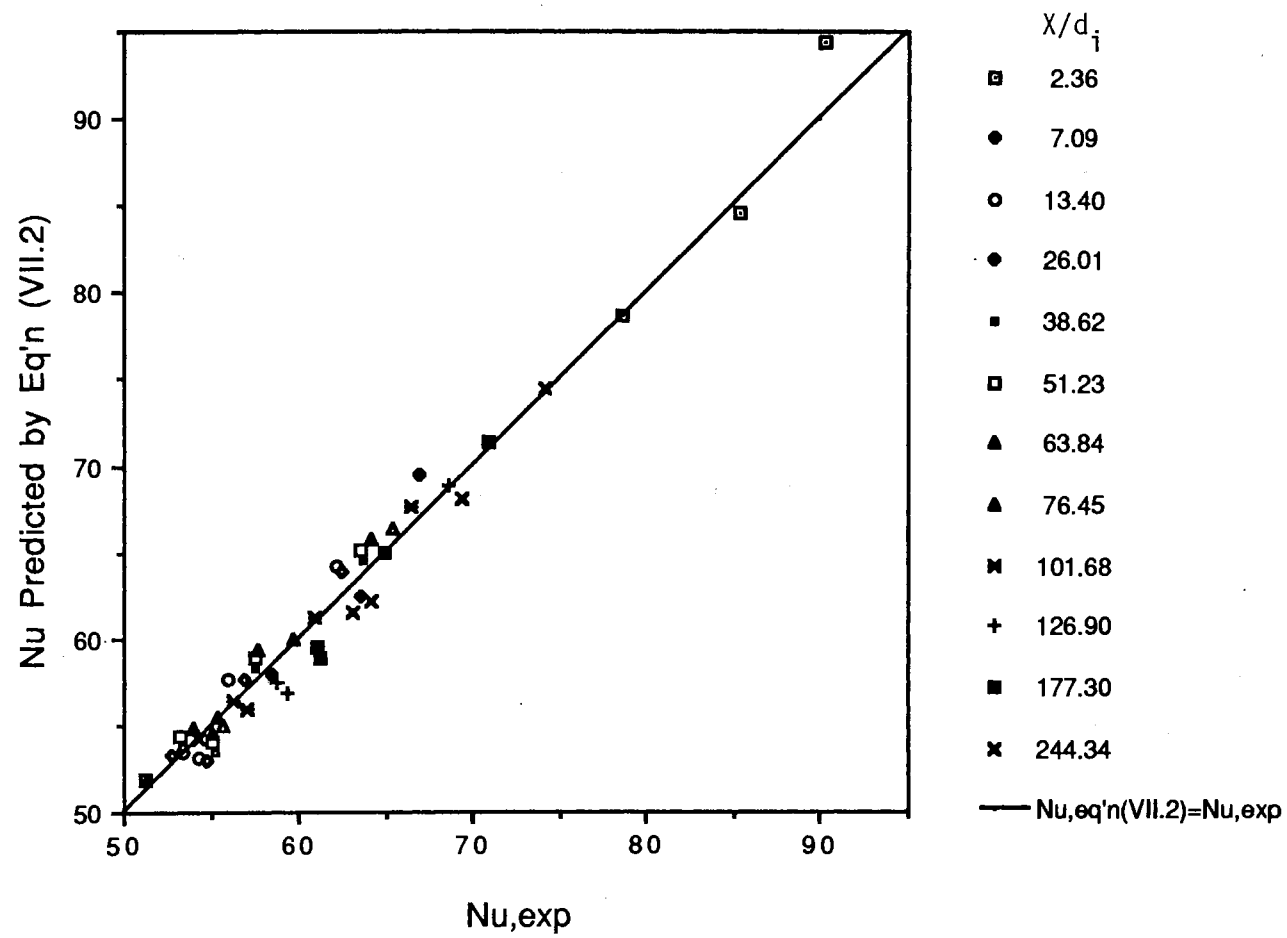


Figure 39: Comparison between the Experimental Nusselt Numbers and the Nusselt Numbers Predicted by Equation (VII.2)

Equation (VII.3) was compared with the experimental data as shown in Figures 40 and 41. Equation (VII.3) has a lower magnitude of entrance effect, 1.19, than equation (VII.1) and a similar but slightly higher entrance effect than equation (VII.2).

#### Lower Transition Flow

The experimental data in the flow regime with the Reynolds number between 2,100 and 4,600 scatter so much that no satisfactory correlation was derived. Linear interpolation of equations (VII.1) and (VII.2) is recommended as following:

$$y = (\text{Re} - 2100) / (4600 - 2100) \quad (\text{VII.4})$$

$$\text{Nu} = [(1-y) \cdot \text{Nu}_{(\text{VII.1})} + y \cdot \text{Nu}_{(\text{VII.3})}] \quad (\text{VII.5})$$

Figures 42 and 43 show the comparison between the experimental Nusselt numbers and the Nusselt numbers derived from equations (VII.4) and (VII.5). The average deviation for the Nusselt numbers calculated by equations (VII.4) and (VII.5) is 15.6 % which is only slightly higher than 12.9 % for equation (VII.1). Further study in this flow range is recommended.

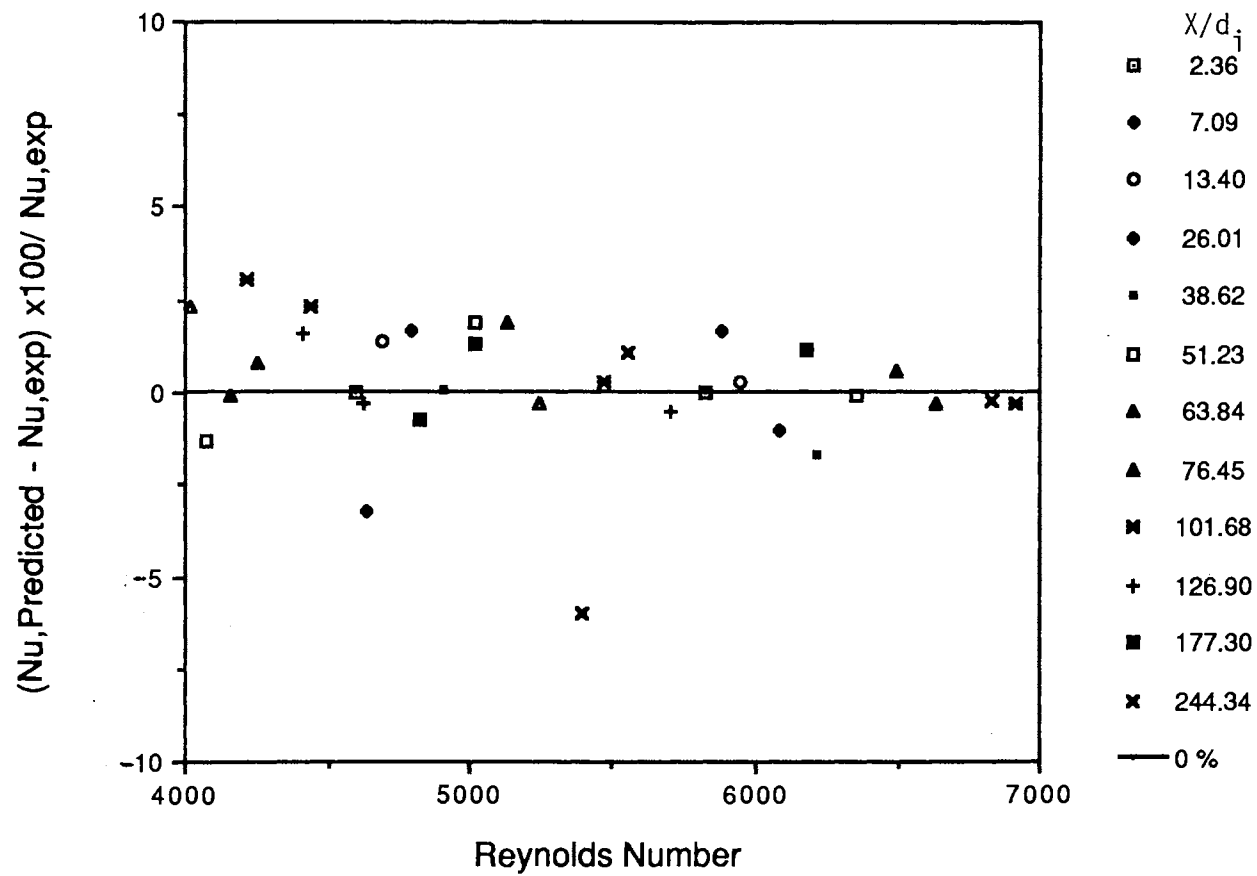


Figure 40: Comparison between the Experimental Nusselt Numbers and the Nusselt Numbers Predicted by Equation (VII.3) as a Function of Reynolds Number for  $4,000 < Re < 7,000$

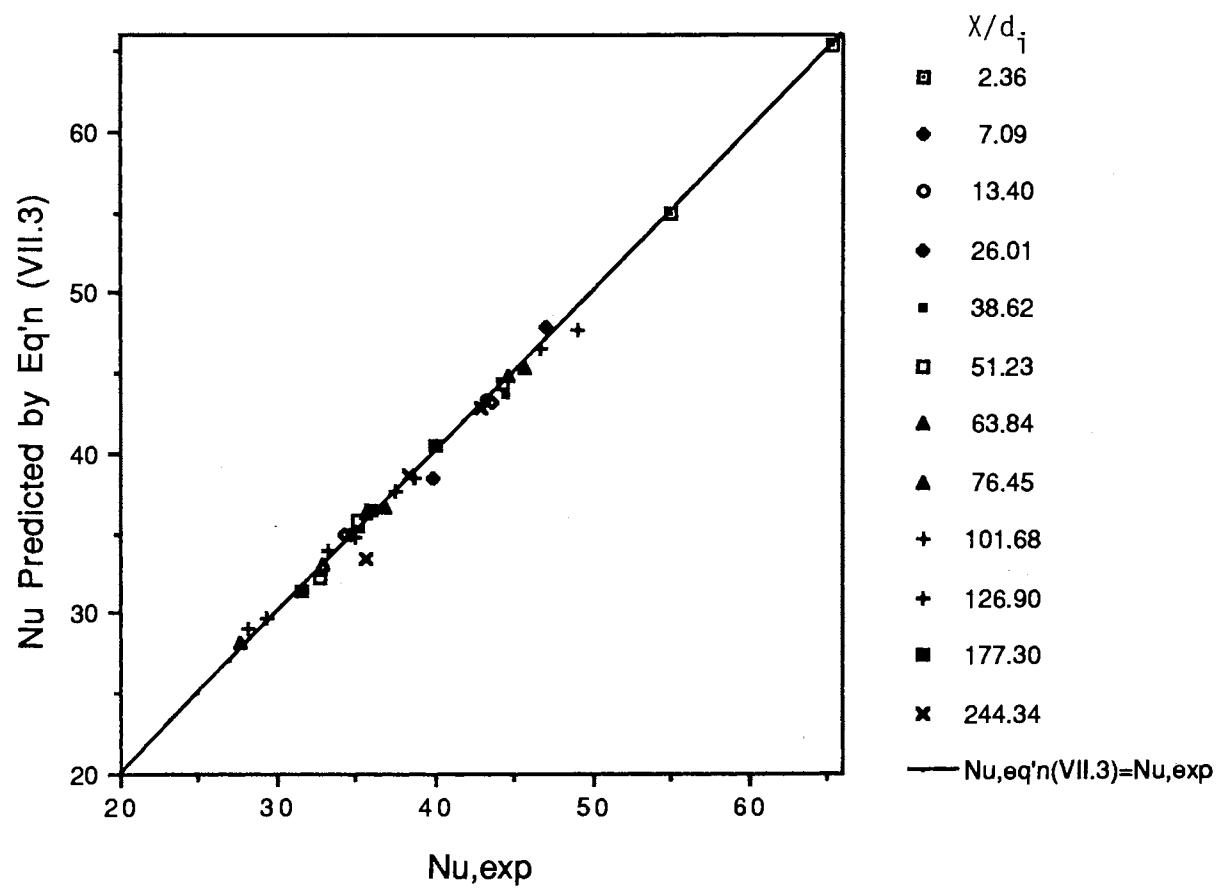


Figure 41: Comparison between the Experimental Nusselt Numbers and the Nusselt Numbers Predicted by Equation (VII.3)

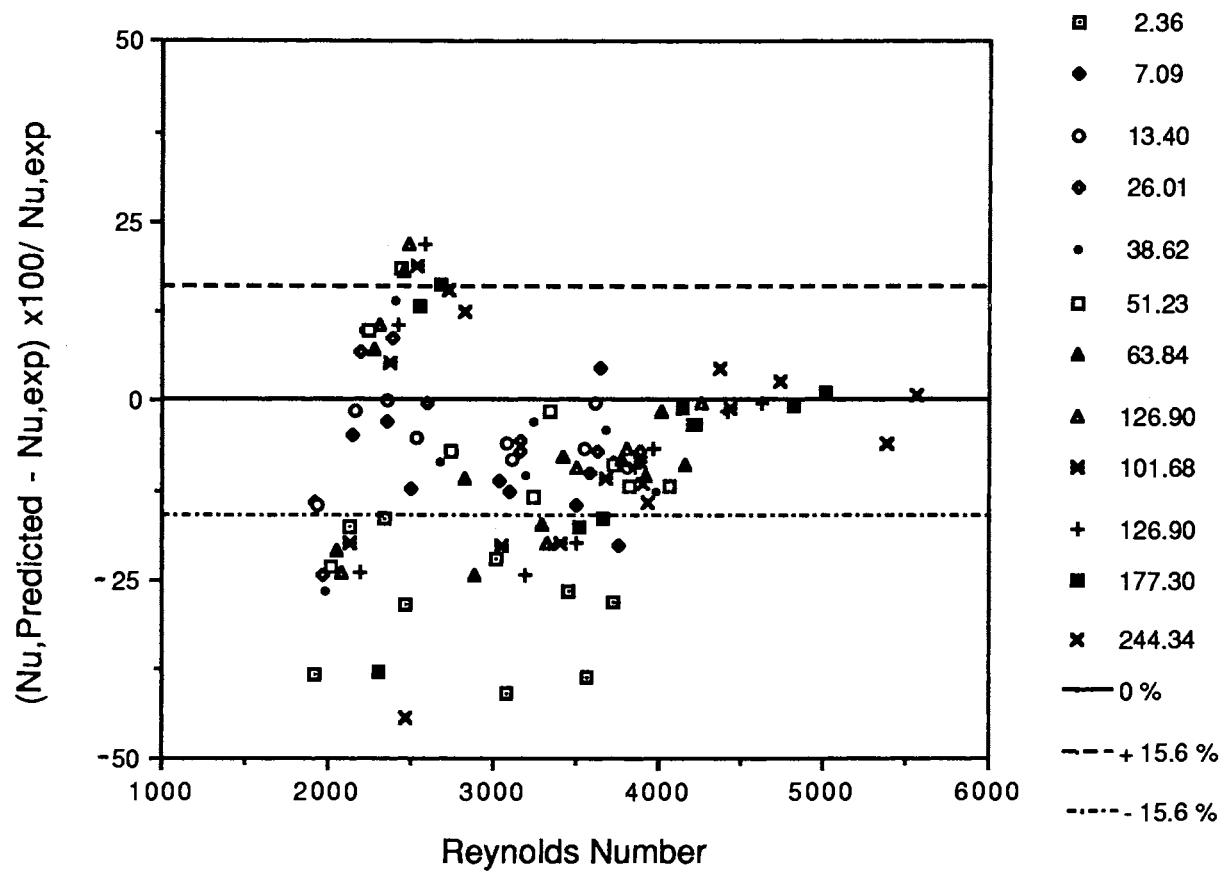


Figure 42: Comparison between the Experimental Nusselt Numbers and the Nusselt Numbers Calculated by Equations (VII.4) and (VII.5) as a Function of Reynolds Number for  $1,900 < Re < 5,500$

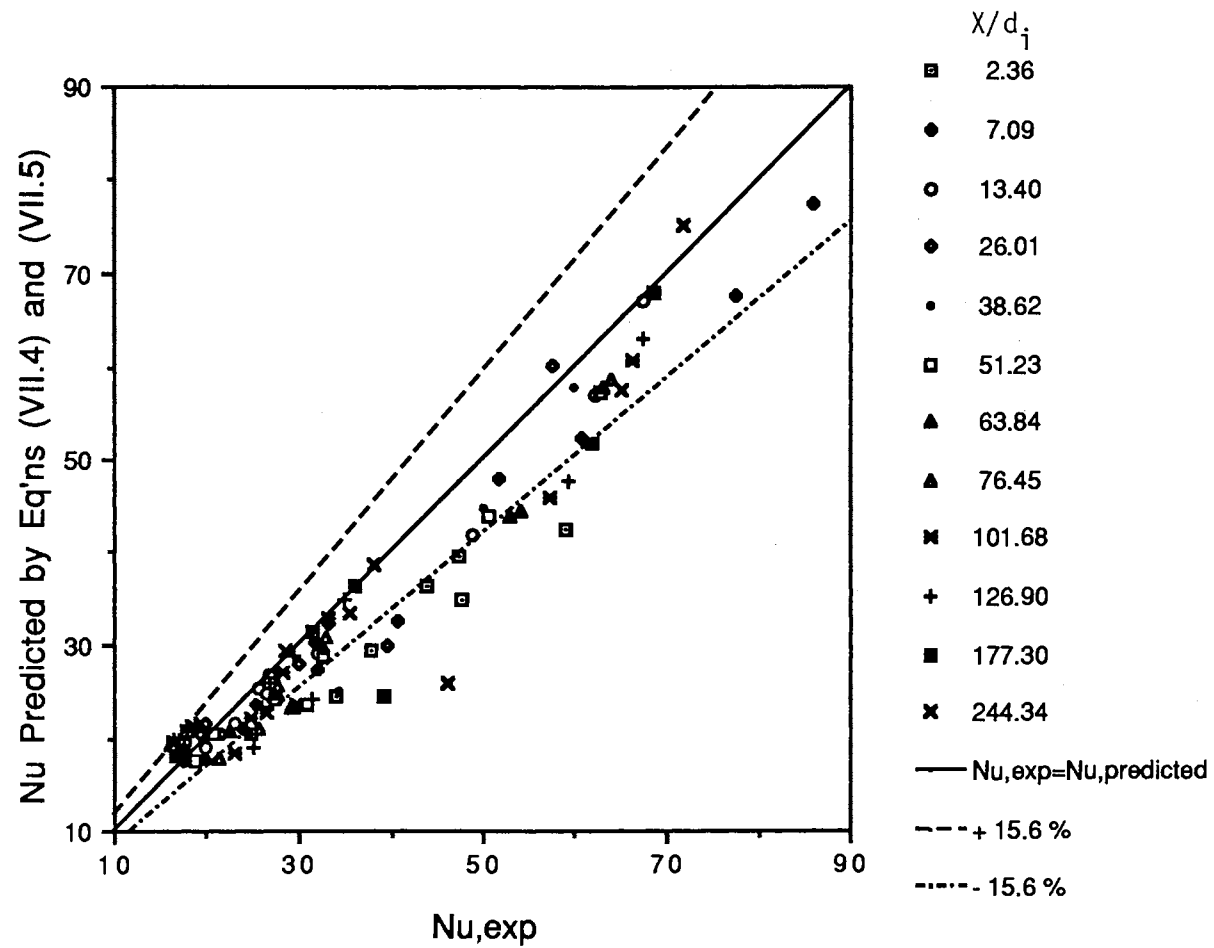


Figure 43: Comparison between the Experimental Nusselt Numbers and the Nusselt Numbers Calculated by Equations (VII.4) and (VII.5)

## CHAPTER VIII

### CONCLUSIONS AND RECOMMENDATIONS

#### Conclusions

The effects of a square-edged entrance, natural convection, and forced convection on heat transfer in a horizontal circular tube for high laminar, transition, and lower turbulent flow regimes were investigated. The test section was heated electrically with nominally constant heat flux.

In the high laminar flow regime, the entrance effect persists longer than those in the transition and lower turbulent flow regimes. According to the recommended calculation, it takes about  $X/d_i = 115$  for the laminar flow entrance effect to reduce to within a factor of 1.01 times the fully developed forced convection heat transfer, to 1 % on the forced convection term and about  $X/d_i = 110$  to damp to within 1 % on the natural convection term. The entrance effect gives only 1 % increase on the forced convection term at about  $X/d_i = 14$  for lower turbulent flow and at about  $X/d_i = 16$  for the flow with Reynolds number in the range of 4,600 to 7,000.

Natural convection is a major factor in laminar flow.



The magnitude of the natural convection contribution on heat transfer is proportional to the product of the Grashof number and the Prandtl number to the  $1/4$  power. However, over the range of parameters considered in this work, natural convection has no effect on the heat transfer for flows with Reynolds numbers greater than 4,600.

Correlations (VII.1) for Re between 121 and 2,100, (VII.2) for Re between 7,000 and 12,400, and (VII.3) for Re between 4,600 and 7,000 to predict the local average heat transfer coefficients for the square-edged contraction entrance are proposed.

#### Recommendations

The validity of equations (VII.2) and (VII.3) should be checked experimentally for the Prandtl number range above 10 and the Grashof number range below 45,000.

Correlation (VII.1) was derived based on the heat transfer data in the thermally developing regime. And since most heat exchangers are built the thermally developing flow regime, this study may be enough to derive correlations for design purposes. In order to cover the heat transfer for the entire thermally developing flow region to both hydrodynamically and thermally developed flow, a longer test section and more thermocouple stations are required.

It is better to have a solitary room or at least a much larger space to run similar experiments. The ideal

laboratory for heat transfer experiments will have its own temperature control system for the room temperature.`

## BIBLIOGRAPHY

1. Abdelmessih, A., Laminar Flow Heat Transfer Downstream from U-Bends, PhD Thesis, Oklahoma State University (1986).
2. Beers, Y., Introduction to the Theory of Error, Addison-Wesley (Mass.), 3rd. ed., 1962.
3. Bergles, A. E. and R. R. Simonds, 'Combined Forced and Free Convection for Laminar Flow in Horizontal Tubes with Uniform Heat Flux', Int. J. Heat Mass Transfer, 14, 1989-2000 (1971).
4. Chandler, J. P., personal communication (1987),
5. Colburn, A. P., 'A Method of Correlating Forced Convection Heat Transfer Data and a Comparison with Fluid Friction', Trans. Am. Inst. Chem. Engrs., 29, 174-210 (1933).
6. Doric Scientific Manual 350-4440-03 'Digital Thermocouple Indicators, Model DS 350-T3', Emerson Electric Co., San Diego, California.
7. Ede, A. J. 'The Heat Transfer for Flow in a Pipe', Int. J. Heat Mass Transfer, 4, 105-110 (1961).
8. Ede, A. J., C. I. Hislop and R. Morris, 'Effect on the Local Heat-Transfer Coefficients in a Pipe of an Abrupt Disturbance of the Fluid Flow: Abrupt Convergence and Divergence of Diameter Ratio 2/1' Proc. Instn. Mech. Engrs, 170, 1113-1130 (1956).
9. Eubank, O. C. and W. S. Proctor, S.M. Thesis in Chemical Engineering, MIT (1951).
10. Gallant, R. W., Physical Properties of Hydrocarbons, Gulf Pub. (Houston, Texas), 1, 114 (1968).
11. Haar, L.; J. S. Gallagher and G. S. Kell, Steam Tables, Hemisphere Pub. Corp. (New York), 1983.
12. Hausen, H., 'Darstellung des Warmenüberganges in Rohren durch Verallgemeinerte

Potenzbeziehungen', ZVDI Benheft  
Verfahrenstechnik, 4, p. 91(1943).

13. Hong, S. W. and A. E. Bergles, 'Laminar Flow Heat Transfer in the Entrance Region of Semi-Circular Tubes with Uniform Heat Flux', Int. J. Heat Mass Transfer, 19, 123-124(1976).
14. Hussain, N. A. and S. T. McComas, 'Experimental Investigation of Combined Convection in a Horizontal Circular Tube with Uniform Heat Flux', Int. Heat Transfer Conf., Paris, 4, paper no. NC3.4 (1970).
15. Hwang, G. J. and K. C. Cheng, 'Boundary Vorticity Method for Convective Heat Transfer with Secondary Flow-Application to the Combined Free and Forced Laminar Convection in Horizontal Tubes', Int. Heat Transfer Conf., Paris, 4, paper no. NC3.5(1970).
16. Kakac, S.; R. K. Shah and A. E. Bergles, Low Reynolds Number Flow Heat Exchangers, Hemisphere Pub. Corp.(New York), 1981.
17. Leeds and Northrup 'Catalog No. 8069-B: Mueller Temperature Bridge'.
18. Leeds and Northrup 'Operations Manual No. 177626: Numatron Series, Numeric Display'.
19. Lincoln Electric Company 'Operating Manual, IM-205-B, Lincolnweld SA-750', Cleveland, Ohio.
20. McAdams, W. H., Heat Transmission, McGraw-Hill(New York), 3rd. ed., 1954.
21. McComas, S. T. and E. R. G. Eckert, 'Combined Free and Forced Convection in a Horizontal Circular Tube', J. Heat Transfer Trans. ASME, 88, 147-153 (1966).
22. Metais, B. and E. R. G. Eckert, 'Forced, Mixed, and Free Convection Regimes', J. Heat Transfer Trans. ASME, 295-296(1964).
23. Minco Products Inc., 'Certificate for Platinum Resistance Thermometer, Model S7928P120S, Serial No. 1009', March(1982)
24. Morcos, S. M. and A. E. Bergles, 'Experimental Investigation of Combined Forced and Free Laminar Convection in Horizontal Tubes', J. Heat Transfer

Trans. ASME, 91, 212-219(1975).

25. Mori, Y. and K. Futagami, 'Forced Convection Heat Transfer in Uniformly Heated Horizontal Tubes (2nd Report)', Int. J. Heat Mass Transfer, 10, p. 1801 (1967).
26. Mori, Y., K. Futagami, S. Tokuda and M. Nakamura, 'Forced Convective Heat Transfer in Uniformly Heated Horizontal Tubes', Int. J. Heat Mass Transfer, 9, 453-463 (1966).
27. Morton, B. R., 'Laminar Convection in Uniformly Heated Horizontal Pipes at Low Rayleigh Numbers', Quar. J. Mech. Appl. Math., 12, p. 410 (1963).
28. Moshfeghian, M., Fluid Flow and Heat Transfer in U-Bends, PhD Thesis, Oklahoma State University (1978).
29. Obermeier, E., S. Fischer and D. Bohne, 'Thermal Conductivity, Density, Viscosity, and Prandtl Number of Di- and Triethylene Glycol-Water Mixtures', Ber. Bunsenges. Phys. Chem., 89, 805-809 (1985).
30. Omega Engineering Inc., 'Temperature Measurement Handbook and Encyclopedia', Stamford, Connecticut (1985).
31. Peckner, D. and I. M. Bernstein, Handbook of Stainless Steel, McGraw Hill (New York), 1977.
32. Petukhov, B. S. and A. F. Polyakov, 'Experimental Investigation of Viscogravitational Fluid Flow in a Horizontal Tube', High Temperature, 5, 75-81 (1967).
33. Petukhov, B. S. and A. F. Polyakov, 'Effect of Free Convection on Heat Transfer During Forced Flow in Horizontal Pipe', High Temperature, 5, 348-351 (1967).
34. Petukhov, B. S., A. F. Polyakov and B. K. Strigin, 'Heat Transfer in Tubes with Viscous-gravity Flow', Heat Transfer-Soviet Research, 1, 24-31 (1969).
35. Petukhov, B. S. and V. N. Popov, 'Theoretical Calculation of Heat Exchange and Frictional Resistance in Turbulent Flow in Tubes of an Incompressible Fluid with Variable Physical

- Properties', Teplifiz. Vys. Temp., 1, 85-101 (1963).
36. Precision Scientific Co., 'Operating Instructions for Precision Constant Temperature Circulating System', TS-66600-5, Chicago, Illinois.
  37. Reynolds, O., 'An Experimental Investigation of the Circumstances which Determine whether the Motion of Water shall be Direct or Sinuous, and the Law of Resistance in Parallel Channels', Phil. Trans. Roy. Soc., London, 174, p. 935 (1883).
  38. Readal, T. C., Effect of Density Gradients on the Rate of Heat Transfer for Flow Through a Horizontal Pipe, M.S. Thesis, University of Illinois, Urbana (1969).
  39. Rosemount Inc., 'Instruction Manual No., 12671D: Variable Temperature Oil Bath, Model 910AD', Minneapolis, Minnesota.
  40. Roy, D. N. 'Laminar Heat Transfer in the Inlet of a Uniformly Heated Tube', J. Heat Transfer Trans. ASME, 87, 425-426(1965).
  41. Schott-Gerate GmbH, 'Operating Instructions: KPG-Viscometers Cannon Fenske', Im Langgewann, West Germany.
  42. Shah, R. K. and A. L. London, Laminar Flow Forced Convection in Ducts, A Supplement to Advances in Heat Transfer, Academic Press (New York), 1978.
  43. Shannon, R. L. and C. A. Depew, 'Combined Free and Forced Laminar Convection in a Horizontal Tube with Uniform Heat Flux', J. Heat Transfer Trans. ASME, 90, 353-357(1968).
  44. Shannon, R. L. and C. A. Depew, 'Forced Laminar Flow Convection in a Horizontal Tube with Variable Viscosity and Free Convection Effect', J. Heat Transfer Trans. ASME, 91, 251-258 (1969).
  45. Sieder, E. N. and G. E. Tate, 'Heat Transfer and Pressure Drop of Liquids in Tubes', Ind. and Eng. Chem., 28, 1429-1435 (1936).
  46. Siegel, R., E. M. Sparrow, T. M. Hallman, 'Steady Laminar Heat Transfer in a Circular Tube with Prescribed Wall Heat Flux', Appl. Sci. Res., Sec. A, 7, 386-392(1958).

47. Siegwarth, D. P., R. D. Mikesell, T. C. Readal and T. J. Hanratty, 'Effect of Secondary Flow on the Temperature Field and Primary Flow in a Heated Horizontal Tube', Int. J. Heat Mass Transfer, 12, 1535-1552 (1969).
48. Union Carbide Chemical Co., Glycols, 1959.
49. White, F. M., Viscous Fluid Flow, McGraw-Hill, 429-444 (1982).
50. Wrap-On Co., Inc. User's Instruction, 1987.

## APPENDIX A

### CALIBRATION OF THE STREAM THERMOCOUPLES

#### Calibration Equipment

The thermocouples which measured the temperatures of the room, the constant temperature bath, and the inlet and exit of the test section were calibrated with the thermocouple indicator against a platinum resistance thermometer (S7928P120S) manufactured by Minco Products, Inc.(23). The thermocouple temperatures were read directly from the Doric DS-350 direct readout thermocouple indicator. The platinum thermocouple was connected to a Leeds and Northrup resistance bridge, Model 8096-B(17). A Leeds and Northrup galvanometer (Model 9834-2) was used as a null detector. An adjustable constant temperature bath manufactured by Rosemount Inc. (Model 910AD) was used to provide constant temperature environment for the calibrated thermocouples.

#### Temperature Calibration Procedures

The thermocouples that were not attached to the test section were calibrated directly against the platinum thermometer together with the thermocouple indicator from 32 to 210 °F (0-98.89 °C). Polyethylene glycol was used as



the bath fluid. A mixture of ice and distilled water was used to fix a reference temperature of 32.0 °F (0 °C).

The constant temperature fluid bath was set at the desired temperature and allowed to run for more than one hour to reach the desired temperature range. The resistance of the resistance bridge was adjusted for the zero correction according to the manual (18) before connecting it to the platinum thermometer. Eight readings with twenty minute intervals were taken for each thermocouple. The readings from the platinum thermometer and the thermocouple indicator for each thermocouple were correlated by a computer program using the linear least square method for further calculation use.

The calibration data obtained are within  $\pm 0.3$  °F and are available upon request as indicated in Appendix H.

## APPENDIX B

### CALIBRATION OF THE SURFACE THERMOCOUPLES

#### Calibration Procedures

All surface thermocouples were calibrated in situ by running distilled water or DEG in the test section at constant temperature for at least one hour and comparing their readings with the readings from the calibrated thermocouples measuring the inlet and outlet temperatures.

The readings were also correlated by the linear least square method. About 80 % of the readings are within  $\pm 0.5$  °F of their corresponding actual temperatures. When the fluid temperature goes higher, the deviation between the reading and the actual temperature increases. This is due to the increase in the temperature difference between the fluid and its surroundings so the heat loss increases. These data are available upon request as indicated in Appendix H.

## APPENDIX C

### FLOW RATE CALIBRATION

#### Calibration Equipment

The rotameters were only calibrated for water. The volumetric flow rate for those runs with DEG-distilled water solution was directly measured after each run.

A stop watch with a precision of 0.01 second was used to time the liquid flow rate. A five-gallon tank was used to collect the liquid. A one-liter volumetric flask was used to measure the volume of the liquid. The accuracy of the volumetric flask was within one milliliter.

#### Calibration Procedures

The flow rate was adjusted to the desired float setting on the rotameter. The liquid was allowed to circulate for one hour. The liquid was collected in the five-gallon tank and the collecting time was measured by the stop watch. The constant temperature bath has about 10 gallons of liquid in it (total volume of liquid in the system was about 15 gallons). Only about 1.5 liters of liquid were collected to measure the volume. So, the liquid level in the constant temperature batch was almost constant during the calibration and there was no noticeable change in the

rotameter reading. The liquid bath temperature was recorded and assumed to be the rotameter liquid temperature. Usually the liquid in the tank was very close to the room temperature and the volume of the collected liquid was measured by volumetric flask.

The flow rates versus rotameter readings were correlated by the linear least square method. These data are available upon request as indicated in Appendix H.

## APPENDIX D

### EVALUATION OF THE COMPOSITION OF DIETHYLENE GLYCOL

#### Apparatus

The composition of the DEG-distilled water solutions was determined in two ways: by measuring the kinematic viscosity by a Cannon-Fenske viscometer and by measuring the density by a pycnometer. The viscometers used were Ref. Nos. 24513-01, 24513-10, 24513-20 and 24513-23. The electronic balance, manufactured by the Aldinger Comp., was located in the Biochemistry Department; it had a sensitivity of 0.1 mg. The pycnometer had approximately 10 ml volume.

#### Procedures

##### Kinematic Viscosity Method

The viscometer was dried with a stream of nitrogen gas first. Then, the flask with the fluid to be measured and the viscometer were put in the constant temperature bath and set for 30 minutes to reach the bath temperature. Then the viscometer was operated according to the Schott Gerate Operating Instructions for Cannon-Fenske Viscometer (41). A stop watch measured the time of fall of the meniscus

between two marks. For a correctly selected viscometer, the flow time was usually around 200 seconds. A thermocouple measured the temperature of the bath. The kinematic viscosity was calculated by the equation:

$$\nu = K \cdot (t - \theta) \quad (D.1)$$

where  $\nu$  = kinematic viscosity,  $\text{mm}^2/\text{sec}$ .

$K$  = constant, found in the Operating Instructions (41).

$t$  = average flow time, seconds.

$\theta$  = Hagenbach correction, sec. (41)

The composition was then calculated by Equations (E.7) and (E.8).

The viscometer was cleaned by dichromate solution (120 g sodium dichromate in 1000 ml water and 1600 ml concentrated sulfuric acid) and rinsed with distilled water.

#### Density Method

The liquid was allowed to sit for at least two hours in the room to reach room temperature. The empty pycnometer was weighed by the electronic balance. Then the pycnometer was filled with distilled water at room temperature and was weighed again. The pycnometer was emptied and dried. The test liquid was transferred into the pycnometer and was weighed by the electronic balance. The volume of the

pycnometer was calculated from the weight of the distilled water in the pycnometer divided by the density of water at the measured temperature. The density of the test liquid was then calculated by the weight of the liquid measured by the electronic balance and divided by the volume of the pycnometer. Finally the composition was calculated by Eq'n (E.7) in Appendix E.

The average of the value from the two methods was used for the liquid composition. Usually the difference of the DEG concentration between the results from the two methods was less than 0.3 % of their average value.

## APPENDIX E

### PHYSICAL PROPERTIES

#### Water

The correlation equations used for water were those used by Abdelmessih (1) except density and coefficient of thermal expansion, which were derived from the data in the steam tables by Haar, Gallagher and Kell (11).

##### Density

The equation for the density of water was derived from values in the data in the steam tables by Haar, Gallagher and Kell (11).

$$\begin{aligned} \rho = & 999.86 + 0.061464T - 0.0084648T^2 + 6.8794 \times 10^{-5}T^3 \\ & - 4.4214 \times 10^{-7}T^4 + 1.2505 \times 10^{-9}T^5 \end{aligned} \quad (E.1)$$

where  $\rho$  = density,  $\text{kg/m}^3$

$T$  = temperature,  $^{\circ}\text{C}$

This equation is valid for the temperature range from 0 to  $100^{\circ}\text{C}$  and is within the accuracy of the steam table (11) which is  $\pm 0.05 \text{ kg/m}^3$ .



### Viscosity

The viscosity of water is calculated by the following equation used by Abdelmessih(1).

$$\log_{10}\left(\frac{\mu_T}{\mu_{20}}\right) = \{1.327(20 - T) - 0.001053(20 - T)^2\} / (T + 105) \quad (\text{E.2})$$

where  $\mu_{20}$  = viscosity of water at 20 °C, Ns/m

$\mu_T$  = viscosity of water at T °C, Ns/m

T = temperature, °C

This equation is valid within the temperature range from 10 to 100 °C. It has an accuracy within 1 %.

### Specific Heat

The specific heat of water is calculated by the following equation:

$$C_p = 4.216 - 2.2 \cdot 10^{-3}T + 3.66 \cdot 10^{-5}T^2 - 1.475 \cdot 10^{-7}T^3 \quad (\text{E.3})$$

where  $C_p$  = specific heat, kJ/(kgK), and 1 kJ/(kgK) is

equal to 0.2388 Btu/(lb<sub>m</sub>·°F)

T = temperature, °C

This equation has an accuracy within 1 % for the range from 0 to 100°C.

### Thermal Conductivity

The thermal conductivity of water is calculated by:

$$k = 0.56276 + 1.874 \times 10^{-3} T - 6.80 \times 10^{-6} T^2 \quad (\text{E.4})$$

where  $k$  = thermal conductivity of water, W/(m·K)

$T$  = temperature, °C.

This equation is applied in the temperature range of 0 to 100 °C. It has an accuracy within 1 %.

#### Coefficient of Thermal Expansion

The coefficient of thermal expansion was calculated from its definition by using the density equation (E.1).

The definition of thermal expansion coefficient is:

$$\beta = \rho \left[ \frac{\partial(1/\rho)}{\partial T} \right]_P \quad (\text{E.5})$$

Substituting equation (E.1) into equation (E.5) gives:

$$\beta = \{0.0615 - 0.01694T - 2.06 \cdot 10^{-4} T^2 - 1.77 \cdot 10^{-6} T^3 + 6.3 \cdot 10^{-9} T^4\} / \\ \{999.86 + 0.06146T - 0.00847T^2 + 6.879 \cdot 10^{-5} T^3 - 4.42 \cdot 10^{-7} T^4 + 1.25 \cdot 10^{-9} T^5\}^2 \quad (\text{E.6})$$

where  $\beta$  = coefficient of thermal expansion, 1/K.

$\rho$  = density at  $T$ , kg/m<sup>3</sup>

$T$  = temperature, °C

This equation is applied in the temperature range of 0 to 100 °C. It is accurate within the accuracy of the steam table (11).

## Diethylene Glycol-Water Solutions

The correlations used for DEG-water solutions are available from ref.(29) except that the coefficient of thermal expansion was calculated from the density by Equation (E.5), ,and the specific heat data were taken from ref.(10) .

### Density

The density for the DEG-water solutions is given by the following equation:

$$\begin{aligned} \rho = & (998.80 + 207.29x - 72.103x^2) \\ & + (-0.10357 - 1.0797x + 0.42904x^2)T \\ & + (-3.2251 \times 10^{-3} + 3.4321 \times 10^{-3}x - 4.5246 \times 10^{-4}x^2)T^2 \quad (E.7) \end{aligned}$$

where  $\rho$  = density, kg/m<sup>3</sup>

$T$  = temperature, °C

$x$  = mass fraction of DEG in DEG-water solution

The equation has an accuracy of  $\pm 0.5$  %. It is good for the temperature range from -10 °C to 140 °C.

### Viscosity

The viscosity of DEG-distilled water solution is calculated by the following equation:

$$\ln \mu = (0.63513 + 3.0176x - 0.49609x^2)^{1.3514} \\ + (-0.029276 - 0.040815x + 0.0099051x^2) T \\ + (1.8238 \times 10^{-6} + 5.765 \times 10^{-6}x - 2.6245 \times 10^{-6}x^2)^{0.6803} T^2 \quad (\text{E.8})$$

where  $\mu$  = viscosity, mPas

$T$  = temperature, °C

$x$  = DEG mass fraction

The equation has an accuracy of  $\pm 4.0$  %. It is good for the temperature range from  $-10$  °C to  $80$  °C.

### Thermal Conductivity

The thermal conductivity of DEG-distilled water solution is calculated by:

$$k = (1 - x) \cdot k_w + x \cdot k_{\text{DEG}} - \lambda \cdot (k_w - k_{\text{DEG}}) \cdot (1 - x) \cdot x \quad (\text{E.9})$$

where  $k_w = 0.56276 + 1.874 \times 10^{-3}T - 6.8 \times 10^{-6}T^2$

$$k_{\text{DEG}} = 0.19589 + 1.689 \times 10^{-4}T - 8.1 \times 10^{-7}T^2$$

$$\lambda = 0.4052 + 0.0594x - 8.4 \times 10^{-4}T$$

$k$  = thermal conductivity, W/(m·K)

$T$  = temperature, °C

$x$  = DEG mass fraction

The equation has an accuracy of  $\pm 0.3$  %. It is good for the temperature range from  $-20$  °C to  $200$  °C.

### Specific Heat

$$\begin{aligned}
 C_p = & (1.027 - 0.52469x + 0.021435x^2) \\
 & + (-2.6187 \times 10^{-4} + 3.8054 \times 10^{-3}x - 2.5793 \times 10^{-3}x^2)T \\
 & + (-2.3096 \times 10^{-7} + 6.0706 \times 10^{-7}x)T^2
 \end{aligned} \tag{E.10}$$

where  $C_p$  = specific heat, kJ/(kgK)

$T$  = temperature, °C

$x$  = DEG mass fraction

The equation has an accuracy of  $\pm 0.5$  %. It is good for temperature range from -20 °C to 200 °C.

### Coefficient of Thermal Expansion

Coefficient of thermal expansion was derived from its definition i.e., equation (E.5)

$$\beta = \rho \left[ \frac{\partial (1/\rho)}{\partial T} \right]_P \tag{E.5}$$

where  $\beta$  = thermal expansion coefficient, 1/K

$\rho$  = density at  $T$ , kg/m<sup>3</sup>

$T$  = temperature, °C

Equation (E.1) was substituted into eq'n (E.5). The following equation was obtained:

$$\begin{aligned}
 \beta = & \{(-0.10357 - 1.0797x + 0.42904x^2) \cdot T \\
 & + (-6.45 \cdot 10^{-3} + 6.864 \cdot 10^{-3}x - 9.05 \cdot 10^{-4}x^2) \cdot T^2\} / \rho_T^2
 \end{aligned} \tag{E.11}$$

where  $\rho_T$  = density at T °C from eq'n (E.7).

The equation has an accuracy of  $\pm 1$  %. It is good for the temperature range from -20 °C to 200 °C.

### Stainless Steel

The test section was made of 316 stainless steel. The physical properties of 316 stainless steel were taken from ref. (31).

#### Thermal Conductivity

$$k = 12.791 + 0.0122 \cdot T + 1.045 \cdot 10^{-5} T^2 - 1.887 \cdot 10^{-8} T^3 \quad (\text{E.12})$$

where  $k$  = thermal conductivity, W/(m·K)

$T$  = temperature, °C

The equation has an accuracy of  $\pm 0.3$  %. It is good for the temperature range from -20 °C to 200 °C.

#### Electrical Resistivity

$$R = 6.93 \cdot 10^{-7} + 3.17 \cdot 10^{-10} T - 2.62 \cdot 10^{-13} T^2 + 1.63 \cdot 10^{-16} T^3 \quad (\text{E.13})$$

where  $R$  = electrical resistivity, ohm·m<sup>2</sup>/m

$T$  = temperature, °C

## APPENDIX F

### NUMERICAL SOLUTION OF THE WALL TEMPERATURE GRADIENT

The numerical solution of the wall temperature gradient is based on the following assumptions:

1. Peripheral and radial wall conduction are significant.
2. Axial conduction is negligible.
3. Steady state conduction prevails.
4. The electrical resistivity and thermal conductivity of the tube wall are functions of temperature.
5. There are heat losses from the test section to the surroundings.

The tube wall thickness was sliced into ten concentric equal thickness cylinders, while the tube cross section was divided into octants (for eight-thermocouple station) or quadrants (for four-thermocouple stations) about the tube axis. In the axial direction, the tube wall was divided into twelve length segments with each thermocouple station placed at the center of the corresponding segment.

An energy balance on an interior element (Figure 44) gives:

$$Q = Q_1 + Q_2 + Q_3 + Q_4 \quad (F.1)$$

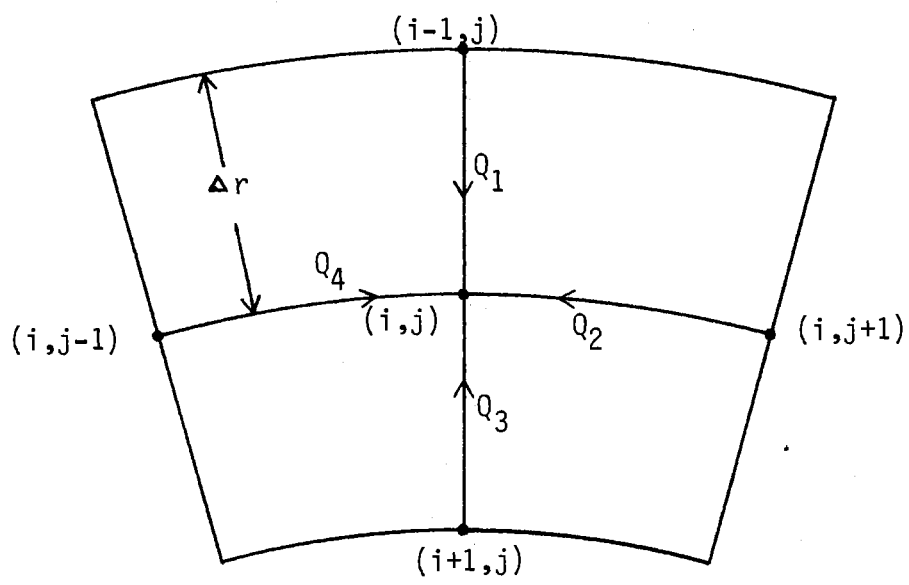


Figure 44: Interior Nodes



From Fourier's law

$$Q_1 = -k \cdot A \cdot \frac{dT}{dx} \quad (F.2)$$

Substituting Fourier's law and applying the finite difference approach for the radial(i) and peripheral(j) directions to equation (F.1) we obtain:

$$Q_1 = (k_{i-1,j} + k_{i,j}) \cdot \frac{(T_{i,j} - T_{i-1,j}) \cdot \pi \cdot (r_i + \frac{1}{2}\Delta r) \cdot \Delta z}{\Delta r \cdot I_p} \quad (F.3)$$

$$Q_2 = (k_{i,j+1} + k_{i,j}) \cdot \frac{(T_{i,j} - T_{i,j+1}) \cdot \Delta r \cdot \Delta z \cdot I_p}{4\pi \cdot r_i} \quad (F.4)$$

$$Q_3 = (k_{i+1,j} + k_{i,j}) \cdot \frac{(T_{i,j} - T_{i+1,j}) \cdot \pi \cdot (r_i - \frac{1}{2}\Delta r) \cdot \Delta z}{\Delta r \cdot I_p} \quad (F.5)$$

$$Q_4 = (k_{i,j-1} + k_{i,j}) \cdot \frac{(T_{i,j} - T_{i,j-1}) \cdot \Delta r \cdot \Delta z \cdot I_p}{4\pi \cdot r_i} \quad (F.6)$$

The heat generation,  $Q$ , is calculated as follows:

$$Q = I^2 \cdot R \quad (F.7)$$

where  $R = 3.412 \cdot \gamma \cdot \Delta z / A$

$\gamma$  = electrical resistivity at node(i,j), ohm-in. or  
ohm-m

$$A = \frac{2 \cdot \pi \cdot r_i \cdot \Delta r}{I_p}$$

$I_p$  = number of thermocouples at the station

Substituting equations (F.3), (F.4), (F.5), (F.6) and (F.7)

into equation (F.1) and rearranging gives:

$$\begin{aligned}
 T_{i+1} = & T_i - \left\{ -3.412 \cdot R \cdot I^2 \cdot I_p / (2 \cdot \pi \cdot r_i \cdot \Delta r) \right. \\
 & + (\pi / (I_p \cdot \Delta r)) \cdot (k_{i-1,j} + k_{i,j}) \cdot (r_{i-1} - \Delta r / 2) \cdot (T_{i-1,j} - T_{i,j}) \\
 & + (I_p \cdot \Delta r / (4 \cdot \pi)) \cdot (k_{i,j+1} + k_{i,j}) \cdot (T_{i,j+1} - T_{i,j}) / r_i \\
 & + (I_p \cdot \Delta r / (4 \cdot \pi)) \cdot (k_{i,j-1} + k_{i,j}) \cdot (T_{i,j-1} - T_{i,j}) / r_i \left. \right\} \\
 & / \{ (\pi / (I_p \cdot \Delta r)) \cdot (k_{i+1,j} + k_{i,j}) \cdot (r_{i+1} + \Delta r / 2) \} \quad (F.8)
 \end{aligned}$$

Equation (F.8) is good for all the interior nodes. There is heat loss to the surroundings for the exterior nodes. The following equation was used to substitute equation (F.3) for exterior nodes:

$$Q_i = \frac{\Delta z \cdot Q_{\text{loss}}}{I_p \cdot L} \quad (F.9)$$

where  $\Delta z$  = axial length of the element, ft or m

$L$  = total length of the test section, ft or m

$I_p$  = number of thermocouples at the station.

## APPENDIX G

### ERROR ANALYSIS

#### Error Analysis

An error analysis for all the experimental variables has to be included in order to determine the error in the experimental heat transfer coefficient. Variables are assumed to be independent unless specified. The following equation is used to calculate independent errors for dependent properties(2)

$$S_R = \sqrt{\left(\frac{\partial R}{\partial y_1}\right)^2 \cdot S_{y_1}^2 + \left(\frac{\partial R}{\partial y_2}\right)^2 \cdot S_{y_2}^2 + \dots} \quad (G.1)$$

where  $R$  = the quantity whose error is to be estimated

$y_1, y_2$  = independent variables

$S$  = standard deviation of  $R$

Quantities with a (') denote the average values.

Table II presents the maximum and minimum values of the variables in the experiments and their maximum absolute error. The maximum absolute error was obtained from either manual or from the calibration data. The maximum absolute error is assumed to be three times of the corresponding standard deviation.

Table II  
RANGE OF PROPERTIES MEASURED AND THEIR ACCURACY

Variable	Maximum value	Minimum value	Maximum abs error
Current, amperes	440.5	121.3	7.5
Voltage drop, volts	16.88	5.03	0.02
Rotameter(1.96 gpm), gpm	1.76	0.303	0.005
Rotameter(11.0 gpm), gpm	5.16	2.41	0.02
Thermocouples, °F			
bath	113.45	55.43	0.3
room,	98.14	55.38	0.3
inlet,	113.15	55.41	0.3
outlet	137.90	66.20	0.3
surface(test section),	239.15	67.08	0.3

The calculation of the standard deviation of power input is used as an example for standard deviation calculation. The power input,  $P$ , is equal to:

$$P = I V$$

We have two independent variables which are  $I = y_1$  and  $V = y_2$ .  $P$  is corresponding to  $R$  in eq'n (G.1).

$$(\partial R / \partial y_1) = (\partial P / \partial I) = V. \quad (\partial R / \partial y_2) = (\partial P / \partial V) = I.$$

$$S_{y_1} = 7.5 \text{ amp} / 3 = 2.5 \text{ amp. and}$$

$$S_{y_2} = 0.02 \text{ volt} / 3 = 0.00667 \text{ volt. For run 1111,}$$

$V = 16.76$  volts and  $I = 437$  amperes. Substituting the above values into equation (G.1) gives:

$$S_p = \sqrt{16.76^2 \cdot 2.5^2 + 437^2 \cdot 0.00667^2}$$

$$= 42.0 \text{ W}$$

So, the input power for run 1111 has a maximum absolute error of  $42.0 \text{ W} \cdot 3 = 126 \text{ W}$ . The input power for run 1111 can be expressed as,  $P = 7324 \pm 126 \text{ W}$ . The same reasoning is used for the rest of the properties.

The standard deviation for power input is calculated by the above procedures except that the average  $V'$  and average  $I'$  were used instead of individual  $V$  and  $I$ .

For the standard deviation of an individual property, the following equation is used to calculate standard deviation(2):

$$S = \sqrt{\frac{\left(\sum_{n=1}^k z_n^2\right) - k \cdot \bar{z}^2}{k - 1}} \quad (G.2)$$

where  $z$  is individual property and  $k$  is total number of individual properties.  $S$  is the standard deviation.

All runs attempted had an error less than 20 % in heat balance. 47 runs had heat balance error less than 10.0 %. For these 47 runs, the average heat balance error is 2.003 %. Only these runs were used in any calculations in the thesis. Thus for the 47 runs included in the calculations,  $\bar{z} = 2.003 \%$  and  $k = 47$ . Substituting into Eq'n (G.2), the standard deviation for the heat balance is 2.06 %.

Table III has standard deviations for some major properties.

#### Correction of the Outside Wall Temperature

The computer listing of the main program in Appendix I does not take into account the thickness of the adhesive thin layer between the thermocouple bead and the outside surface of the test section. However, the main program did take into the account the heat loss to the surroundings. The adhesive thin layer is approximately 0.1 mm thick. As we can see from Figure 45, the difference between the apparent outside temperature of the tube,  $T_{app}$ , and the actual outside wall temperature,  $T_{wo}$ , is:

Table III  
PERCENTAGE STANDARD DEVIATIONS

property	Standard deviation %
Power	1.2
Volumetric flow rate	1.5
Mass flow rate	1.6
Heat loss to surroundings,	1.4
Heat input	1.3
Heat output	1.2
Heat balance	1.5
Length of test section,	0.001
Radius of test section	0.8
Area	0.8
Heat flux	1.5
Heat transfer coefficient*	2.1

\*: Heat transfer coefficient,  $h$ , is calculated by:

$$h = Q / (A_i \cdot \Delta T)$$

where  $Q/A_i$  is the heat flux at the inside wall and  $\Delta T$  is the temperature difference between the inside wall temperature and the bulk fluid temperature. The standard deviation of  $Q$ ,  $A_i$  and  $\Delta T$  are calculated separately by eq'n (G.2). The standard deviation of  $h$  is then calculated by (G.1). The maximum possible error for heat transfer coefficient is estimated to be 6.3 %, three times the standard deviation.

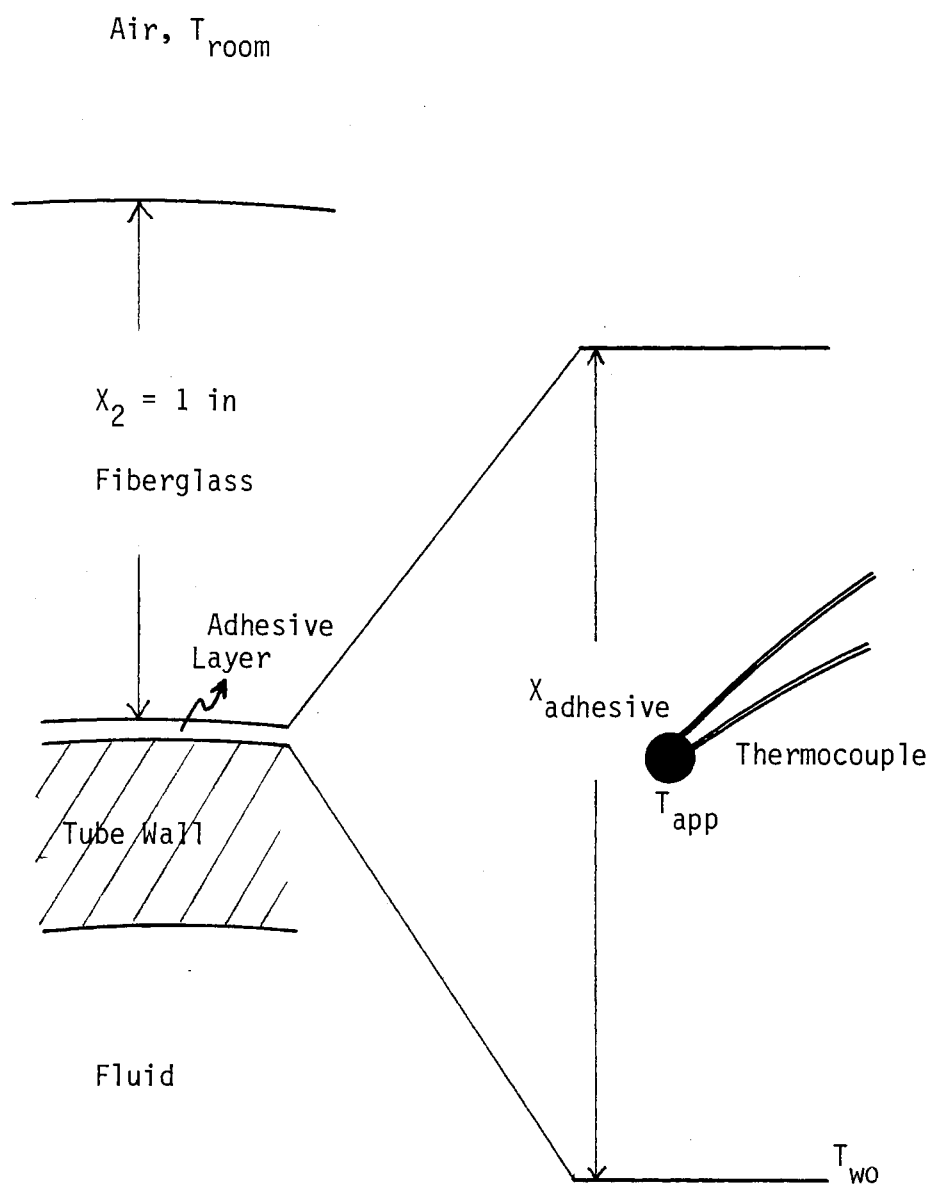


Figure 45: Correction for Outside Wall Temperature



$$T_{wo} - T_{app} = (Q/A)_{loss} \cdot X_{adhesive} / k_{adhesive} \quad (G.3)$$

where  $X_{adhesive}$  is the thickness of adhesive thin layer.

Overall heat generated by electric current,  $Q$ , can be divided into two parts: the heat transferred to the fluid flowing inside the tube,  $Q_{fluid}$ , and the heat loss to the surroundings,  $Q_{loss}$ .

$$Q = Q_{loss} + Q_{fluid} \quad (G.4)$$

$Q_{loss}$  can be estimated either by the fluid inlet and outlet temperatures as we do in Appendix J or by the following equation:

$$Q_{loss} = U_{wo} \cdot A_{wo} \cdot \Delta T \quad (G.5)$$

where  $U_{wo}$  = overall heat transfer coefficient for heat

loss, Btu/(ft<sup>2</sup>·hr·°F)

$A_{wo}$  = tube outside surface area, ft<sup>2</sup>

$\Delta T = T_{app} - T_{room}$

While

$$U_{wo} = \frac{1}{\frac{r_0 \ln\left(\frac{r_0 + 2x_1}{r_0 + x_1}\right)}{k_{adhesive}} + \frac{r_0 \ln\left(\frac{r_0 + x_2}{r_0}\right)}{k_{insulation}} + \frac{r_0 \ln\left(\frac{r_0 + x_2 + x_3}{r_0 + x_2}\right)}{k_{air}}} \quad (G.6)$$

For  $x_1 = 0.004$  in.,  $x_2 = 1$  in.,  $k_{adhesive} = 0.6$

Btu/(ft·hr·°F) (ref. 30),  $k_{insulation} = 0.0225$

Btu/(ft·hr·°F) (ref. 49),  $h_{air} = 0.015$  Btu/(ft·hr·°F) (ref.

$$T_{wo} - T_{app} = (Q/A)_{loss} \cdot X_{adhesive} / k_{adhesive} \quad (G.3)$$

where  $X_{adhesive}$  is the thickness of adhesive thin layer.

Overall heat generated by electric current,  $Q$ , can be divided into two parts: the heat transferred to the fluid flowing inside the tube,  $Q_{fluid}$ , and the heat loss to the surroundings,  $Q_{loss}$ .

$$Q = Q_{loss} + Q_{fluid} \quad (G.4)$$

$Q_{loss}$  can be estimated either by the fluid inlet and outlet temperatures as we do in Appendix J or by the following equation:

$$Q_{loss} = U_{wo} \cdot A_{wo} \cdot \Delta T \quad (G.5)$$

where  $U_{wo}$  = overall heat transfer coefficient for heat

loss, Btu/(ft<sup>2</sup>·hr·°F)

$A_{wo}$  = tube outside surface area, ft<sup>2</sup>

$\Delta T = T_{app} - T_{room}$

While

$$U_{wo} = \frac{1}{\frac{r_0 \ln\left(\frac{r_0 + 2x_1}{r_0 + x_1}\right)}{k_{adhesive}} + \frac{r_0 \ln\left(\frac{r_0 + x_2}{r_0}\right)}{k_{insulation}} + \frac{r_0 \ln\left(\frac{r_0 + x_2 + x_3}{r_0 + x_2}\right)}{k_{air}}} \quad (G.6)$$

For  $x_1 = 0.004$  in.,  $x_2 = 1$  in.,  $k_{adhesive} = 0.6$

Btu/(ft·hr·°F) (ref. 30),  $k_{insulation} = 0.0225$

Btu/(ft·hr·°F) (ref. 49),  $h_{air} = 0.015$  Btu/(ft·hr·°F) (ref.

20), and  $r_0 = 0.075$  in., we have

$$\begin{aligned} U_{w0} &= 1/(0.00054+3.61+1.24) \\ &= 0.206 \text{ Btu}/(\text{ft}^2 \cdot \text{hr} \cdot ^\circ\text{F}) \end{aligned}$$

For run 1111, the average  $T_{\text{app}}$  is about  $130^\circ\text{F}$  and  $T_{\text{room}}$  is  $75.0^\circ\text{F}$ . From equation (G.5),

$$\begin{aligned} Q_{\text{loss}} &= 0.206 \cdot 2.544 \cdot (130-75) \\ &= 28.8 \text{ Btu/hr} \end{aligned}$$

And  $(Q/A)_{\text{loss}} = 11.33 \text{ Btu}/(\text{ft}^2 \cdot \text{hr})$

While  $Q_{\text{loss}}$  estimated from the fluid inlet and outlet temperatures is  $22.9 \text{ Btu/hr}$  (Appendix H),  $Q_{\text{loss}} = 28.8 \text{ Btu/hr}$  is used here. From equation (G.3),

$$\begin{aligned} T_{w0} - T_{\text{app}} &= 11.33 \cdot (0.1/304.8)/0.6 \\ &= 0.0062 ^\circ\text{F} \end{aligned}$$

From this estimation the difference between  $T_{w0}$  and  $T_{\text{app}}$  is less than  $0.01^\circ\text{F}$  which is negligible. So we can use the apparent temperatures (thermocouple readings) as the outside surface temperatures.

## APPENDIX H

### EXPERIMENTAL DATA AND CALCULATED RESULTS

Run Number	Test Fluid
1101-1120	water
2101-2143	DEG-water

The experimental data and calculated results are available from:

Professor Kenneth J. Bell  
School of Chemical Engineering  
Oklahoma State University  
Stillwater, Oklahoma 74078

All runs are listed with their major parameters on Table IV, such as DEG mass fraction,  $Re_1$ ,  $Re_{12}$ ,  $Pr_1$ ,  $Pr_{12}$ ,  $Gr_1$ ,  $Gr_{12}$ ,  $Nu_1$ ,  $Nu_{12}$ , bulk fluid velocity, average heat flux, and heat balance error. Subscript 1 denotes the property at station 1 ( $X/d_i = 2.36$ ) and subscript 12 denotes the property at station 12 ( $X/d_i = 244.34$ ).

The calculated results include: bulk parameters, uncorrected outside temperatures, corrected outside temperatures, Reynolds numbers at the inside tube wall,

inside surface temperatures, inside surface heat fluxes, peripheral heat transfer coefficients, average heat transfer coefficients, ratio of heat transfer coefficient to the value predicted by literature, summary of local parameters and the values of local dimensionless groups, and summary of overall parameters and heat balance error.

Only Run 1111 results, which are used as in the sample calculation in Appendix J, are listed in the following pages.

TABLE IV  
SUMMARY OF EXPERIMENTAL DATA AND CALCULATED RESULTS

Run number	x	Re <sub>1</sub>	Re <sub>12</sub>	Pr <sub>1</sub>	Pr <sub>12</sub>	Gr <sub>1</sub>	Gr <sub>12</sub>	V <sup>a</sup>	Nu <sub>1</sub>	Nu <sub>12</sub>	Q/A <sup>b</sup>	HB%error <sup>c</sup>
1101	0.9987 <sup>d</sup>	3725	5552	7.9	5.1	43764	300953	0.84	59.1	38.3	6238	1.69
1103	0.9987	2474	3941	6.2	3.7	131460	746603	0.45	34.0	26.4	4459	0.23
1105	0.9987	3460	5388	6.0	3.7	133889	710869	0.61	47.5	35.6	5846	0.37
1107	0.9987	4593	6829	5.9	3.8	133485	620611	0.80	59.0	42.9	6754	-0.35
1109	0.9987	6868	10098	5.5	3.6	179777	697821	1.13	78.5	64.0	9777	1.86
1111	0.9987	7405	11247	5.6	3.5	187264	804850	1.24	85.3	69.2	11603	1.62
1114	0.9987	8446	12398	5.6	3.6	186370	714767	1.40	90.2	74.1	11778	0.02
1115	0.9987	3010	4733	5.9	3.6	154832	827114	0.53	37.8	28.5	5190	0.26
1116	0.9987	6886	9939	5.4	3.6	172559	672482	1.12	82.1	63.0	9405	3.66
1117	0.9987	5827	8604	5.5	3.6	178436	689615	0.96	65.3	54.2	8238	-0.24
2101	0.9987	499	732	205	141	3219	10754	1.56	34.1	23.3	4015	0.24
2104	0.9987	410	616	207	139	3447	11275	1.30	30.6	22.7	3556	0.54
2105	0.9987	354	585	209	128	3482	12648	1.13	28.9	23.7	3863	-0.16

TABLE IV (Continued)

Run number	x	Re <sub>1</sub>	Re <sub>12</sub>	Pr <sub>1</sub>	Pr <sub>12</sub>	Gr <sub>1</sub>	Gr <sub>12</sub>	V <sup>a</sup>	Nu <sub>1</sub>	Nu <sub>12</sub>	Q/A <sup>b</sup>	HB%error <sup>c</sup>
2107	0.9987	222	452	221	111	3448	15714	0.75	25.2	25.7	3691	-0.19
2108	0.9987	121	266	250	117	2398	10482	0.47	18.7	23.7	2490	1.16
2109	0.9305	841	1305	116	76	11941	44790	1.52	36.8	24.6	6393	2.01
2110	0.9305	1361	1809	116	88	8836	33951	2.44	53.0	23.7	7723	0.72
2111	0.9305	1779	2344	108	83	8144	33146	2.97	75.0	32.8	10430	-0.41
2112	0.9201	3570	4372	94	77	6719	23211	5.21	162.0	71.6	10447	-0.03
2113	0.9201	3087	3900	92	74	7940	28434	4.42	144.0	64.9	7950	1.52
2114 <sup>e</sup>	0.9201	1917	2468	114	89	5539	20427	3.38	100.0	46.1	1835	16.60
2115	0.9250	371	427	282	246	1027	2225	1.64	19.4	12.5	2592	5.75
2116 <sup>e</sup>	0.9250	718	820	236	207	1365	3520	2.65	29.9	15.4	2647	9.88
2117	0.9250	913	1015	227	204	1061	3541	3.23	42.4	16.1	2762	4.92
2118	0.9250	1050	1164	227	206	931	3523	3.73	49.9	16.5	2777	3.59
2119	0.9250	1189	1304	226	207	977	3472	4.20	48.5	16.8	2848	1.58
2121	0.6584	1580	1833	53	46	8577	39856	1.48	45.4	14.6	2779	1.20

TABLE IV (Continued)

Run number	x	Re <sub>1</sub>	Re <sub>12</sub>	Pr <sub>1</sub>	Pr <sub>12</sub>	Gr <sub>1</sub>	Gr <sub>12</sub>	V <sup>a</sup>	Nu <sub>1</sub>	Nu <sub>12</sub>	Q/A <sup>b</sup>	HB%error <sup>c</sup>
2122	0.6584	1336	1577	57	48	9147	31697	1.33	37.0	15.9	3148	4.07
2123	0.6584	1030	1276	66	53	8161	33007	1.19	34.1	14.5	2175	5.28
2124	0.6584	868	1039	63	52	7533	26020	0.95	28.5	13.3	2529	1.99
2126	0.4850	468	676	66	45	7180	23401	0.59	18.0	14.0	3464	-0.09
2127	0.4850	1304	1592	61	50	5596	24732	1.52	37.4	14.1	3361	-1.62
2128	0.4850	1097	1384	61	48	5638	25014	1.28	35.7	14.5	3282	-1.20
2129	0.4850	984	1264	61	48	6043	25474	1.15	32.4	14.5	2751	-1.37
2130	0.4850	724	955	64	48	5504	20821	0.88	27.5	14.6	5799	6.32
2131	0.4850	613	821	64	48	6442	21677	0.75	22.6	13.9	4697	1.33
2132	0.4850	349	537	64	41	7764	24042	0.43	15.2	14.3	7608	2.12
2133	0.4850	1201	1480	64	52	3476	9224	1.46	56.4	14.6	7544	4.06
2134	0.2803	2344	2818	27	22	10864	41582	1.34	47.2	19.2	3489	4.06
2135	0.2803	514	749	28	19	16765	47250	0.31	12.7	12.7	1619	1.82
2136	0.2803	990	1211	29	23	8841	28248	0.61	22.7	13.1	1653	1.54



TABLE IV (Continued)

Run number	x	Re <sub>1</sub>	Re <sub>12</sub>	Pr <sub>1</sub>	Pr <sub>12</sub>	Gr <sub>1</sub>	Gr <sub>12</sub>	V <sup>a</sup>	Nu <sub>1</sub>	Nu <sub>12</sub>	Q/A <sup>b</sup>	HB%error <sup>c</sup>
2137	0.2803	1769	2284	26	20	14102	67298	1.00	37.9	16.1	3580	1.46
2138	0.2803	2137	2726	26	20	14884	65925	1.19	44.0	18.4	4165	4.00
2139	0.2803	1104	1249	22	19	9280	26882	0.52	21.8	11.9	964	4.22
2140	0.2803	1109	1301	22	18	12558	34459	0.52	20.2	12.7	1204	-0.37
2141	0.2803	1119	1364	21	16	15194	44131	0.52	21.2	13.9	1481	-2.15
2142	0.2803	1134	1449	21	16	19312	60007	0.52	21.2	15.3	1890	-0.59
2143	0.2803	1155	1555	21	15	22838	82620	0.52	24.6	16.8	2344	-0.27

1: property at station 1 ( $X/d_i = 2.36$ ).

12: property at station 12 ( $X/d_i = 244.34$ ).

a: bulk average velocity, ft/s.

b: overall average heat flux, Btu/ft<sup>2</sup>

c: heat balance % error.

d: pure DEG.

e: runs not used in developing correlations.

\*-----\*  
 RUN NUMBER 1111  
 \*-----\*

FLOW RATE	=	611.172	LBM/HR	=	1.226	GPM	=	77.310	CC/SEC
CURRENT TO TUBE	=	437.000	AMPS						
VOLTAGE DROP IN TUBE	=	16.760	VOLTS						
ROOM TEMPERATURE	=	83.080	F	=	28.378	C			
UNCORRECTED INLET TEMPERATURE	=	83.100	F	=	28.389	C			
UNCORRECTED OUTLET TEMPERATURE	=	123.400	F	=	50.778	C			
BATH TEMPERATURE	=	83.100	F	=	28.389	C			

\*\*\*\*\* TEST FLUID IS DISTILLED WATER \*\*\*\*\*

UNCORRECTED OUTSIDE SURFACE TEMPERATURES - DEGREES F

	1	2	3	4	5	6	7	8	9	10	11	12
1	106.20	114.10	118.90	120.35	121.95	123.50	125.35	126.25	128.90	132.25	138.80	148.95
2		113.85	117.95		121.40		124.95					
3	105.70	113.40	117.60	119.20	120.55	122.60	124.45	125.35	128.45	131.95	139.35	148.25
4		113.00	117.20		120.30		124.15					
5	106.35	112.70	117.05	118.55	119.75	122.30	123.90	124.75	128.25	131.35	138.20	146.90
6		113.00	117.35		120.50		124.20					
7	105.95	113.35	117.70	119.00	120.65	122.85	124.55	125.50	128.60	131.90	139.30	148.65
8		113.90	118.00		121.15		125.20					

UNCORRECTED OUTSIDE SURFACE TEMPERATURES - DEGREES C

	1	2	3	4	5	6	7	8	9	10	11	12
1	41.22	45.61	48.28	49.08	49.97	50.83	51.86	52.36	53.83	55.69	59.33	64.97
2		45.47	47.75		49.67		51.64					
3	40.94	45.22	47.56	48.44	49.19	50.33	51.36	51.86	53.58	55.53	59.64	64.58
4		45.00	47.33		49.06		51.19					
5	41.31	44.83	47.25	48.08	48.75	50.17	51.06	51.53	53.47	55.19	59.00	63.83
6		45.00	47.42		49.17		51.22					
7	41.08	45.19	47.61	48.33	49.25	50.47	51.42	51.94	53.67	55.50	59.61	64.81
8		45.50	47.78		49.53		51.78					

## CORRECTED OUTSIDE SURFACE TEMPERATURES -DEGREES F

	1	2	3	4	5	6	7	8	9	10	11	12
1	106.22	114.30	118.94	120.44	122.59	123.80	125.85	126.12	129.60	132.32	140.73	150.22
2		113.84	118.13		121.73		125.58					
3	105.59	113.25	117.79	119.32	120.91	123.08	125.07	126.52	129.90	132.95	140.36	149.40
4		113.24	117.47		120.51		124.75					
5	106.18	112.54	117.20	118.70	120.38	122.59	124.36	126.16	129.10	132.61	139.30	148.61
6		112.68	117.40		120.70		124.65					
7	105.78	113.38	117.94	119.20	120.85	123.10	125.05	125.97	129.92	132.62	140.40	149.60
8		113.96	117.96		121.22		125.68					

## CORRECTED OUTSIDE SURFACE TEMPERATURES -DEGREES C

	1	2	3	4	5	6	7	8	9	10	11	12
1	41.24	45.72	48.30	49.13	50.33	51.00	52.14	52.29	54.22	55.74	60.40	65.68
2		45.47	47.85		49.85		51.99					
3	40.88	45.14	47.66	48.51	49.39	50.60	51.71	52.51	54.39	56.08	60.20	65.22
4		45.13	47.48		49.17		51.53					
5	41.21	44.75	47.33	48.17	49.10	50.33	51.31	52.31	53.94	55.89	59.61	64.78
6		44.82	47.45		49.28		51.47					
7	40.99	45.21	47.74	48.44	49.36	50.61	51.69	52.20	54.40	55.90	60.22	65.33
8		45.53	47.76		49.57		52.04					

## REYNOLDS NUMBER AT THE INSIDE TUBE WALL

	1	2	3	4	5	6	7	8	9	10	11	12
1	9210.5	10006.5	10475.7	10624.9	10849.4	10968.7	11180.9	11207.7	11570.7	11857.2	12758.6	13800.9
2		9959.0	10388.0		10755.6		11152.7					
3	9147.4	9897.8	10354.4	10508.9	10669.9	10893.5	11098.7	11249.2	11603.5	11924.9	12718.1	13709.3
4		9899.7	10321.4		10629.8		11066.1					
5	9206.6	9826.9	10293.1	10445.8	10615.5	10842.3	11023.4	11211.5	11517.2	11887.9	12601.3	13619.9
6		9841.5	10314.3		10649.9		11055.2					
7	9166.0	9913.0	10370.4	10496.6	10664.3	10895.7	11096.1	11191.5	11605.4	11889.8	12723.4	13731.7
8		9970.7	10369.5		10700.8		11162.8					

\*-----\*  
 RUN NUMBER 1111  
 \*-----\*

INSIDE SURFACE TEMPERATURES - DEGREES F

	1	2	3	4	5	6	7	8	9	10	11	12
1	102.87	110.96	115.63	117.09	119.29	120.45	122.50	122.76	126.24	128.96	137.37	146.87
2		110.49	114.76		118.37		122.23					
3	102.22	109.87	114.43	115.95	117.54	119.72	121.71	123.16	126.55	129.60	137.00	146.04
4		109.89	114.10		117.14		121.39					
5	102.83	109.16	113.82	115.33	117.00	119.22	120.98	122.80	125.73	129.25	135.92	145.24
6		109.31	114.03		117.34		121.29					
7	102.41	110.03	114.59	115.83	117.48	119.74	121.68	122.61	126.57	129.27	137.05	146.25
8		110.60	114.58		117.84		122.33					

INSIDE SURFACE TEMPERATURES - DEGREES C

	1	2	3	4	5	6	7	8	9	10	11	12
1	39.37	43.87	46.46	47.27	48.49	49.14	50.28	50.42	52.36	53.87	58.54	63.82
2		43.60	45.98		47.99		50.13					
3	39.01	43.26	45.79	46.64	47.52	48.73	49.84	50.64	52.53	54.22	58.33	63.36
4		43.27	45.61		47.30		49.66					
5	39.35	42.87	45.46	46.30	47.22	48.46	49.43	50.44	52.07	54.03	57.73	62.91
6		42.95	45.57		47.41		49.60					
7	39.12	43.35	45.88	46.57	47.49	48.74	49.82	50.34	52.54	54.04	58.36	63.47
8		43.67	45.88		47.69		50.18					

BULK FLUID TEMPERATURE - DEGREES F

1	2	3	4	5	6	7	8	9	10	11	12
83.49	84.26	85.30	87.36	89.43	91.50	93.56	95.63	99.76	103.90	112.16	123.14

BULK FLUID TEMPERATURE - DEGREES C

1	2	3	4	5	6	7	8	9	10	11	12
28.60	29.03	29.61	30.76	31.91	33.05	34.20	35.35	37.65	39.94	44.53	50.63

CORRECTED OUTLET TEMPERATURE = 123.400 DEG F = 50.778 DEG C

CORRECTED INLET TEMPERATURE = 83.100 DEG F = 28.389 DEG C

INSIDE SURFACE HEAT FLUXES BTU/HR/FT2

	1	2	3	4	5	6	7	8	9	10	11	12
1	10862.2	10858.7	10801.4	10909.7	10781.4	10952.0	10956.4	11007.6	11034.1	11058.6	11062.4	11095.9
2		10915.9	10993.0		10974.3		10973.6					
3	10912.9	10978.3	10956.6	10974.7	11010.1	10989.6	11012.5	10985.0	10997.2	11016.6	11064.3	11129.9
4		10873.5	10961.1		10998.4		10991.7					
5	10864.0	11002.4	10997.2	10990.5	11015.6	11008.7	11056.9	11005.8	11057.4	11045.4	11129.2	11170.4
6		10978.6	10984.6		10961.7		11006.1					
7	10904.1	10919.0	10912.2	10980.1	10993.2	10989.2	11015.8	11010.8	10996.2	11031.2	11062.0	11120.2
8		10907.9	11034.4		11056.4		10956.3					

INSIDE SURFACE HEAT FLUXES W PER SQ.M.

	1	2	3	4	5	6	7	8	9	10	11	12
1	34269.1	34258.1	34077.6	34419.2	34014.3	34552.5	34566.4	34728.1	34811.6	34888.9	34900.8	35006.7
2		34438.7	34681.9		34622.9		34620.7					
3	34429.4	34635.5	34567.0	34624.1	34735.8	34671.1	34743.6	34656.8	34695.1	34756.4	34906.8	35113.8
4		34304.8	34581.2		34698.8		34677.8					
5	34274.9	34711.6	34695.2	34673.9	34753.3	34731.5	34883.6	34722.3	34885.1	34847.1	35111.7	35241.7
6		34636.5	34655.4		34583.1		34723.2					
7	34401.6	34448.5	34426.9	34641.3	34682.6	34669.8	34753.7	34738.2	34692.2	34802.5	34899.6	35083.1
8		34413.6	34812.6		34882.1		34566.1					

\*-----\*  
 RUN NUMBER 1111  
 \*-----\*

AVERAGE REYNOLDS NUMBER	= 0.925E+04		
AVERAGE PRANDTL NUMBER	= 0.439E+01		
MASS FLUX	= 0.278E+06	LBM/(SQ.FT-HR)	= 0.378E+03 KG.PER.(S.SQ.M.)
AVERAGE HEAT FLUX	= 0.116E+05	BTU/(SQ.FT-HR)	= 0.366E+05 W PER SQ.M.
Q=AMP*VOLT	= 0.250E+05	BTU/HR	= 0.732E+04 W
Q=M*C*(T2-T1)	= 0.246E+05	BTU/HR	= 0.720E+04 W
HEAT LOST	= 0.573E+01	BTU/HR	= 0.168E+01 W
HEAT BALANCE ERROR %	= 0.167E+01		

PERIPHERAL HEAT TRANSFER COEFFICIENT BTU/SQ.FT-HR-F)

	1	2	3	4	5	6	7	8	9	10	11	12
1	560.4	406.7	356.1	366.9	361.1	378.3	378.6	405.7	416.7	441.2	438.8	467.6
2		416.2	373.1		379.1		382.8					
3	582.6	428.7	376.1	383.8	391.7	389.4	391.3	399.0	410.5	428.6	445.4	486.0
4		424.3	380.5		396.9		394.9					
5	561.7	441.9	385.5	392.9	399.5	397.1	403.3	405.1	425.8	435.7	468.4	505.5
6		438.4	382.3		392.7		397.0					
7	576.2	423.8	372.5	385.7	391.9	389.1	391.7	408.2	410.2	434.8	444.5	481.3
8		414.1	376.8		389.2		380.9					

PERIPHERAL HEAT TRANSFER COEFFICIENT W/(SQ.M. K)

	1	2	3	4	5	6	7	8	9	10	11	12
1	3182.1	2309.2	2022.1	2083.5	2050.2	2147.8	2149.8	2303.7	2366.4	2505.5	2491.4	2655.4
2		2363.5	2118.5		2152.8		2173.5					
3	3308.3	2434.1	2135.6	2179.5	2224.3	2211.0	2221.7	2265.7	2331.0	2433.9	2529.3	2759.4
4		2409.1	2160.6		2253.5		2242.6					
5	3189.2	2509.4	2189.1	2231.2	2268.5	2254.6	2289.9	2300.2	2418.0	2473.8	2659.9	2870.6
6		2489.3	2170.6		2230.1		2254.1					
7	3271.9	2406.6	2115.4	2189.9	2225.2	2209.2	2224.3	2317.7	2329.2	2468.9	2523.8	2732.9
8		2351.3	2139.8		2209.9		2162.8					

AVERAGE HEAT TRANSFER COEFFICIENT-BTU/(SQ.FT.HR-F)

	1	2	3	4	5	6	7	8	9	10	11	12
(H1)	570.23	424.26	375.37	382.34	387.76	388.44	390.05	404.50	415.82	435.08	449.28	485.11
(H2)	570.09	424.01	375.22	382.13	387.47	388.34	389.91	404.47	415.74	435.04	449.03	484.76

AVERAGE HEAT TRANSFER COEFFICIENT-W/(SQ.M. K)

	1	2	3	4	5	6	7	8	9	10	11	12
(H1)	3237.89	2409.08	2131.46	2171.04	2201.80	2205.68	2214.83	2296.83	2361.14	2470.51	2551.11	2754.57
(H2)	3237.12	2407.64	2130.62	2169.83	2200.18	2205.09	2214.01	2296.70	2360.68	2470.29	2549.69	2752.62

RATIO OF CALCULATED HEAT TRANSFER COEFFICIENT TO THOSE PREDICTED BY LITERATURE

	1	2	3	4	5	6	7	8	9	10	11	12
LIT(1)	1.625	1.192	1.043	1.050	1.052	1.041	1.033	1.060	1.065	1.091	1.079	1.105
LIT(2)	1.493	1.106	0.973	0.980	0.983	0.974	0.967	0.992	0.999	1.024	1.016	1.045
LIT(3)	1.571	1.164	1.023	1.030	1.032	1.022	1.015	1.040	1.046	1.070	1.059	1.082
LIT(5)	8.768	6.458	5.684	5.787	5.865	5.868	5.887	6.105	6.267	6.552	6.740	7.248
LIT(6)	3.946	4.191	4.060	5.207	5.277	5.280	5.297	5.494	7.104	7.427	9.625	11.378
LIT(7)	2.219	1.612	1.393	1.368	1.338	1.292	1.252	1.254	1.203	1.177	1.079	1.105
LIT(8)	2.597	2.797	2.725	3.501	3.544	3.544	3.553	3.678	4.746	4.950	6.341	7.405

LIT(1) IS BY SIEDER-TATE  
LIT(2) IS BY DITTUS-BOELTER  
LIT(3) IS BY EAGLE-FERGUSON  
LIT(5) IS BY HAUSEN  
LIT(6) IS BY MCADAMS  
LIT(7) IS BY SIEDER-TATE AND HAUSEN

\*-----\*  
 RUN NUMBER 1111  
 \*-----\*

	1	2	3	4	5	6	7	8	9	10	11	12
X, INCH	1.00	4.00	8.00	16.00	24.00	32.00	40.00	48.00	64.00	80.00	112.00	154.50
TB, F	83.49	84.26	85.30	87.36	89.43	91.50	93.56	95.63	99.76	103.90	112.16	123.14
RE.NO.	7404.80	7474.12	7566.93	7753.86	7942.54	8132.93	8325.01	8518.76	8911.19	9310.05	10126.40	11247.25
PR.NO.	5.62	5.56	5.48	5.34	5.20	5.06	4.93	4.80	4.57	4.35	3.96	3.53
NU.NO.	85.358	63.442	56.054	56.938	57.589	57.537	57.624	59.602	60.960	63.469	64.922	69.280
GR.NO.	187224.5	260172.4	306962.6	327326.3	350454.8	377955.6	405201.5	419169.4	470420.1	512872.1	640555.1	804715.1
UB/UW.	1.2401	1.3265	1.3692	1.3566	1.3461	1.3402	1.3339	1.3165	1.2988	1.2771	1.2542	1.2194
HT/HB	0.998	0.920	0.924	0.934	0.904	0.953	0.939	1.002	0.979	1.013	0.937	0.925
HJ	0.369E+02	0.274E+02	0.245E+02	0.256E+02	0.266E+02	0.273E+02	0.281E+02	0.298E+02	0.322E+02	0.352E+02	0.397E+02	0.477E+02
V, FT/S	1.23656	1.23656	1.23656	1.23656	1.23656	1.23656	1.23656	1.23656	1.23656	1.23656	1.23656	1.23656
GR/RE2	0.00	0.00	0.01	0.01	0.01	0.01	0.01	0.01	0.01	0.01	0.01	0.01
PW	0.921E+03	0.684E+03	0.605E+03	0.614E+03	0.621E+03	0.621E+03	0.622E+03	0.643E+03	0.658E+03	0.685E+03	0.700E+03	0.747E+03
NU*PR-.3	48.02	35.81	31.79	32.58	33.25	33.52	33.86	35.32	36.74	38.88	41.02	45.51

NO	RUN #	RE	PR	AVG HEAT FLUX	HEAT GENERATED	HEAT GAINED	HEAT LOST	H.B.% ERROR
1	1111	9247	4.4	11609	24990.9	24568.3	5.7	1.669



# APPENDIX I

## COMPUTER LIST OF THE MAIN PROGRAM

```

C *****
C *
C *   A PROGRAM TO CALCULATE THE INSIDE WALL TEMPERATURES AND
C *   LOCAL HEAT TRANSFER COEFFICIENTS FOR GIVEN OUTSIDE WALL
C *   TEMPERATURES AND COMPARE THE RESULTS WITH SEVERAL LITERATURE
C *   RESULTS.
C *
C *   INSTALLATION   : OKLAHOMA STATE UNIVERSITY.
C *   WRITTEN BY     : A. N. ABDELMESSIH ET AL.
C *   MODIFIED BY    : CHEN, JENG-HO
C *   DATE MODIFIED  : SPRING, 1987
C *   LANGUAGE       : FORTVCG
C *
C *****
C *
C *                               MAIN PROGRAM
C *
C *****
C
C   DIMENSION TSAVE1(12,8),TSAVE2(12,8),SITOC(12,8),REN(12,8),
C $         TCHCK1(8),TCHCK2(8)
C   COMMON /READ1/TBATH,TROOM,VOLTS,TAMPS,RMFL,MFLUID,X2,FLOWRT,NRUN
C   COMMON /READ2/ TIN,TOUT,TIN2,TOUT1
C   COMMON /READ3/ TOSURF(12,8),TISURF(12,8),NTH(12)
C   COMMON /TCOND/ CONDK(12,9)
C   COMMON /TEMP1/ TWALL(12,8),AMPS(12,8),RESIS(12,8),POWERS(13),
C $         TPOWER
C   COMMON /MAIN1/ IST,KOUNT
C   COMMON /MAIN2/ AMP,OHMS,OHMS12,OHMS13
C   COMMON/GEOM1/XAREA(12),R(12),LTP(13),LTH(13),DELZ(12),LHEAT,LTEST
C   COMMON /GEOM2/ DOUT,DIN,DEL,R,NODES,NSLICE,PI
C   COMMON /THERM1/TSAT(13),TSTART,TEND,QLOSS1,QLOSS2
C   COMMON /ERESIS/ RSVTY(12,8)
C   COMMON /OUTT/  INO,IRNO(50),IRENO(50),PRDNO(50),
C $         IQFLUX(50),QGEN(50),QGAIN(50),QL(50),QER(50)
C   COMMON /CORT/  AA(12,8),BB(12,8),CC(12,8),DD(12,8)
C   COMMON M,N
C   REAL*4 LTH,LTP,LTEST,LHEAT
C   DATA NTH/4,8,8,4,8,4,8,4,4,4,4,4/
C
C
C   M=5
C   N=6
C   INO=0
C 1 READ(M,100) NRUN
C   IF (NRUN .EQ. 0) GO TO 2000
C   INO=INO+1
C   CALL READS
C   CALL GEOM
C   CALL CORECT

```

```

DO 2 IST=1,12
  IP = NTH(IST)
  DO 2 IPR=1,IP
    2    SITOC(IST,IPR)=(TOSURF(IST,IPR)-32.0)/1.8
    WRITE(N,120)IPR,(SITOC(IST,IPR),IST=1,12)
    SIRMFL=RMFL*1.259979E-4
    IRNO(INO)=NRUN
    NNODE=NODES-1
C ----- START SOLUTION WITH STATION 1
  DO 1000 T=1,12
    IP = NTH(IST)
C SET ALL RADIAL TEMPERATURES EQUAL TO THE OUTSIDE SURFACE TEMPERATURES
    DO 4 ISL=1,NODES
      DO 4 IPR=1,IP
        4    TWALL(ISL,IPR)=TOSURF(IST,IPR)
C ----- CALCULATE THERMAL CONDUCTIVITY FOR EACH NODE
        5    CALL THCOND
C ----- CALCULATE ELECTRICAL CONDUCTIVITY FOR EACH NODE
        CALL ERSTVT
C ----- CALCULATE RESISTANCE FOR EACH SEGMENT, ALSO
C    CALCULATE EQUIVALENT RESISTANCE FOR PARALLEL CIRCUITS
        CALL GEOMST
        DO 6 ISL=1,NODES
          DO 6 IPR=1,IP
            RESIS(ISL,IPR) = RSVTY(ISL,IPR)*DELZ(IST)/XAREA(ISL)
        6    RINV = RINV +1.0/RESIS(ISL,IPR)
C ----- CALCULATE CURRENT FOR EACH SEGMENT
        OHMS = 1.0/RINV
        DO 7 ISL=1,NODES
          DO 7 IPR=1,IP
            AMPS(ISL,IPR) = TAMPS*OHMS/RESIS(ISL,IPR)
        7    AMP=AMP+AMPS(ISL,IPR)
C ----- CALCULATE TEMPERATURES AT NODE 2
C    TEMPERATURES AT NODE 1 ARE OUTSIDE WALL TEMPERATURES
        DO 8 IPR=1,IP
          IMINS=IPR-1
          IPLUS=IPR+1
          NMINS = ISL - 1
          NPLUS = ISL + 1
          IF(IMINS.EQ.0 .AND. IP .EQ. 8) IMINS=8
          IF(IMINS.EQ.0 .AND. IP .EQ. 4) IMINS=4
          IF(IPLUS.EQ.9 .AND. IP .EQ. 8) IPLUS=1
          IF(IPLUS.EQ.5 .AND. IP .EQ. 4) IPLUS=1
          A = 3.41214*12.0*AMPS(ISL,IPR)*AMPS(ISL,IPR)
          $    *RSVTY(ISL,IPR)/XAREA(ISL)
          B = 12.0*(QLOSS2+QLOSS1)/(2.0*IP*LHEAT)
          C = IP*DELK*(CONDK(ISL,IPR)+CONDK(ISL,IPLUS))
          $    *(TWALL(ISL,IPR)-TWALL(ISL,IPLUS))/(8.0*PI*R(ISL))
          D = IP*DELK*(CONDK(ISL,IPR)+CONDK(ISL,IMINS))
          $    *(TWALL(ISL,IPR)-TWALL(ISL,IMINS))/(8.0*PI*R(ISL))
          X = PI*(R(ISL)-DELK/2.0)*(CONDK(ISL,IPR)+CONDK(NPLUS,IPR))
          $    /(IP*DELK)
          TWALL(NPLUS,IPR) = TWALL(ISL,IPR)- (A-B-C-D)/X
C ----- CALCULATE REMAINING NODAL TEMPERATURES
        DO 9 ISL=2,NNODE
          DO 9 IPR=1,IP
            IMINS=IPR-1
            IPLUS=IPR+1
            NMINS=ISL-1
            NPLUS=ISL+1
            IF(IMINS.EQ.0 .AND. IP .EQ. 8) IMINS=8
            IF(IMINS.EQ.0 .AND. IP .EQ. 4) IMINS=4
            IF(IPLUS.EQ.9 .AND. IP .EQ. 8) IPLUS=1
            IF(IPLUS.EQ.5 .AND. IP .EQ. 4) IPLUS=1

```

```

      A= 3.41214*12.0*AMPS(ISL,IPR)*AMPS(ISL,IPR)
$      *RSVTY(ISL,IPR)/XAREA(ISL)
      B =PI*(R(ISL)+DELR/2)*(CONDK(ISL,IPR)+CONDK(NMINS,IPR))
$      *(TWALL(ISL,IPR)-TWALL(NMINS,IPR))/(IP*DELR)
      C = IP*DELR*(CONDK(ISL,IPR)+CONDK(ISL,IPLUS))
$      *(TWALL(ISL,IPR)-TWALL(ISL,IPLUS))/(4.*PI*R(ISL))
      D = IP*DELR*(CONDK(ISL,IPR)+CONDK(ISL,IMINS))
$      *(TWALL(ISL,IPR)-TWALL(ISL,IMINS))/(4.*PI*R(ISL))
      X =PI*(R(ISL)-DELR/2)*(CONDK(ISL,IPR)+CONDK(NPLUS,IPR))
$      /(IP*DELR)
      9      TWALL(NPLUS,IPR) = TWALL(ISL,IPR)- (A-B-C-D)/X
C ----- CHECK FOR THE CONVERGENCE OF THE WALL TEMPERATURES
      DO 10 IPR=1,IP
          TCHCK2(IPR)=TWALL(NODES,IPR)
      10      TCHCK = TCHCK + ABS(TCHCK2(IPR)-TCHCK1(IPR))
          IF (TCHCK .GT. 0.001) GO TO 11
          GO TO 14
      11      DO 12 IPR=1,IP
      12      TCHCK1(IPR) = TCHCK2(IPR)
          IF (KOUNT .GT. 20) GO TO 13
          KOUNT = KOUNT+1
          GO TO 5
      13      WRITE(N,135) IST,KOUNT
      14      DO 15 IPR=1,IP
      15      TISURF( IST ,IPR)=TWALL(NODES,IPR)
C ----- CALCULATE POWER GENERATED IN EACH SEGMENT IN BTU/HOUR
      DO 16 ISL=1,NODES
          DO 16 IPR=1,IP
      16      POWER=POWER+AMPS(ISL,IPR)*AMPS(ISL,IPR)*RESIS(ISL,IPR)
C CALCULATE POWER GENERATED IN SEGMENTS 12 & 13 BY SAVING VARIABLES FOR
C      STATIONS 1,2,10,AND 11
      POWERS(IST)=POWER*3.41214
      IF(IST.GT.0) GO TO 32
      IF(IST.GT.2) GO TO 25
      IF(IST.EQ.2) GO TO 18
      DO 25 ISL=1,NODES
          DO 17 IPR=1,IP
      17      TSAVE1(ISL,IPR)=TWALL(ISL,IPR)
          GO TO 23
      18      DO 19 ISL=1,NODES
          DO 19 IPR=1,IP
      19      TSAVE2(ISL,IPR)=TWALL(ISL,IPR)
          DO 22 ISL=1,NODES
          DO 22 IPR=1,IP
              IF((IPR .EQ. 1) .OR. (IPR .EQ. 3)) GO TO 20
              IF((IPR .EQ. 5) .OR. (IPR .EQ. 7)) GO TO 20
              IF (IPR .EQ. 8) GO TO 21
              IP1 = IPR/2
              TWALL(ISL,IPR)=(TSAVE1(ISL,IP1)
$                  +TSAVE1(ISL,IP1+1)
$                  +TSAVE2(ISL,IPR)*2.)/4.0
              GO TO 22
      20      IP2 = (IPR-1)/2+1
              TWALL(ISL,IPR)=(TSAVE1(ISL,IP2)+
$                  TSAVE2(ISL,IPR))/2.0
              GO TO 22
      21      TWALL(ISL,IPR)=(TSAVE1(ISL,1)+TSAVE1(ISL,4)
$                  +2.0*TSAVE2(ISL,IPR))/4.0
      22      CONTINUE
          CALL ERSTVT
          DO 23 ISL=1,NODES
          DO 23 IPR=1,IP
              RESIS(ISL,IPR) = RSVTY(ISL,IPR)*DELR(IST)/XAREA(ISL)
              RINV=RINV+1.0/RESIS(ISL,IPR)

```

```

23          TWALL(ISL,IPR) = TSAVE2(ISL,IPR)
C ----- REDEFINE WALL TEMPERATURES AT STATION 2
          OHMS12=1.0/RINV
          DO 24 IPR=1,IP
            DO 24 ISL=1,NODES
              AMPS(ISL,IPR)= TAMPS*OHMS12/(RESIS(ISL,IPR))
24          POWER=POWER +AMPS(ISL,IPR)*AMPS(ISL,IPR)*RESIS(ISL,IPR)
          POWERS(IST)=POWER*3.41214
25          IF(IST.LT.11) GO TO 32
          IF(IST.EQ.12) GO TO 27
          DO 26 ISL=1,NODES
            DO 26 IPR=1,IP
26          TSAVE1(ISL,IPR)=TWALL(ISL,IPR)
          GO TO 32
27          DO 28 ISL=1,NODES
            DO 28 IPR=1,IP
28          TSAVE2(ISL,IPR)=TWALL(ISL,IPR)
          DO 29 ISL=1,NODES
            DO 29 IPR=1,IP
29          TWALL(ISL,IPR)=(TSAVE1(ISL,IPR)+TSAVE2(ISL,IPR))/2.0
          CALL ERSTVT
          DO 30 ISL=1,NODES
            DO 30 IPR=1,IP
              RESIS(ISL,IPR) = RSVTY(ISL,IPR)*DELZ(IST)/XAREA(ISL)
              RINV=RINV+1.0/RESIS(ISL,IPR)
              TWALL(ISL,IPR) = TSAVE2(ISL,IPR)
30          CONTINUE
C ----- REDEFINE WALL TEMPERATURES AT STATION 10
          OHMS13=1.0/RINV
          DO 32 IPR=1,IP
            DO 31 ISL=1,NODES
              AMPS(ISL,IPR)= TAMPS*OHMS13/(RESIS(ISL,IPR))
31          POWER=POWER + AMPS(ISL,IPR)*AMPS(ISL,IPR)*RESIS(ISL,IPR)
          POWERS(IST)=POWER*3.41214
32          CONTINUE
          CALL QFLUX
1000 CONTINUE
C ---- CALCULATE RENOLDS NUMBERS AT THE INSIDE SURFACE OF THE TUBE.
          DO 33 IST=1,12
            DO 33 IPR=1,IP
              TR=TISURF(IST,IPR)
              CALL MEW(TR,MFLUID,X2,VISS)
              REN(IST,IPR)=RMFL*48.0/(PI*DIN*VISS)
33          CONTINUE
          WRITE(N,125)IPR,(REN(IST,IPR),IST=1,12)
C ----- CALCULATE TOTAL POWER GENERATED IN BTU/HOUR
          DO 34 IST=1,12
34          TPOWER=TPOWER+POWERS(IST)
          CALL TLIQD
          GO TO 1
2000 WRITE(N,170)
          DO 35 I=1,INO
            WRITE(N,190)I,IRNO(I),IRENO(I),PRDNO(I),IQFLUX(I),
              $          QGEN(I),QGAIN(I),QL(I),QER(I)
35          CONTINUE
C
100 FORMAT(I5)
110 FORMAT(1H1,////35X,'CORRECTED OUTSIDE SURFACE TEMPERATURES ',
  $      '-DEGREES F',//15X,'1',7X,'2',7X,'3',7X,'4',7X,
  $      '5',7X,'6',7X,'7',7X,'8',7X,'9',6X,'10',
  $      6X,'11',6X,'12',/)
120 FORMAT(8X,I1,F9.2,11F8.2 )
125 FORMAT(8X,I1,F9.1,11F8.1 )
130 FORMAT(8X,I1,F17.2,F8.2,2F16.2)

```

```

135 FORMAT(//5X,'TEMPERATURES AT STATION',I3,'DO NOT CONVERGE AFTER',
$      I3,' ITERATIONS. JUMP TO NEXT STATION')
140 FORMAT(8X,I1,F17.1,F8.1,2F16.1)
150 FORMAT(1H0,///35X,'CORRECTED OUTSIDE SURFACE ',
$      'TEMPERATURES -DEGREES C',//15X,'1',7X,'2',7X,
$      '3',7X,'4',7X,'5',7X,'6',7X,'7',7X,'8',
$      '9',6X,'10',6X,'11',6X,'12',/)
160 FORMAT(1H0,///40X,'REYNOLDS NUMBER AT THE INSIDE TUBE WALL'
$      //14X,'1',7X,'2',7X,'3',7X,'4',7X,'5',7X,'6',7X,
$      '7',7X,'8',7X,'9',6X,'10',6X,'11',6X,'12',/)
170 FORMAT(1H1)
180 FORMAT(/////14X,'NO',3X,'RUN #',5X,'RE',6X,'PR',
$ 4X,'AVG HEAT FLUX',5X,'HEAT GENERATED',3X,'HEAT GAINED',3X,'HEAT
$ LOST',3X,'H.B.% ERROR')
190 FORMAT(//11X,I5,I8,I8,F8.1,I12,10X,F10.1,5X,F10.1,F12.1,F14.3)
      STOP
      END

C
C
      SUBROUTINE BET(TF,MFLUID,X,BETA)
C
C COEFFICIENT OF THERMAL EXPANSION 1/DEGF.
      T1 = TF + 0.50
      T2 = TF - 0.50
      CALL DENS(T1,MFLUID,X,ROW1)
      CALL DENS(T2,MFLUID,X,ROW2)
      CALL DENS(TF,MFLUID,X,ROW)
      BETA= ROW*(ROW2-ROW1)/ROW1/ROW2
      RETURN
      END

C
C
      SUBROUTINE CONDFL(TF,MFLUID,X,COND)
C
C THERMAL CONDUCTIVITY OF THE TEST FLUID IN BTU/(HR.FT.DEGF)
      T=(TF-32.0)/1.8
      CONW=0.56276+1.874E-3*T-6.8E-6*T**2
      IF(MFLUID.GT.1) GO TO 100
      COND=CONW/1.729577
      GO TO 101
100 CN=0.4052+0.0594*X-8.40E-4*T
      CONDEG=0.19589+1.689E-4*T-8.10E-7*T**2
      CONSI=(1.0-X)*CONW+X*CONDEG-CN*(CONDEG-CONW)*(1.0-X)*X
      COND=CONSI/1.729577
101 RETURN
      END

C
C
      SUBROUTINE CORECT
C
C COMMON /READ1/ TBATH,TROOM,VOLTS,TAMPS,RMFL,MFLUID,X2,FLOWRT,NRUN
COMMON /READ2/ TIN,TOUT,TIN2,TOUT1
COMMON /READ3/ TOSURF(12,8),TISURF(12,8),NTH(12)
COMMON/GEOM1/XAREA(12),R(12),LTP(13),LTH(13),DELZ(12),LHEAT,LTEST
COMMON /THERM1/ TSAT(13),TSTART,TEND,QLOSS1,QLOSS2
COMMON /OUTT/ INO,IRNO(50),IRENO(50),PRDNO(50),
$      IQFLUX(50),QGEN(50),QGAIN(50),QL(50),QER(50)
COMMON /CORT/ AA(12,8),BB(12,8),CC(12,8),DD(12,8)
REAL*4 LTH,LTP,LTEST,LHEAT
C
      IF (INO .GT. 1) GO TO 202
      DO 200 IST=1,12
          IP = NTH(IST)
          DO 200 IPR=1,IP

```

```

200      READ(M,201)AA(IST,IPR),BB(IST,IPR),CC(IST,IPR),DD(IST,IPR)
201      FORMAT(4E15.5)
C ----- CORRECT INLET AND OUTLET MIXTURE TEMPERATURES
202  TIN2=TIN2
      TOUT1=TOUT1
C ----- CORRECT OUTSIDE SURFACE TEMPERATURES.
      DO 203 IST=1,12
          IP = NTH(IST)
          DO 203 IPR=1,IP
203      TOSURF(IST,IPR)=AA(IST,IPR)+BB(IST,IPR)*TOSURF(IST,IPR)
          $
          $      +CC(IST,IPR)*TOSURF(IST,IPR)**2.0+
          $      DD(IST,IPR)*TOSURF(IST,IPR)**3.0
C ----- CALCULATION OF VOLUMETRIC FLOW RATE IN GPM.
      VFLOW=FLOWRT*60./3785
C ----- CALCULATION OF MASS FLOW RATE IN LBM/HR
      CALL DENS(TBATH,MFLUID,X2,ROW)
      RMFL=VFLOW*0.133666*60.0*ROW
C ----- CALCULATION OF HEAT LOSS FROM TEST SECTION IN BTU/HR.
C      BASED ON INLET TEMPERATURE.
      T1=(TIN+TOUT1)/2.0
      CALL SPHEAT(T1,MFLUID,X2,SPHT)
      QLOST1=RMFL*SPHT*(TIN-TOUT1)
C ----- BASED ON EXIT TEMPERATURE.
      T2=(TIN2+TOUT)/2.0
      CALL SPHEAT(T2,MFLUID,X2,SPHT)
      QLOST2=RMFL*SPHT*(TIN2-TOUT)
C --- CALCULATION OF HEAT LOSS FROM HEAT TRANSFER LOOP IN BTU/HR
      QLOSS1 = QLOST1*LHEAT/(LHEAT+5.0)
      QLOSS2 = QLOST2*LHEAT/(LHEAT+5.0)
      RETURN
      END

C
C
C      SUBROUTINE DENS(TF,MFLUID,X,ROW)
C
C      DENSITY IN LBM/CU.FT
C      T=(TF-32.0)/1.8
C ----- H2O DENSITY IN LB/FT**3
      IF(MFLUID.GT.1) GO TO 300
      ROWSI=999.86+0.061464*T-0.008468*T**2+6.8794E-5*T**3
      $      -4.4214E-7*T**4 + 1.2505E-9*T**5
      ROW=ROWSI*0.062427
      GO TO 301
300  A1 = 0.9988+0.20729*X-0.072103*X*X
      A2 = -1.0357E-4-1.0797E-3*X+4.2904E-4*X*X
      A3 = -3.2251E-6+3.432E-6*X-4.5246E-7*X*X
      ROW=(A1+A2*T+A3*T*T)*62.428
301  RETURN
      END

C
C
C      SUBROUTINE ERSTVT
      COMMON /READ1/ TBATH,TROOM,VOLTS,TAMPS,RMFL,MFLUID,X2,FLOWRT,NRUN
      COMMON /TEMP1/ TWALL(12,8),AMPS(12,8),RESIS(12,8),POWERS(13)
      $      ,TPOWER
      COMMON /GEOM2/ DOUT,DIN,DELR,NODES,NSLICE,PI
      COMMON /READ3/ TOSURF(12,8),TISURF(12,8),NTH(12)
      COMMON /ERESIS/ RSVTY(12,8)
      COMMON /MAIN1/ IST,KOUNT
C ELECTRICAL RESISTIVITY OF STAINLESS STEEL IN OHMS-SQIN/IN
      DO 400 ISL=1,NODES
          IP = NTH(IST)
          DO 400 IPR=1,IP
              RSVTY(ISL,IPR)=.27668E-4 + 0.21346E-7*TWALL(ISL,IPR)

```

```

$          -0.31386E-10*TWALL(ISL,IPR)*TWALL(ISL,IPR)
$          +0.37334E-13*TWALL(ISL,IPR)**3
400 CONTINUE
    RETURN
    END
C
C
SUBROUTINE GEOM
COMMON /READ1/ TBATH,TROOM,VOLTS,TAMPS,RMFL,MFLUID,X2,FLOWRT,NRUN
COMMON/GEOM1/XAREA(12),R(12),LTP(13),LTH(13),DELZ(12),LHEAT,LTEST
COMMON /GEOM2/ DOUT,DIN,DELR,NODES,NSLICE,PI
COMMON /MAIN1/ IST,KOUNT
REAL*4 LTH,LTP,LTEST,LHEAT
DATA LTP/1.0,3.0,4.0,8.0,8.0,8.0,8.0,8.0,16.0,16.0,32.0,42.5,1.0/
DATA LTH/1.0,4.,8.,16.,24.,32.,40.,48.,64.,80.,112.,154.5,155.5/
DATA DELZ/2.0,4.0,4.5,9.5,8.0,8.0,8.0,9.0,19.0,24.0,37.50,22.00/
C
NSLICE=10
NODES= NSLICE + 1
LTEST = 156.0
LHEAT = 155.5
RETURN
END
C
C
SUBROUTINE GEOMST
COMMON /MAIN1/ IST,KOUNT
COMMON /READ3/ TOSURF(12,8),TISURF(12,8),NTH(12)
COMMON/GEOM1/XAREA(12),R(12),LTP(13),LTH(13),DELZ(12),LHEAT,LTEST
COMMON /GEOM2/ DOUT,DIN,DELR,NODES,NSLICE,PI C
DELR = (DOUT-DIN)/2.0/NSLICE
R(1) = DOUT/2.0
DO 500 I=1,NSLICE
500   R(I+1)=R(I)-DELR
    IP = NTH(IST)
    XAREA(1)=(R(1)-DELR/4.0)*PI*DELR/IP
    XAREA(NODES)=(R(NODES)+DELR/4.0) *PI*DELR/IP
    DO 501 I=2,NSLICE
501   XAREA (I)= 2.0*R(I)*PI*DELR/IP
    RETURN
    END
C
C
SUBROUTINE MEW(TF,MFLUID,X,VISC)
C
C      VISCOSITY IN LBM/(HR.FT.)
T=(TF-32.0)/1.8
IF(MFLUID.GT.1) GO TO 600
VISC=2.419*1.0019*10.0**((1.3272*(20.0-T)-0.001053*(20-T)
$      **2)/(T+105.0))
GO TO 601
600 A1=6.3513E-1+3.0176*X-4.9609E-1*X**2
    A2=(9.9051E-3*X*X-4.0815E-2*X-2.9276E-2)
    A3=(1.8238E-6+5.7651E-6*X-2.6245E-6*X*X)
    V = A1**1.3514+A2*T+A3**0.6803*T*T
    VISC = 2.419*EXP(V)
601 RETURN
    END
C
C
SUBROUTINE QFLUX
COMMON /MAIN1/ IST,KOUNT
COMMON/GEOM1/XAREA(12),R(12),LTP(13),LTH(13),DELZ(12),LHEAT,LTEST
COMMON /READ3/ TOSURF(12,8),TISURF(12,8),NTH(12)

```

```

COMMON /GEOM2/ DOUT,DIN,DELR,NODES,NSLICE,PI
COMMON /TCOND/ CONDK(12,9)
COMMON /TEMP1/ TWALL(12,8),AMPS(12,8),RESIS(12,8),POWERS(13),
$          TPOWER
COMMON /QFLUX1/ QFLXID(12,8)
COMMON /QFLUX2/ Q1,Q2,Q4,QGEN
COMMON /ERESIS/ RSVTY(12,8)

C
C          CALCULATE HEAT FLUX AT INSIDE SURFACE
ISL=NODES
DO 700 IPR=1,IP
    IPLUS=IPR+1
    IMINS=IPR-1
    IF(IMINS.EQ.0 .AND. IP .EQ. 8) IMINS=8
    IF(IMINS.EQ.0 .AND. IP .EQ. 4) IMINS=4
    IF(IPLUS.EQ.9 .AND. IP .EQ. 8) IPLUS=1
    IF(IPLUS.EQ.5 .AND. IP .EQ. 4) IPLUS=1
    Q1 = PI*(CONDK(ISL-1,IPR)+CONDK(ISL,IPR))*(R(ISL-1)-DELR/2.0)*
$      (TWALL(ISL,IPR)-TWALL(ISL-1,IPR))/(IP*DELR)
    Q2 = IP*(CONDK(ISL,IPLUS)+CONDK(ISL,IPR))*DELR
$      *(TWALL(ISL,IPR)-TWALL(ISL,IPLUS))/(PI*R(ISL)*8.0)
    Q4 = IP*(CONDK(ISL,IPR)+CONDK(ISL,IMINS))*DELR
$      *(TWALL(ISL,IPR)-TWALL(ISL,IMINS))/(PI*R(ISL)*8.0)
    QGEN=3.41214*12.0*AMPS(ISL,IPR)*AMPS(ISL,IPR)
$      *RSVTY(ISL,IPR)/XAREA(ISL)
700  QFLXID(IST,IPR) =(QGEN-Q1-Q2-Q4)*IP*12.0/(2.0*PI*R(ISL))
    RETURN
END

C
C
SUBROUTINE READS
DIMENSION SITOS(12,8)
COMMON /READ1/ TBATH,TROOM,VOLTS,TAMPS,RMFL,MFLUID,X2,FLOWRT,NRUN
COMMON /READ2/ TIN,TOUT,TIN2,TOUT1
COMMON /READ3/ TOSURF(12,8),TISURF(12,8),NTH(12)
COMMON /MAIN1/ IST,KOUNT
COMMON M,N

C
    READ (M,15)MFLUID,X2,FLOWRT,TAMPS,VOLTS,TBATH,TIN,TOUT,
$      TIN2,TOUT1,TROOM
    DO 800 IST=1,12
        IP = NTH(IST)
800  READ (M,20)(TOSURF(IST,IPR),IPR=1,IP)
        SITR=(TROOM-32.0)/1.8
        SITIN=(TIN-32.0)/1.8
        SITOUT=(TOUT-32.0)/1.8
        SITBA=(TBATH-32.0)/1.8
        SITIN2=(TIN2-32.0)/1.8
        SITO1=(TOUT1-32.0)/1.8
        VFLOW = FLOWRT*60/3785
        CALL DENS(TBATH,MFLUID,X2,ROW)
        RMFL = VFLOW*0.133666*60.0*ROW
        WRITE(N,25)NRUN,RMFL,VFLOW,FLOWRT,TAMPS,VOLTS,TROOM,
$      SITR,TIN,SITIN,TOUT,SITOUT,TBATH,SITBA
        IF(MFLUID.GT.1)GO TO 801
        GO TO 802
801  WRITE(N,35)X2
802  WRITE(N,45)IPR,(TOSURF(IST,IPR),IST=1,12)
        DO 803 IST=1,12
            DO 803 IPR=1,IP
803      SITOS(IST,IPR) = (TOSURF(IST,IPR)-32.0)/1.8
        WRITE(N,45)IPR,(SITOS(IST,IPR),IST=1,12)

C
10  FORMAT(1H1)

```



```

15 FORMAT(I2,F7.2,F7.4,8F7.2)
20 FORMAT(8F7.2)
25 FORMAT(///46X,'*',15('-'),'*/47X,'RUN NUMBER ',I4,
$      /46X,'*',15('-'),'*/20X,
$      'FLOW RATE',23X,'=',F9.3,2X,'LBM/HR',3X,'=',F9.3,2X,
$      'GPM',3X,'=',F9.3,2X,'CC/SEC',
$      /20X,'CURRENT TO TUBE',17X,'=',F9.3,4X,'AMPS',
$      /20X,'VOLTAGE DROP IN TUBE',12X,'=',F9.3,3X,'VOLTS',
$      /20X,'ROOM TEMPERATURE',16X,'=',F9.3,7X,'F',3X,
$      ' ',F9.3,4X,'C',
$      /20X,'UNCORRECTED INLET TEMPERATURE  ',F9.3,7X,'F',3X,
$      ' ',F9.3,4X,'C',
$      /20X,'UNCORRECTED OUTLET TEMPERATURE  ',F9.3,7X,'F',3X,
$      ' ',F9.3,4X,'C',
$      /20X,'BATH TEMPERATURE',16X,'=',F9.3,7X,'F',3X,
$      ' ',F9.3,4X,'C')
30 FORMAT(///32X,7('*'),' TEST FLUID IS DISTILLED WATER ',7('*'))
35 FORMAT(///15X,'MASS FRACTION OF DIETHYLENE GLYCOL =',F8.4)
40 FORMAT(///32X,'UNCORRECTED OUTSIDE SURFACE TEMPERATURES - ',
$      'DEGREES F',//15X,'1',7X,'2',7X,'3',7X,'4',7X,'5',7X,
$      '6',7X,'7',7X,'8',7X,'9',6X,'10',6X,'11',6X,'12',/)
45 FORMAT(8X,I1,F9.2,11F8.2)
50 FORMAT(8X,I1,F17.2,F8.2,2F16.2)
55 FORMAT(///32X,'UNCORRECTED OUTSIDE SURFACE TEMPERATURES - ',
$      'DEGREES C',//15X,'1',7X,'2',7X,'3',7X,'4',7X,'5',7X,
$      '6',7X,'7',7X,'8',7X,'9',6X,'10',6X,'11',6X,'12',/)
C
      RETURN
      END
C
C
      SUBROUTINE SPHEAT(T,MFLUID,X,SPHT)
C
C          SPECIFIC HEAT IN BTU/(LBM-DEGF)
      IF(MFLUID .GT. 1.0)GO TO 850
      SPHT=1.01881-0.4802E-3*T+0.3274E-5*T**2-0.604E-8*T**3
      GO TO 851
850      CALL MEW(T,MFLUID,X,VISC)
      CALL CONDFL(T,MFLUID,X,COND)
      T = (T-32.0)/1.8
      PNPR = (1.4539+0.95616*X-0.21388*X*X)**2.5
$      -(1.0111E-3+2.8728E-3*X-3.6635E-4*X*X)**0.5*T
$      +(1.6878E-10+1.4891E-9*X-6.7294E-10*X*X)**0.4*T*T
      SPHT = EXP(PNPR)*COND/VISC
851 RETURN
      END
C
C
      SUBROUTINE THCOND
      COMMON /READ3/ TOSURF(12,8),TISURF(12,8),NTH(12)
      COMMON /READ1/ TBATH,TRODM,VOLTS,TAMPS,RMFL,MFLUID,X2,SET,NRUN
      COMMON /TCOND/ CONDK(12,9)
      COMMON /TEMP1/ TWALL(12,8),AMPS(12,8),RESIS(12,8),POWERS(13)
$      ,TPOWER
      COMMON /GEOM2/ DOUT,DIN,DELR,NODES,NSLICE,PI
      COMMON /MAIN1/ IST,KOUNT
C
C      THERMAL CONDUCTIVITY OF STAINLESS STEEL IN BTU/(HR-FT-DEGF)
      IF (IST .GT. 12) IST=12
      DO 860 ISL=1,NODES
          DO 860 IPR=1,IP
860              CONDK(ISL,IPR)=7.270+0.37822E-2*TWALL(ISL,IPR)+0.2042
4E-5*
$              TWALL(ISL,IPR)**2-0.18698E-8*TWALL(ISL,IPR)**3

```

```

      RETURN
      END
C
C
      SUBROUTINE TLIQD
      COMMON /READ1/ TBATH,TROOM,VOLTS,TAMPS,RMFL,MFLUID,X2,FLOWRT,NRUN
      COMMON /READ2/ TIN,TOUT,TIN2,TOUT1
      COMMON /READ3/ TOSURF(12,8),TISURF(12,8),NTH(12)
      COMMON /TEMP1/ TWALL(12,8),AMPS(12,8),RESIS(12,8),POWERS(13)
      $      ,TPOWER
      COMMON/GEOM1/XAREA(12),R(12),LTP(13),LTH(13),DELZ(12),LHEAT,LTEST
      COMMON /GEOM2/ DOUT,DIN,DELR,NODES,NSLICE,PI
      COMMON /THERM1/ TSAT(13),TSTART,TEND,QLOSS1,QLOSS2
      COMMON /THERM2/ HTCOFF(12,8),QUALTY(13),HSTART,HEND,XSTART,XEND,
      $      ENTH(13)
      COMMON /QFLUX1/ QFLXID(12,8)
      COMMON /TCOND/ CONDK(12,9)
      COMMON /TLIQ1/ TBULK(13),HLIQ(13)
      COMMON /TLIQ2/HTDBL(12),HNUSLT(12),HSTATE(12),HAVG(12),HHAUSN(12)
      &      ,HPP(12),HMX(12),HMCADM(12)
      COMMON /OUTT/ INO,IRNO(50),IRENO(50),PRDNO(50),
      $      IQFLUX(50),QGEN(50),QGAIN(50),QL(50),QER(50)
      COMMON M,N
      DIMENSION QAVG(12),TAVG(12),H(12),PWP(12),SIH(12),SIHP(12,8)
      DIMENSION GRNO(12),GRRE2(12),RENO(12),PR(12),HU(12),XD(12),
      $      VISBW(12)
      DIMENSION XX(22),YY(22),SIHAV(12),SITIS(12,8),SITB(12)
      DIMENSION SIQIN(12,8),PRNU(12),SHTHB(13)
      DIMENSION RATIO(12),HCAL(12),VEL(12),HTMP(12)
      REAL*4 LTH,LTP,LTEST,LHEAT,H,HAV,HAVG,HTCOFF,HEF,HSTATE,
      $      HTDBL,HNUSLT,HMB,HAUSEN,HHAUSN,HPP,HIPP,HSTH,HMIX,HCAL
C
      G=32.174
      WRITE(N,105)NRUN
      WRITE(N,115)IPR,(TISURF(IST,IPR),IST=1,12)
      DO 900 IST=1,12
        DO 900 IPR=1,IP
          SITIS(IST,IPR)=(TISURF(IST,IPR)-32.0)/1.8
      900 CONTINUE
      WRITE(N,115)IPR,(SITIS(IST,IPR),IST=1,12)
C ----- CALCULATE BULK FLUID TEMPERATURE AT EACH STATION,DEG.F
      TBULK(1) = TIN + (TOUT-TIN)*1.5/LTEST
      DO 901 IST =2,12
      901   TBULK(IST) = TBULK(IST-1) + (TOUT-TIN)*LTP(IST)/LTEST
      WRITE(N,115)(TBULK(IST),IST=1,12)
      DO 902 IST=1,12
      902   SITB(IST)=(TBULK(IST)-32.0)/1.8
      WRITE(N,115)(SITB(IST),IST=1,12)
      SITOUT=(TOUT-32.0)/1.8
      SITIN=(TIN-32.0)/1.8
      WRITE(N,145)TOUT,SITOUT,TIN,SITIN
      WRITE(N,105)IPR,(QFLXID(IST,IPR),IST=1,12)
      DO 903 IST=1,12
        DO 903 IPR=1,IP
      903   SIQIN(IST,IPR)=QFLXID(IST,IPR)*3.15491
      WRITE(N,105)IPR,(SIQIN(IST,IPR),IST=1,12)
C ----- CALCULATION OF INPUT AND OUTPUT HEAT TRANSFER RATE,BTU/HR
      QGCALC=TPOWER
      QGEXPT =TAMPS*VOLTS*3.41214
      QLOSS=(QLOSS1+QLOSS2)*LHEAT/(2.0*(LHEAT+5.0))
      QIN=QGEXPT-QLOSS
      T=(TOUT+TIN)/2.0
      CALL SPHEAT(T,MFLUID,X2,SPHT)
      QBALNC=RMFL*SPHT*(TOUT-TIN)

```

```

      QPCT=(QIN-QBALNC)*100.0/QIN
      AID=PI*DIN*DIN/4.0/144.0
      GW=RMFL/AID
C ----- CALCULATION OF PERIPHERAL HEAT TRANSFER COEFFICIENT FROM
C      EXPERIMENTAL DATA, BTU/(HR-SQ.FT-DEG.F)
      DO 904 IST=1,12
        DO 904 IPR=1,IP
          904      HTCOFF(IST,IPR) =QFLXID(IST,IPR)/((TISURF(IST,IPR)-TBULK(IST) )
C ----- CALCULATION OF OVERALL HEAT TRANSFER COEFFICIENT
      DO 906 IST=1,12
        DO 905 J=1,IP
          TT=TT+TISURF(IST,J)
          905      QQ=QQ+QFLXID(IST,J)
          TAVG(IST)=TT/IP
          QAVG(IST)=QQ/IP
          906      H(IST)=QAVG(IST)/((TAVG(IST)-TBULK(IST))
      DO 908 IST=1,12
        DO 907 IPR=1,IP
          TIS=TIS+TISURF(IST,IPR)
          907      HAV = HAV+HTCOFF(IST,IPR)
          T=TBULK(IST)
          CALL MEW(T,MFLUID,X2,VISC)
          CALL SPHEAT(T,MFLUID,X2,SPHT)
          CALL CONDFL(T,MFLUID,X2,COND)
          CALL DENS(T,MFLUID,X2,ROW)
          CALL BET(T,MFLUID,X2,BETA)
          PR(IST) = VISC*SPHT/COND
          RENO(IST) = GW*DIN/12.0/VISC
          GRNO(IST)=G*BETA*ROW**2*DIN**3*((TAVG(IST)-TBULK(IST))/VIS
$          C**2 *3600.0**2/12.0/12.0 /12.0
          GRRE2(IST)=GRNO(IST)/RENO(IST)**2
C ----- AVERAGE HEAT TRANSFER COEFFICIENT AT EACH STATION
C      FROM EXPERIMENTAL DATA, BTU/HR-SQ.FT-DEG.F
          T=TIS/IP
          CALL MEW(T,MFLUID,X2,VISWL)
          T=TBULK(IST)
          CALL MEW(T,MFLUID,X2,VISC)
          CALL SPHEAT(T,MFLUID,X2,SPHT)
          CALL CONDFL(T,MFLUID,X2,COND)
          VISBW(IST) = VISC/VISWL
          REYNO=GW*DIN/12.0/VISC
          PRNO=VISC*SPHT/COND
          HAVG(IST)=HAV/IP
          TH=(DOUT-DIN)/2.0
          TWALL(IST,1)=TAVG(IST)
          CALL THCOND
          HMB=ABS(H(IST))
C      ++++++
C      TURBULENT FLOW.
          PW=HMB*(DIN/12.0)**2/(COND*TH/12.0)
          PWP(IST)=PW
C ---- DITTUS-BOETLER HEAT TRANSFER COEFFICIENT, BTU/(HR-SQ.FT-DEG.F)
          HTDB=0.023*REYNO**0.8*PRNO**0.4*COND/DIN*12.0
C ----- SIEDER-TATE HEAT TRANSFER COEFFICIENT AT EACH STATION,
C      BTU/HR-SQ.FT-DEG.F
          HSTATE(IST)=0.023*REYNO**0.8*PRNO**0.3333*((VISC/VISWL)**0.14
$          *COND/DIN*12.0
C ----- EAGLE-FERGUSON HEAT TRANSFER COEFFICIENT
C      BTU/HR-SQ.FT-DEG.F
          V=GW/ROW/3600.0
          T=TBULK(IST)
          HEF=(1.75*T +160.0)*V**0.80
          C=0.9109 - 0.4292*ALOG10(DIN)
          HEF=C*HEF

```

```

C ----- HEAT TRANSFER COEFFECIENT BY PETUKHOV AND POPOV
      FF = 1.0/(3.64*ALOG10(REYNO)-3.28)**2
      A = 1.07+12.7*(FF/2.)**.5*(PRNO**0.6667-1.0)
      HIPP = 12.0*COND*FF*REYNO*PRNO/(2.*A*DIN)
C
C
C
C ----- HEAT TRANSFER COEFFECIENT BY HAUSEN
      A = 0.0668*REYNO*PRNO*DIN/LTEST
      B = 1.0+0.04*(REYNO*PRNO*DIN/LTEST)**0.6667
      HAUSEN = COND*12.0/DIN*(4.364+A/B)*(VISC/VISWL)**0.14
      PEC = REYNO*PRNO*DIN/LTP(IST)
      H11 = 4.364 + (0.038*PEC**0.8+0.01482741*PEC**1.267)
      $ /((1.0 + 0.117*PEC**0.467)**2)
C ----- HEAT TRANSFER COEFFECIENT BY MCADAMS
      HMC = COND*12.0/DIN*1.75*(RMFL*SPHT/(COND*LTP(IST)))*0.3333
      $ *(VISC/VISWL)**0.14
C ----- HEAT TRANSFER COEFFECIENT BY SIEDER-TATE AND HAUSEN
      HSTH = HAUSEN + (REYNO-2100.0)*(HSTATE(IST)-HAUSEN)/7900.0
      IF (REYNO .GT. 10000.) HSTH = HSTATE(IST)
      IF (REYNO .LT. 2100.) HSTH = HAUSEN
C ---- RATIO OF HEAT TRANSFER COEFFICIENTS:THIS WORK TO LITERATURES
      HTDBL(IST)=HAVG(IST)/HTDB
      HSTATE(IST)=HAVG(IST)/HSTATE(IST)
      HNUSLT(IST)=HAVG(IST)/HEF
      HHAUSN(IST)=HAVG(IST)/HAUSEN
      HMCADM(IST)=HAVG(IST)/HMC
      HPP(IST)=HAVG(IST)/HIPP
      HMIK(IST)=HAVG(IST)/HSTH
      HU(IST) = 1.0/(PRNO*0.4*(VISC/VISWL)**0.14)
      HLIQ(IST)=HAVG(IST)*DIN/(12.0*COND)
      HTMP(IST)=HLIQ(IST)/H11
      HCAL(IST) = HLIQ(IST)/HMCADM(IST)
      RATIO(IST) = (HLIQ(IST)-HCAL(IST))*100.0/HLIQ(IST)
C ----- VELOCITY IN FT/SEC
      VEL(IST) = FLOWRT/(49.4535*3.14159*DIN*DIN)
908 CONTINUE
C
      T=(TIN+TOUT)/2.0
      CALL CONDFL(T,MFLUID,X2,COND)
      CALL MEW(T,MFLUID,X2,VISC)
      CALL SPHEAT(T,MFLUID,X2,SPHT)
      PRNO=VISC*SPHT/COND
      REYNO=GW*DIN/12.0/VISC
      QFLXAV=QIN/(3.1416*DIN/12.0*(LHEAT/12.0))
      IRENO(INO)=REYNO
      PRDNO(INO)=PRNO
      IQFLUX(INO)=QFLXAV
      SIGW=GW/737.33806
      SIQAV=QFLXAV*3.154591
      WRITE(N,160)NRUN,REYNO,PRNO,GW,SIGW,QFLXAV,SIQAV
      SIQG=QGEXPT*0.2930711
      SIQBAL=QBALNC*0.2930711
      SIQLOS=QLOSS*0.2930711
      WRITE(N,165)QGEXPT,SIQG,QBALNC,SIQBAL,QLOSS,SIQLOS,QPCT
      QGEN(INO)=QGEXPT
      QGAIN(INO)=QBALNC
      QL(INO)=QLOSS
      QER(INO)=QPCT
      WRITE(N,180)IPR,(HTCOFF(IST,IPR),IST=1,12)
      DO 909 IST=1,12
        DO 909 IPR=1,IP
909      SIHP(IST,IPR)=HTCOFF(IST,IPR)*5.678263
      DO 911 IST=1,12

```

```

      IF (IP .EQ. 4) GO TO 910
      SHTHB(IST)=HTCOFF(IST,1)/HTCOFF(IST,5)
      GO TO 911
910    SHTHB(IST)=HTCOFF(IST,1)/HTCOFF(IST,3)
911    CONTINUE
      WRITE(N,180)IPR,(SIHP(IST,IPR),IST=1,12)
      WRITE(N,195)(HAVG(IST),IST=1,12)
      WRITE(N,200)(H(I),I=1,12)
      DO 912 IST=1,12
912    SIHAV(IST)=HAVG(IST)*5.678263
      DO 913 I=1,12
913    SIH(I)=H(I)*5.678263
      WRITE(N,195)(SIHAV(IST),IST=1,12)
      WRITE(N,200)(SIH(I),I=1,12)
      DO 914 IST=1,12
          CALL CONDFL(T,MFLUID,X2,COND)
          HLIQ(IST)=HAVG(IST)*DIN/(12.0*COND)
          HJ(IST)=HLIQ(IST)*HJ(IST)
914    PRNU(IST) = HLIQ(IST)/PR(IST)**0.3333
      WRITE(N,215)(HSTATE(IST),IST=1,12)
      WRITE(N,220)(HTDBL(IST),IST=1,12)
      WRITE(N,225)(HNUSLT(IST),IST=1,12)
      WRITE(N,230)(HHAUSN(IST),IST=1,12)
      WRITE(N,235)(HMCADM(IST),IST=1,12)
      WRITE(N,240)(HMX(IST),IST=1,12)
      WRITE(N,245)(HTMP(IST),IST=1,12)
      WRITE(N,105)NRUN
      WRITE(N,260)(LTH(IST),IST=1,12)
      WRITE(N,265)(TBULK(IST),IST=1,12)
      WRITE(N,270)(RENO(IST),IST=1,12)
      WRITE(N,275)(PR(IST),IST=1,12)
      WRITE(N,280)(HLIQ(IST),IST=1,12)
      WRITE(N,285)(GRNO(IST),IST=1,12)
      WRITE(N,290)(VISBW(IST),IST=1,12)
      WRITE(N,295)(SHTHB(IST),IST=1,12)
      WRITE(N,300)(HJ(IST),IST=1,12)
      WRITE(N,305)(VEL(IST),IST=1,12)
      WRITE(N,310)(GRRE2(IST),IST=1,12)
      WRITE(N,315)(PWP(IST),IST=1,12)
      WRITE(N,320)(PRNU(IST),IST=1,12)
C
100  FORMAT(1H1)
105  FORMAT(/45X,'*',15('-'),'*/46X,'RUN NUMBER ',
$      I4/45X,'*',15('-'),'*)
110  FORMAT(/35X,'INSIDE SURFACE TEMPERATURES - DEGREES F',//15X,
$      '1',7X,'2',7X,'3',7X,'4',7X,'5',7X,'6',7X,'7',7X,'8',
$      7X,'9',6X,'10',6X,'11',6X,'12',/)
115  FORMAT(8X,I1,F9.2,11F8.2 )
120  FORMAT(/35X,'INSIDE SURFACE TEMPERATURES - DEGREES C',//15X,
$      '1',7X,'2',7X,'3',7X,'4',7X,'5',7X,'6',7X,'7',7X,'8',
$      7X,'9',6X,'10',6X,'11',6X,'12',/)
125  FORMAT(8X,I1,F17.2,F8.2,2F16.2)
125  FORMAT(/41X,'BULK FLUID TEMPERATURE - DEGREES F',//15X,'1',
$      7X,'2',7X,'3',7X,'4',7X,'5',7X,'6',7X,'7',7X,'8',
$      7X,'9',6X,'10',6X,'11',6X,'12',/)
130  FORMAT(/41X,'BULK FLUID TEMPERATURE - DEGREES C',//15X,'1',
$      7X,'2',7X,'3',7X,'4',7X,'5',7X,'6',7X,'7',7X,'8',
$      7X,'9',6X,'10',6X,'11',6X,'12',/)
140  FORMAT(1H0,/)
145  FORMAT(1H1,25X,'CORRECTED OUTLET TEMPERATURE =' ,F9.3,2X,'DEG F',
$      3X,'=' ,F9.3,2X,'DEG C',//25X,
$      'CORRECTED INLET TEMPERATURE =' ,
$      F9.3,2X,'DEG F',3X,'=' ,F9.3,2X,'DEG C')
150  FORMAT(///36X,'INSIDE SURFACE HEAT FLUXES BTU/HR/FT2',//15X,

```

```

$      '1',7X,'2',7X,'3',7X,'4',7X,'5',7X,'6',7X,'7',7X,'8',
$      7X,'9',6X,'10',6X,'11',6X,'12',/)
155 FORMAT(///36X,'INSIDE SURFACE HEAT FLUXES W PER SQ.M.',//15X,
$      '1',7X,'2',7X,'3',7X,'4',7X,'5',7X,'6',7X,'7',7X,'8',
$      7X,'9',6X,'10',6X,'11',6X,'12',/)
160 FORMAT(///44X,'*',15('-'),',*',/45X,'RUN NUMBER ',I4,/44X,'*',
$      15('-'),',*',//15X,
$      'AVERAGE REYNOLDS NUMBER',9X,'=',E10.3,/15X,
$      'AVERAGE PRANDTL NUMBER',10X,'=',E10.3,/15X,
$      'MASS FLUX',23X,'=',E10.3,'LBM/(SQ.FT-HR)',3X,'=',E10.3
$      ,2X,'KG.PER.(S.SQ.M.)',/15X,
$      'AVERAGE HEAT FLUX',15X,'=',E10.3,'BTU/(SQ.FT-HR)',3X,
$      '=',E10.3,2X,'W PER SQ.M.')
165 FORMAT(15X,'Q=AMP*VOLT',22X,'=',E10.3,2X,'BTU/HR',11X,'=',
$      E10.3,2X,'W',/15X,'Q=M*C*(T2-T1)',19X,'=',E10.3,2X,
$      'BTU/HR',11X,'=',E10.3,2X,'W',/15X,
$      'HEAT LOST',23X,'=',E10.3,'BTU/HR',1X,'=',E10.3,2X,'W',
$      /15X,'HEAT BALANCE ERROR %',12X,'=',E10.3)
170 FORMAT(///38X,'PERIPHERAL HEAT TRANSFER COEFFICIENT BTU/',
$      'SQ.FT-HR-F'))
175 FORMAT(18X,'1',7X,'2',7X,'3',7X,'4',7X,'5',7X,'6',7X,'7',7X,'8',
$      7X,'9',6X,'10',6X,'11',6X,'12',/)
180 FORMAT(8X,I2,4X,12F8.1)
185 FORMAT(///39X,'PERIPHERAL HEAT TRANSFER COEFFICIENT W/(SQ.M. K)')
190 FORMAT(1H1,///37X,'AVERAGE HEAT TRANSFER COEFFICIENT',
$      '-BTU/(SQ.FT.HR-F)')
195 FORMAT(10X,'(H1)',12F8.2)
200 FORMAT(10X,'(H2)',12F8.2)
205 FORMAT(///38X,'AVERAGE HEAT TRANSFER COEFFICIENT-W/(SQ.M. K)')
210 FORMAT(/24X,'RATIO OF CALCULATED HEAT TRANSFER COEFFICIENT TO ',
$      'THOSE PREDICTED BY LITERATURE')
215 FORMAT(8X,'LIT(1)',12F8.3)
220 FORMAT(8X,'LIT(2)',12F8.3)
225 FORMAT(8X,'LIT(3)',12F8.3)
230 FORMAT(8X,'LIT(5)',12F8.3)
235 FORMAT(8X,'LIT(6)',12F8.3)
240 FORMAT(8X,'LIT(7)',12F8.3)
245 FORMAT(8X,'LIT(8)',12F8.3)
250 FORMAT(//25X,'LIT(1) IS BY SIEDER-TATE',
$      /25X,'LIT(2) IS BY DITTUS-BOELTER',
$      /25X,'LIT(3) IS BY EAGLE-FERGUSON',
$      /25X,'LIT(4) IS BY PETUKHOV AND POPOV',
$      /25X,'LIT(5) IS BY HAUSEN',
$      /25X,'LIT(6) IS BY MCADAMS',
$      /25X,'LIT(7) IS BY SIEDER-TATE AND HAUSEN')
255 FORMAT(//16X,'1',9X,'2',9X,'3',9X,'4',9X,'5',9X,'6',9X,'7',9X
$      ,8',9X,'9',8X,'10',8X,'11',8X,'12')
260 FORMAT(1H0,3X,'X,INCH',12F10.2)
265 FORMAT(1H0,3X,'TB,F ',12F10.2)
270 FORMAT(1H0,3X,'RE.NO.',12F10.2)
275 FORMAT(1H0,3X,'PR.NO.',12F10.2)
280 FORMAT(1H0,3X,'NU.NO.',12F10.3)
285 FORMAT(1H0,3X,'UB/UW.',12F10.4)
290 FORMAT(1H0,3X,'GR.NO.',12F10.1)
295 FORMAT(1H0,3X,'HT/HB ',12F10.3)
300 FORMAT(1H0,3X,' HJ ',12E10.3)
305 FORMAT(1H0,3X,'V,FT/S',12F10.5)
310 FORMAT(1H0,3X,'GR/RE2',12F10.2)
315 FORMAT(1H0,3X,'PW ',12E10.3)
320 FORMAT(1H0,1X,'NU*PR-.3',12F10.2)
325      FORMAT(3F10.3,F15.3,2F10.3)

RETURN
END

```

//

## APPENDIX J

### SAMPLE CALCULATION

Run 1111 is presented as a sample calculation. The first digit of the run number represents the test fluid, i.e., 1 for distilled water and 2 for DEG-water solution. The second digit identifies the test section. The square-edged contraction entrance straight circular tube with 0.632-in. (16.05 mm) inside diameter, 155.5-in (3.95 m) long, used in the present investigation is identified as 1. The last two digits are the run number of the given test fluid and test section. For run 1111, the test fluid was water and the rotameter setting was 75.2 percent for the small rotameter corresponding to a flow rate of 1.226 gpm. The input current was 437.0 amperes and the voltage drop was 16.760 volts. The experimental data of this run are given in Appendix H. The sample calculations given here follow the procedures presented in Chapter V. All calculations are performed in U.S. units and both U.S. units and SI units are reported. All calculations are based on the following assumptions, which are the same as those in Appendix F:

1. Both peripheral and radial wall conduction exist.
2. Axial conduction is negligible.

3. Steady state achieved.
4. There was heat loss from the test section to the surroundings.

#### Calculation of Heat Balance

##### Rate of Heat Input

$$\begin{aligned}
 \text{Power input} &= (F) (I) (V) \\
 &= (3.41214) (437.0 \text{ A}) (16.760 \text{ V}) \\
 &= 24,991 \text{ Btu/hr} \\
 &= 7324 \text{ W}
 \end{aligned}$$

Density of water at bath temperature ( $83.10^\circ\text{F} = 301.54^\circ\text{K}$ )  
from Appendix E.

$$\begin{aligned}
 &= 62.18 \text{ lb}_m/\text{ft}^3 \\
 &= 995.8 \text{ kg/m}^3
 \end{aligned}$$

Mass flow rate is equal to the volumetric flow rate  
multiplied by the density of water at bath temperature

$$\begin{aligned}
 &= (1.226 \text{ gpm}) \cdot (62.18 \text{ lb}_m/\text{ft}^3) \cdot (0.1337 \text{ ft}^3/\text{gal}) \\
 &\quad \cdot (60 \text{ min/hr}) \\
 &= 610.98 \text{ lb}_m/\text{hr} \\
 &= 0.0770 \text{ kg/s}
 \end{aligned}$$

Correction for inlet and exit bulk temperatures is  
made according to the calibration in Appendix A. When the  
test fluid is circulated at a constant temperature equal to  
the inlet temperature:

$$\begin{aligned}
 \text{Inlet temperature} \\
 &= 83.10 + 0.03
 \end{aligned}$$



$$= 83.13 \text{ }^{\circ}\text{F}$$

$$= 301.74 \text{ K}$$

Exit temperature

$$= 83.10 + 0.02$$

$$= 83.12 \text{ }^{\circ}\text{F}$$

$$= 301.73 \text{ K}$$

When the test fluid is circulated at a constant temperature equal to the exit temperature:

Inlet temperature

$$= 123.40 + 0.03$$

$$= 123.43 \text{ }^{\circ}\text{F}$$

$$= 324.13 \text{ K}$$

Exit temperature

$$= 123.40 + 0.02$$

$$= 123.42 \text{ }^{\circ}\text{F}$$

$$= 324.12 \text{ K}$$

Specific heat of water at 83.10  $^{\circ}\text{F}$  from Appendix E

$$= 0.99805 \text{ Btu}/(\text{lb}_m \cdot \text{F})$$

$$= 4.1786 \text{ kJ}/(\text{kg} \cdot \text{K})$$

Specific heat of water at 123.4  $^{\circ}\text{F}$  from Appendix E

$$= 0.99806 \text{ Btu}/(\text{lb}_m \cdot \text{F})$$

$$= 4.1787 \text{ kJ}/(\text{kg} \cdot \text{K})$$

Heat loss when the fluid is circulated at a constant temperature equal to the inlet temperature

$$= (\dot{m}) (C_p) (T_i - T_o)$$

$$= (610.98) (0.99805) (83.13 - 83.12)$$

$$= 6.10 \text{ Btu/hr}$$

$$= 1.79 \text{ W}$$

Heat loss when the fluid is circulated at a constant temperature equal to the exit temperature

$$= (\dot{m}) (C_p) (T_i - T_o)$$

$$= (610.98) (0.99805) (123.43 - 123.42)$$

$$= 6.10 \text{ Btu/hr}$$

$$= 1.79 \text{ W}$$

Heat loss from the test section

$$= (6.10 + 6.10) / 2$$

$$= 6.10 \text{ Btu/hr}$$

$$= 1.79 \text{ W}$$

Rate of heat input

$$= \text{power input} - \text{heat loss}$$

$$= 24991 - 6.1$$

$$= 24985 \text{ Btu/hr}$$

$$= 7322 \text{ W}$$

#### Rate of Heat Output

Specific heat of water at the arithmetic mean of the inlet and exit temperatures ( $103.25^\circ\text{F} = 312.92^\circ\text{K}$ ) from Appendix E.

$$= 0.99805 \text{ Btu}/(\text{lb}_m \cdot ^\circ\text{F})$$

$$= 4.1786 \text{ kJ}/(\text{kg} \cdot \text{K})$$

Rate of heat output

$$= (m) (C_p) (T_i - T_o)$$

$$= (610.98) (0.99805) (123.40 - 83.10)$$

$$= 24574 \text{ Btu/hr}$$

$$= 7202 \text{ W}$$

### Heat Balance

$$\begin{aligned} \text{heat balance error} &= (100 \%) (\text{heat input} - \text{heat output}) \\ &\quad / \text{heat input} \\ &= (100 \%) (24985 - 24574) / 24985 \\ &= 1.7 \% \end{aligned}$$

### Calculation of the Local Inside Wall Temperature and the Local Inside Wall Heat Flux

The computer program in Appendix I solves for the inside wall temperatures numerically from the measured outside wall temperatures. The equations used for the computer program are listed in Appendix F. The numerical solutions involve a converging trial-and-error procedure which will not be attempted here. Typical results are listed in Appendix H, page 122. Due to natural convection, the temperature at the bottom of the tube is lower than the temperature at the top of the tube for Reynolds numbers less than 4,600. The heat flux at the bottom of the tube is higher than the heat flux at the top of the tube for Reynolds numbers less than 4,600.

### Calculation of the Local Heat Transfer Coefficient

For position (12,1), i.e., the thermocouple at the top

of the tube in station 12, the heat transfer coefficient is calculated according to equation (V.4):

$$\begin{aligned} h &= 11102.2 / (146.84 - 123.14) \\ &= 468.45 \text{ Btu} / (\text{ft}^2 \cdot \text{hr} \cdot ^\circ\text{F}) \\ &= 2659.8 \text{ W} / (\text{m}^2 \cdot \text{K}) \end{aligned}$$

The rest of the local heat transfer coefficients are calculated similarly. The average peripheral heat transfer coefficient at station 12 is calculated by equation (V.5):

$$\begin{aligned} h &= (1/8) (11102 / (146.84 - 123.14) + 11129 / (146.15 - 123.14) \\ &\quad + 11170 / (145.35 - 123.14) + 11126 / (146.23 - 123.14)) \\ &= 484.23 \text{ Btu} / (\text{hr} \cdot \text{ft} \cdot ^\circ\text{F}) \\ &= 2750 \text{ W} / (\text{m} \cdot \text{K}) \end{aligned}$$

The average peripheral heat transfer coefficient at station 12 is also calculated by equation (V.6):

$$\begin{aligned} h &= ((11102 + 11129 + 11170 + 11126) / 8) \\ &\quad / ((146.84 + 146.15 + 145.35 + 146.23) / 4 - 123.14) \\ &= 483.95 \text{ Btu} / (\text{hr} \cdot \text{ft} \cdot ^\circ\text{F}) \\ &= 2748 \text{ W} / (\text{m} \cdot \text{K}) \end{aligned}$$

## APPENDIX K

### SAMPLE PROBLEMS

#### Laminar Flow

A DEG-distilled water solution with 20 % DEG mass fraction is flowing at a local bulk temperature of 100 °F (311 °K) inside a 1 in. x 14 BWG stainless steel 316 tube (wall thickness = 0.083 in.). The outside film heat transfer coefficient is assumed to be 300 Btu/(hr·ft<sup>2</sup>·°F) (1700 W/(m<sup>2</sup>·K)), based on the outside surface area. Assume there is no fouling.

The physical properties for DEG-water solution are calculated at the bulk fluid temperature from Appendix E:

$$\rho = 1022 \text{ kg/m}^3 = 63.81 \text{ lb}_m/\text{ft}^3$$

$$\mu = 1.464 \text{ mPa}\cdot\text{s} = 3.542 \text{ lb}/(\text{ft}\cdot\text{hr})$$

$$C_p = 0.9378 \text{ Btu}/(\text{lb}\cdot^\circ\text{F}) = 3.927 \text{ kJ}/(\text{kg}\cdot\text{K})$$

$$k = 0.5134 \text{ W}/(\text{m}\cdot\text{K}) = 0.2967 \text{ Btu}/(\text{hr}\cdot\text{ft}\cdot^\circ\text{F})$$

$$\beta = 1.804\cdot 10^{-5}/\text{K} = 1.002\cdot 10^{-5}/^\circ\text{F}$$

Assume the solution is flowing at 0.24 ft/s (0.0732 m/s).

$$\text{Re} = \rho u d_i / \mu$$

$$= (63.81 \text{ lb}_m/\text{ft}^3) \cdot (0.24 \text{ ft/s}) \cdot (0.834 \text{ ft}/12) \cdot$$

$$\cdot (3600\text{s/hr}) \cdot / (3.542 \text{ lb}/(\text{ft}\cdot\text{hr}))$$

$$= 1081$$

The flow is laminar.

$$\underline{X/d_i = 300}$$

If the outside fluid has a local bulk temperature of 140 °F, we assume for a first trial the tube inside wall temperature to be the average of the inside and outside bulk fluid temperature.

$$\begin{aligned} T_{wi} &= (100 + 140)/2 \\ &= 120 \text{ °F} \\ &= 322.1 \text{ °K} \end{aligned}$$

From Appendix E

$$\begin{aligned} \mu_w @ 120^\circ\text{F} &= 2.184 \text{ lb}/(\text{hr}\cdot\text{ft}) \\ &= 0.9029 \text{ mNs}/\text{m}^2 \end{aligned}$$

Calculate dimensionless parameters

$$\begin{aligned} (\mu_b/\mu_w) &= [3.542 \text{ lb}/(\text{ft}\cdot\text{hr})]/[2.184 \text{ lb}/(\text{hr}\cdot\text{ft})] \\ &= 1.622 \end{aligned}$$

$$\begin{aligned} Gr &= (32.17\text{ft}/\text{s}^2) \cdot (1.002 \cdot 10^{-5}/^\circ\text{F}) \cdot (63.81 \text{ lb}_m/\text{ft}^3)^2 \\ &\quad \cdot (0.834\text{ft}/12)^3 \cdot (120 \text{ °F} - 100 \text{ °F}) \cdot (3600\text{s}/\text{hr})^2 \\ &\quad / [3.542 \text{ lb}/(\text{ft}\cdot\text{hr})]^2 \\ &= 9,106 \end{aligned}$$

$$\begin{aligned} Pr &= [3.542 \text{ lb}/(\text{ft}\cdot\text{hr})] \cdot [0.9378 \text{ Btu}/(\text{lb}\cdot^\circ\text{F})] \\ &\quad / [0.2967 \text{ Btu}/(\text{hr}\cdot\text{ft}\cdot^\circ\text{F})] \\ &= 11.20 \end{aligned}$$

Equation (VII.1) is used to calculate the inside heat transfer coefficient

$$\begin{aligned}
Nu &= \{4.364 + 0.00106 \cdot 1081^{0.81} \cdot 11.2^{0.45} \cdot [1 + 14e^{(-0.063 \cdot 300)}] \\
&\quad \cdot 0.268 \cdot (807,200 \cdot 11.2)^{1/4} \cdot [1 - e^{(-0.042 \cdot 300)}]\} \cdot 1.622^{0.14} \\
&= \{4.364 + 0.9013 \cdot [1.000] + 4.468 \cdot [1.000]\} \cdot 1.0701 \\
&= 10.42
\end{aligned}$$

$$\begin{aligned}
h_i &= Nu \cdot k / d_i \\
&= 10.42 \cdot [0.2967 \text{ Btu}/(\text{hr} \cdot \text{ft} \cdot ^\circ\text{F})] / (0.834 \text{ ft}/12) \\
&= 44.46 \text{ Btu}/(\text{hr} \cdot \text{ft}^2 \cdot ^\circ\text{F}) \\
&= 254 \text{ W}/(\text{m}^2 \cdot \text{K})
\end{aligned}$$

Check for the assumption of surface temperature from heat balance between two bulk temperatures:

$$h_i A_i (T_{wi} - T_{bi}) = k_w (A_i + A_o) (T_{wo} - T_{wi}) / 2\Delta X \quad (\text{K.1})$$

$$h_o A_o (T_{bo} - T_{wo}) = h_i A_i (T_{wi} - T_{bi}) \quad (\text{K.2})$$

where thermal conductivity of the wall (7.75 Btu/(hr·ft·°F)) is calculated from eq'n (E.12).

Substituting and solving equations (K.1) and (K.2) for the inside and outside wall temperatures, we obtain:

$$T_{wi} = 134.4 ^\circ\text{F} = 57.07 ^\circ\text{C}$$

$$T_{wo} = 135.7 ^\circ\text{F} = 57.79 ^\circ\text{C}$$

For the new surface temperature (134.4 °F), recalculate dimensionless parameters and resubstitute these new parameters into eq'n (VII.1), giving:

$$\begin{aligned}
h_i &= 49.4 \text{ Btu}/(\text{hr} \cdot \text{ft}^2 \cdot ^\circ\text{F}) \\
&= 281 \text{ W}/\text{m}^2
\end{aligned}$$

Recheck the inside and outside surface temperature from eq'ns (K.1) and (K.2), we obtain:

$$T_{wi} = 133.8 ^\circ\text{F} = 56.7 ^\circ\text{C}$$

$$T_{wo} = 135.1 \text{ }^{\circ}\text{F} = 57.5 \text{ }^{\circ}\text{C}$$

These temperatures are very close to the previous temperatures (0.6  $^{\circ}\text{F}$  difference). And the heat flux based on the outside surface area is:

$$\begin{aligned}(Q/A_o) &= 300 \text{ Btu}/(\text{hr}\cdot\text{ft}^2\cdot\text{F}) \cdot (140 \text{ }^{\circ}\text{F} - 135.1 \text{ }^{\circ}\text{F}) \\ &= 1470 \text{ Btu}/(\text{hr}\cdot\text{ft}^2) \\ &= 4.637 \text{ kW}/\text{m}^2\text{K}\end{aligned}$$

The overall heat transfer coefficient,  $U_o$  is calculated by:

$$\begin{aligned}U_o &= (Q/A_o) / (T_{bo} - T_{bi}) \\ &= 1470 \text{ Btu}/(\text{hr}\cdot\text{ft}^2) / (140 \text{ }^{\circ}\text{F} - 100 \text{ }^{\circ}\text{F}) \\ &= 36.8 \text{ Btu}/(\text{hr}\cdot\text{ft}^2\cdot\text{F}) \\ &= 209 \text{ W}/\text{m}^2\text{K}\end{aligned}$$

$$\underline{X/d_i = 20}$$

If we have the same case as the above except that we want to calculate the heat transfer coefficient at  $X/d_i = 20$ , for  $T_{wi} = 120 \text{ }^{\circ}\text{F}$  ( $T_{bi} = 100 \text{ }^{\circ}\text{F}$ ), the entrance effect terms in eq'n (VII.1) are no longer negligible.

$$\begin{aligned}\text{Nu} &= \{4.364 + 0.00106 \cdot 1081^{0.81} \cdot 11.2^{0.45} \cdot [1 + 14e^{(-0.063 \cdot 20)}] \\ &\quad \cdot 0.268 \cdot (807,200 \cdot 11.2)^{1/4} \cdot [1 - e^{(-0.042 \cdot 20)}]\} \cdot 1.622^{0.14} \\ &= \{4.364 + 0.9013 \cdot [4.971] + 4.468 \cdot [0.5683]\} \cdot 1.0701 \\ &= 12.18 \\ h_i &= \text{Nu} \cdot k/d_i \\ &= 12.18 \cdot [0.2967 \text{ Btu}/(\text{hr}\cdot\text{ft}\cdot\text{F})] / (0.834 \text{ ft}/12)\end{aligned}$$



$$= 52.0 \text{ Btu}/(\text{hr} \cdot \text{ft}^2 \cdot ^\circ\text{F})$$

$$= 297 \text{ W}/\text{m}^2\text{K}$$

By reestimating the wall temperature at 125.5  $^\circ\text{F}$  and using the similar procedure as the previous case, we obtain the wall temperature at 125.52  $^\circ\text{F}$  (or 52.14  $^\circ\text{K}$ ) and the heat transfer coefficient:

$$h_i = 57.6 \text{ Btu}/(\text{hr} \cdot \text{ft}^2 \cdot ^\circ\text{F})$$

$$= 328 \text{ W}/\text{m}^2\text{K}$$

#### Lower Turbulent Flow

Distilled water is flowing at a local bulk temperature of 100  $^\circ\text{F}$  (311  $^\circ\text{K}$ ) inside a 1 in. x 14 BWG stainless steel 316 tube (wall thickness = 0.083 in.). The outside film heat transfer coefficient is assumed to be 300  $\text{Btu}/(\text{hr} \cdot \text{ft}^2 \cdot ^\circ\text{F})$  ( $1700 \text{ W}/(\text{m}^2 \cdot \text{K})$ ), based on the outside surface area. Assume there is no fouling.

The physical properties for water are calculated at the bulk fluid temperature from Appendix E:

$$\rho = 991 \text{ kg}/\text{m}^3 = 61.87 \text{ lb}_\text{m}/\text{ft}^3$$

$$\mu = 0.730 \text{ mPas} = 1.766 \text{ lb}/(\text{ft} \cdot \text{hr})$$

$$C_p = 0.9979 \text{ Btu}/(\text{lb} \cdot ^\circ\text{F}) = 4.179 \text{ kJ}/(\text{kg} \cdot \text{K})$$

$$k = 0.6241 \text{ W}/(\text{m} \cdot \text{K}) = 0.3607 \text{ Btu}/(\text{hr} \cdot \text{ft} \cdot ^\circ\text{F})$$

$$\beta = 3.743 \cdot 10^{-7}/\text{K} = 2.079 \cdot 10^{-7}/^\circ\text{F}$$

Assume the solution is flowing at 1.14 ft/s (0.35 m/s).

$$\text{Re} = \rho u d_i / \mu$$

$$= (61.87 \text{ lb}_\text{m}/\text{ft}^3) \cdot (1.14 \text{ ft}/\text{s}) \cdot (0.834 \text{ ft}/12) \cdot$$

$$\begin{aligned} & \cdot (3600\text{s/hr}) \cdot / (1.766 \text{ lb}/(\text{ft}\cdot\text{hr})) \\ & = 10,000 \end{aligned}$$

The flow is turbulent.

If the outside fluid has a local bulk temperature of 140 °F and  $h_o = 300 \text{ Btu}/(\text{hr}\cdot\text{ft}^2\cdot^\circ\text{F})$ , we assume the tube inside wall temperature to be the average of the inside and outside bulk fluid temperature.

$$\begin{aligned} T_{wi} &= (100 + 140)/2 \\ &= 120 \text{ }^\circ\text{F} \\ &= 322.1 \text{ }^\circ\text{K} \end{aligned}$$

From Appendix E

$$\mu_w \text{ @ } 120^\circ\text{F} = 1.445 \text{ lb}/(\text{hr}\cdot\text{ft})$$

Calculate dimensionless parameters

$$\begin{aligned} (\mu_b/\mu_w) &= [1.766 \text{ lb}/(\text{ft}\cdot\text{hr})]/[1.445 \text{ lb}/(\text{hr}\cdot\text{ft})] \\ &= 1.222 \\ Pr &= [1.766 \text{ lb}/(\text{ft}\cdot\text{hr})] \cdot [0.9979 \text{ Btu}/(\text{lb}\cdot^\circ\text{F})] \\ &\quad / [0.3607 \text{ Btu}/(\text{hr}\cdot\text{ft}\cdot^\circ\text{F})] \\ &= 4.89 \end{aligned}$$

Equation (VII.2) is used to calculate the inside heat transfer coefficient

$$\begin{aligned} Nu &= 0.01426 \cdot 10000^{0.86} \cdot 4.89^{1/3} \cdot [1 + 1.15 \cdot e^{(-300/3)}] \cdot 1.222^{0.14} \\ &= 68.6 \\ h_i &= Nu \cdot k/d_i \\ &= 68.6 \cdot [0.3607 \text{ Btu}/(\text{hr}\cdot\text{ft}\cdot^\circ\text{F})]/(0.834\text{ft}/12) \\ &= 356 \text{ Btu}/(\text{hr}\cdot\text{ft}^2\cdot^\circ\text{F}) \\ &= 2038 \text{ W}/\text{m}^2\text{K} \end{aligned}$$

After rechecking the inside surface temperature, the

heat transfer coefficient,  $h_i = 382 \text{ Btu}/(\text{hr}\cdot\text{ft}^2\cdot^\circ\text{F})$  (or  $2243 \text{ W}/\text{m}^2\text{K}$ ).

#### Transition Flow

Same conditions as those in the turbulent flow case were used except that velocity is  $0.63 \text{ ft/s}$ . For inside surface temperature  $120^\circ\text{F}$ , we have:

$$\begin{aligned} \text{Re} &= \rho u d_i / \mu \\ &= (61.87 \text{ lb}_m/\text{ft}^3) \cdot (0.63 \text{ ft/s}) \cdot (0.834 \text{ ft}/12) \cdot \\ &\quad \cdot (3600\text{s/hr}) / (1.766 \text{ lb}/(\text{ft}\cdot\text{hr})) \\ &= 5,523 \end{aligned}$$

The flow is in transition flow regime.

Equation (VII.3) is used to calculate the inside heat transfer coefficient

$$\begin{aligned} \text{Nu} &= 0.00392 \cdot 5523 \cdot 4.89^{1/3} \cdot [1 + 1.19 \cdot e^{(-300 \cdot 0.308)}] \cdot 1.222^{0.14} \\ &= 37.8 \end{aligned}$$

$$\begin{aligned} h_i &= \text{Nu} \cdot k / d_i \\ &= 37.8 \cdot [0.3607 \text{ Btu}/(\text{hr}\cdot\text{ft}\cdot^\circ\text{F})] / (0.834\text{ft}/12) \\ &= 196 \text{ Btu}/(\text{hr}\cdot\text{ft}^2\cdot^\circ\text{F}) \\ &= 1123 \text{ W}/\text{m}^2\text{K} \end{aligned}$$

After rechecking the inside surface temperature, the heat transfer coefficient,  $h_i = 210 \text{ Btu}/(\text{hr}\cdot\text{ft}^2\cdot^\circ\text{F})$  (or  $1202 \text{ W}/\text{m}^2\text{K}$ ).

## APPENDIX L

### BEHAVIOR OF THE DEVELOPED CORRELATIONS

Correlations (VII.1), (VII.2) and (VII.3) are for the local average Nusselt number calculations.  $\underline{Nu}$  denotes the overall average Nusselt number for the entire tube.  $\underline{Nu}$  can be derived from the local average Nusselt number equation by assuming that the physical properties remain the same for the entire tube and by taking the integration of the local average Nusselt number with respect to  $X$  from 0 to  $L$ , the total length of the tube, and divided by  $L$  as following:

$$\underline{Nu} = \frac{1}{L} \cdot \int_0^L Nu \cdot dX \quad (L.1)$$

Equation (VII.1) is substituted into eq'n (L.1) and the following eq'n is obtained:

$$\begin{aligned} \underline{Nu} = & \{4.364 + 0.00106 \cdot Re^{0.81} Pr^{0.45} \cdot [1 + 222 \cdot d_i/L (1 - e^{(-0.063L/d_i)})] \\ & + 0.268 \cdot (GrPr)^{1/4} \cdot [1 - 23.8 \cdot d_i/L (1 - e^{(-0.042L/d_i)})]\} \cdot (\mu_b/\mu_w)^{0.14} \end{aligned} \quad (L.2)$$

Equation (VII.2) is substituted into eq'n (L.1) and the following eq'n is obtained:

$$\underline{Nu} = 0.001426 \cdot RePr^{1/3} \cdot [1 + 3.45 \cdot d_i/L - 3.45 \cdot d_i/L \cdot e^{(-L/(3 \cdot d_i))}] \cdot (\mu_b/\mu_w)^{0.14} \quad (L.3)$$

Equation (VII.3) is substituted into eq'n (L.1) and the following eq'n is obtained:

$$\underline{Nu} = 0.00392 \cdot Re^{0.86} Pr^{1/3} \cdot [1 + 3.86 \cdot d_i/L (1 - e^{(-0.308 \cdot L/d_i)})] \cdot (\mu_b/\mu_w)^{0.14} \quad (L.4)$$

Figures 46, 47 and 48 show  $Nu$  and  $\underline{Nu}$  as a function of  $X/d_i$  (for  $Nu$ ) or  $L/d_i$  (for  $\underline{Nu}$ ) at  $Re = 2,000, 1,000$  and  $500$  respectively. Figure 49 shows  $Nu$  and  $\underline{Nu}$  as a function of  $X/d_i$  (for  $Nu$ ) or  $L/d_i$  (for  $\underline{Nu}$ ) at  $Re = 10,000$ . Figure 50 shows  $Nu$  and  $\underline{Nu}$  as a function of  $X/d_i$  (for  $Nu$ ) or  $L/d_i$  (for  $\underline{Nu}$ ) at  $Re = 5,500$ . Also the values calculated by Sieder-Tate (45) and Petukhov-Popov (35) were given in Figures 49 and 50 as reference values.

The assumption of constant properties throughout the entire tube may cause tremendous error if we have the following cases:

- 1) Large heat flux. The fluid flowing inside the tube changes temperature significantly so that the physical properties change dramatically.

- 2) The fluid changes its flow mechanism from one flow regime to another. This will cause an unexpected increase or decrease in heat flux.

In order to solve the above two problems, we have to apply finite difference techniques to divide the entire tube into several sections. The physical properties remain the same within the same section and will be subjected to change for different sections according to the result of

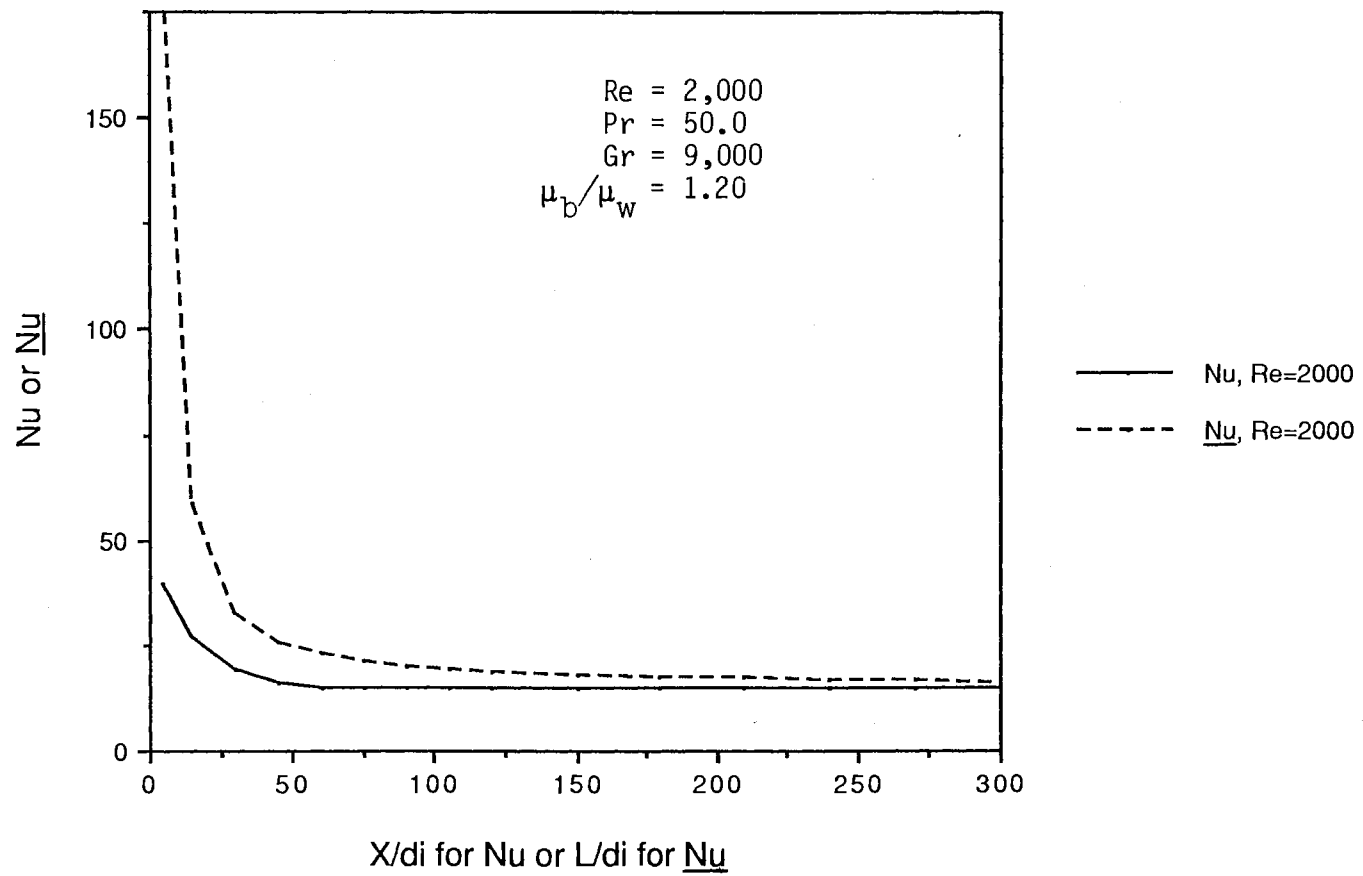


Figure 46:  $Nu$  vs  $X/d_i$  and  $\bar{Nu}$  vs  $L/d_i$  at  $Re = 2,000$

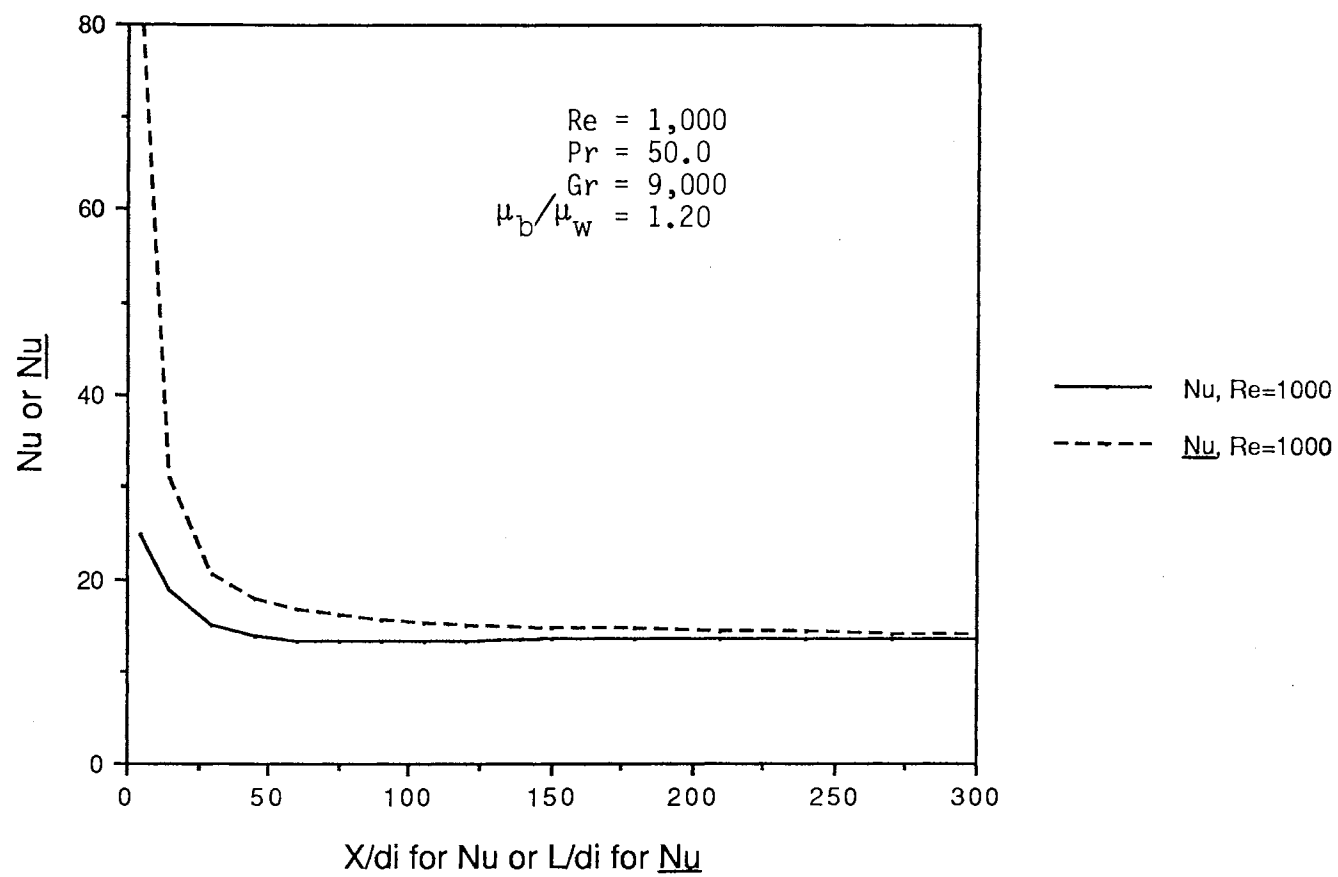


Figure 47:  $Nu$  vs  $X/d_i$  and  $\bar{Nu}$  vs  $L/d_i$  for  $Re = 1,000$

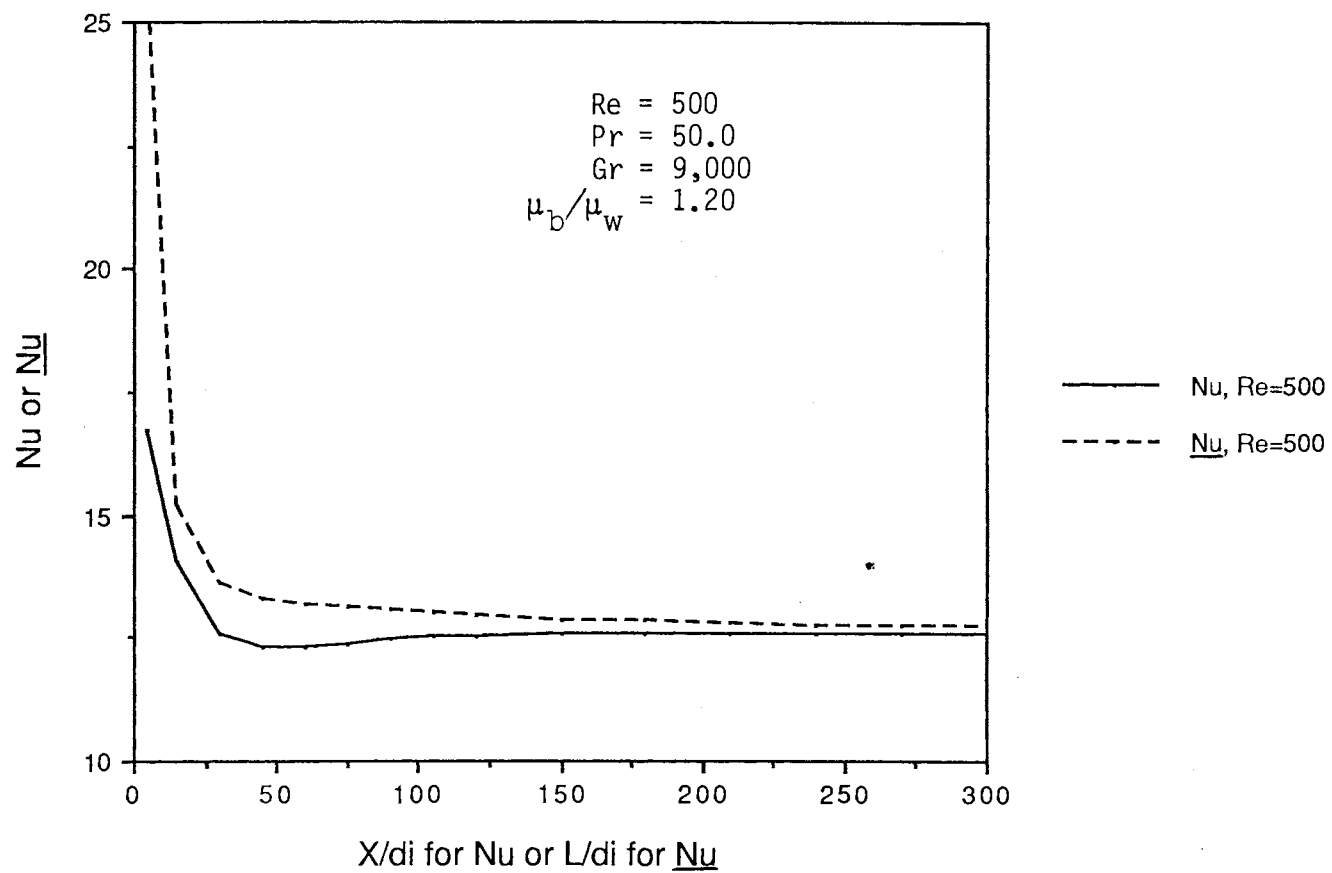


Figure 48:  $Nu$  vs  $X/d_i$  and  $\underline{Nu}$  vs  $L/d_i$  for  $Re = 500$



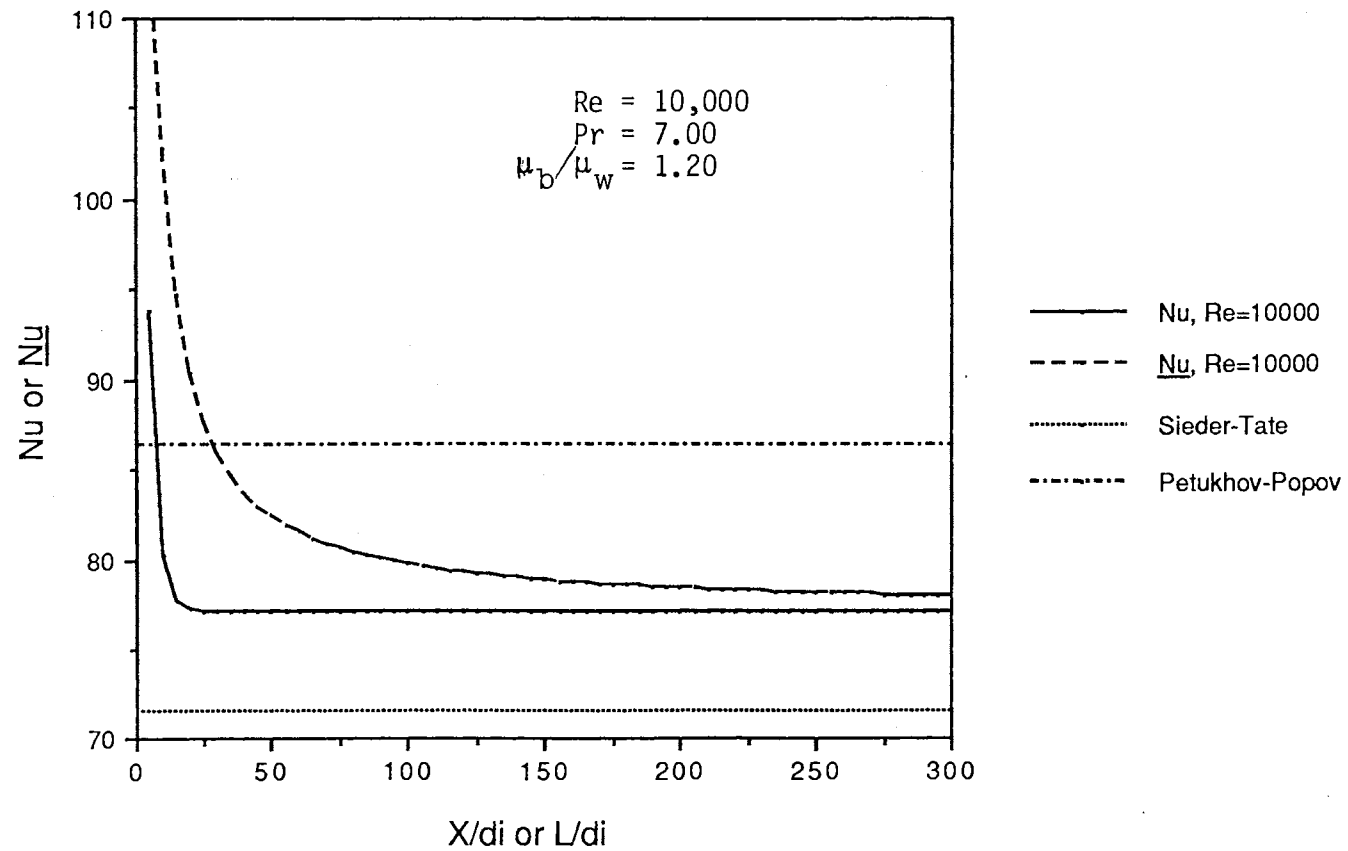


Figure 49: Nu vs  $X/d_i$  and  $\bar{Nu}$  vs  $L/d_i$  for Re = 10,000  
 $\bar{Nu}$  Calculated by Sieder-Tate and Petukhov-Popov Correlations are Shown as References.

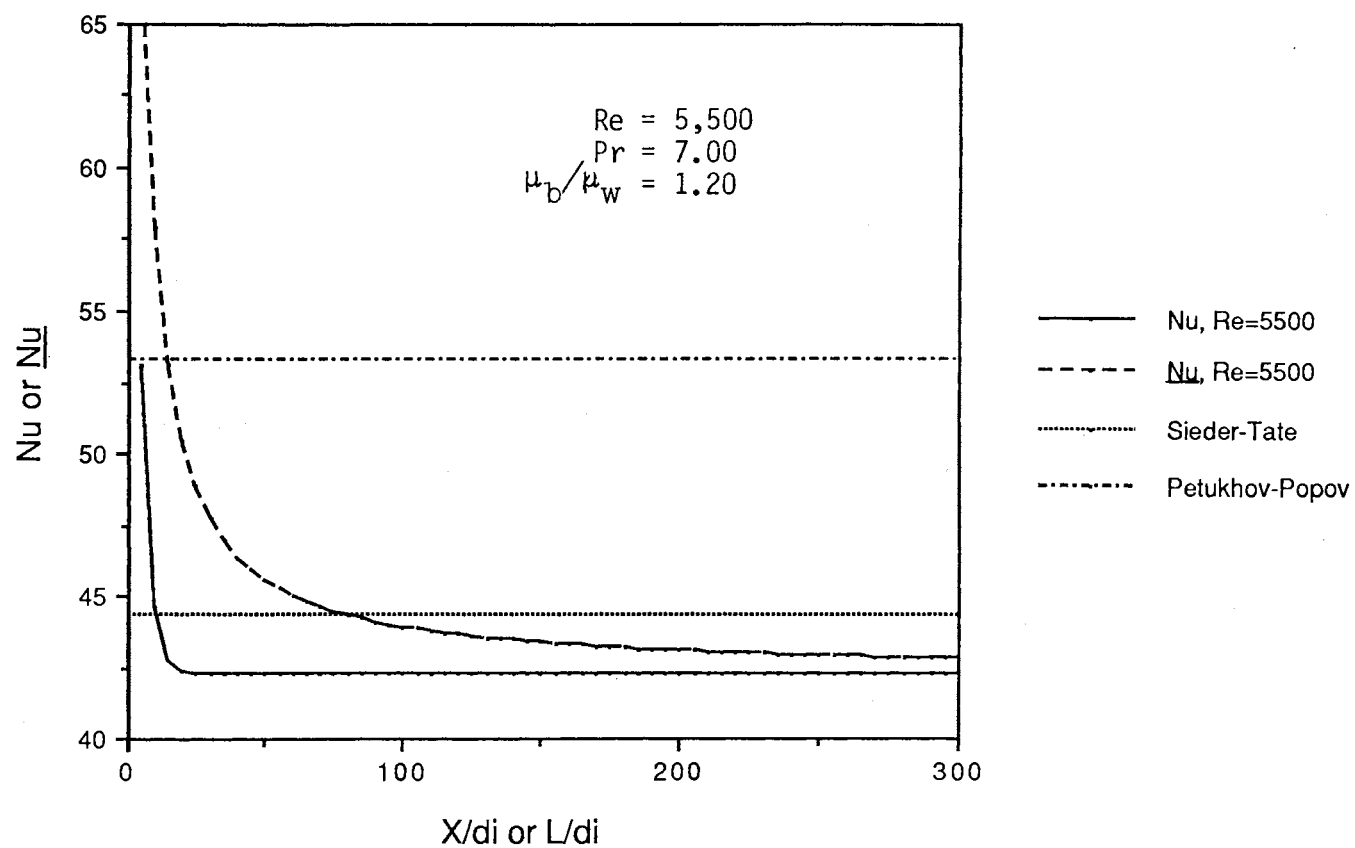


Figure 50: Nu vs  $X/d_i$  and  $\overline{Nu}$  vs  $L/d_i$  for Re = 5,500  
 $\overline{Nu}$  Calculated by Sieder-Tate and Petukhov-Popov Correlations Are Shown as References.

heat balance of the previous section. The calculation will be step by step.

VITA

Jeng-Ho Chen

Candidate for the Degree of

Doctor of Philosophy

Thesis: HEAT TRANSFER IN HIGH LAMINAR, TRANSITION, AND LOWER  
TURBULENT FLOW REGIMES FOR SQUARE-EDGED CONTRACTION  
ENTRANCE IN A CIRCULAR TUBE

Major Field: Chemical Engineering

Biographical:

Education: Received the Bachelor of Science degree in  
Chemical Engineering (1978) and the Master of  
Science degree in Chemical Engineering (1980) from  
National Tsing-Hua University, Hsin-Chu, Taiwan,  
R.O.C. Completed requirements for the Doctor of  
Philosophy degree in Chemical Engineering at  
Oklahoma State University in May, 1989

Professional Experience: Teaching Assistant, School of  
Chemical Engineering, Oklahoma State University,  
September 1983 to May 1987. Research Associate,  
Department of Biochemistry, Oklahoma State  
University, May 1986 to October 1988. Design  
Engineer, January 1980 to March 1981, at Far East  
Mach. Company, Taiwan, R.O.C. Lecturer, March 1981  
to August 1982, at Chinese Army Electronics and  
Communication School, Taiwan, R.O.C.